ON INSTABILITY WAVE CONTROL IN TURBULENT JETS

V. F. Kopiev
Central Aerohydrodinamic Institute (TsAGI), Moscow

18th Workshop of the CEAS/X-Noise
AIRCRAFT NOISE REDUCTION BY FLOW CONTROL AND
ACTIVE/ ADAPTIVE TECHNIQUES

25-26 September 2014
Vilnius Gediminas Technical University, Lithuania

Proposed approach

In supersonic jet one of the mechanisms of sound radiation is identified and is ready to noise control strategy formulation. We issue the same mechanism exists in **hot high speed subsonic** jet.

The Main questions are:

Strategy of excitation?

Original assumptions?

Physical principle for control?

Approaches?

Possible mechanisms of noise generation

Large-scale structures in the mixing layer of a jet do not directly radiate noise, if they travel with a subsonic speed with respect to the ambient air.

Large-scale structures directly radiate noise.(additional mechanism to pairing, tilting, etc.)

Supersonic jet, wavy wall

Low speed subsonic jet

Subsonic jet, vortex ring

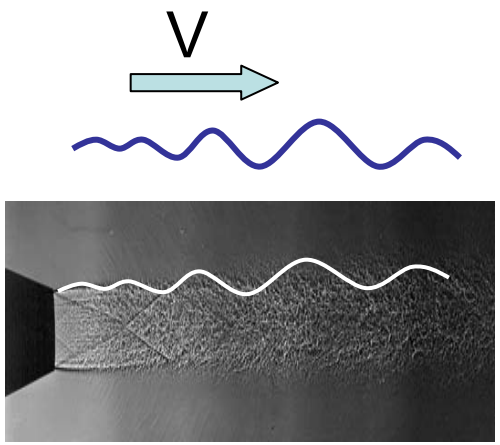

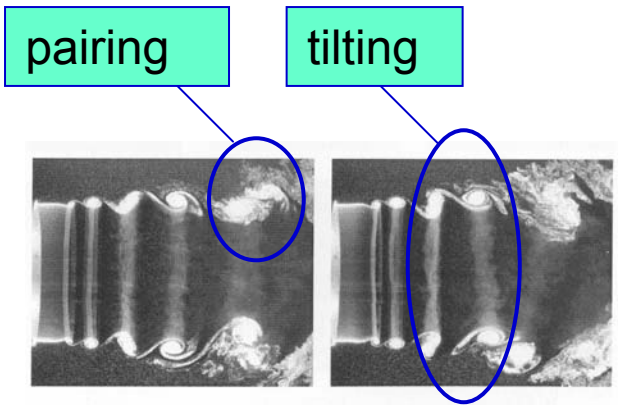

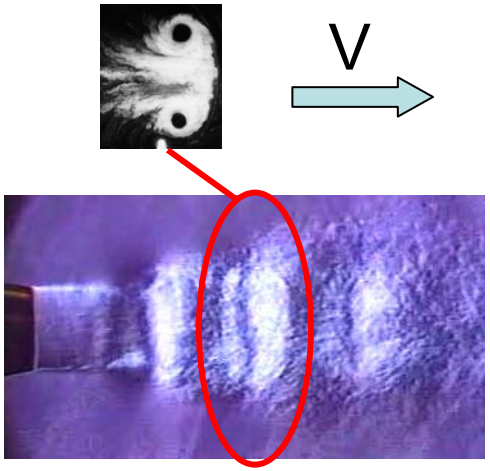

Nozzle exit solutions for intensification of lengthwise vorticity for instability wave control

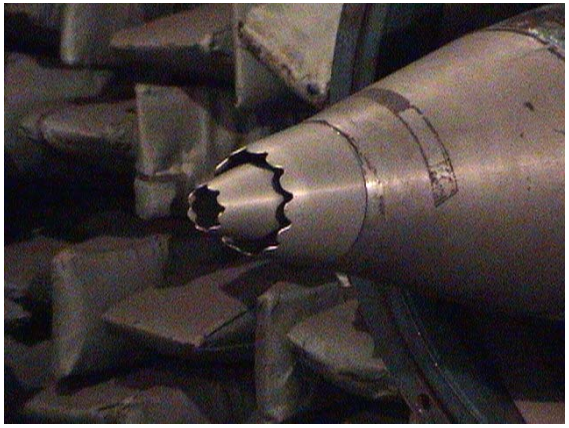

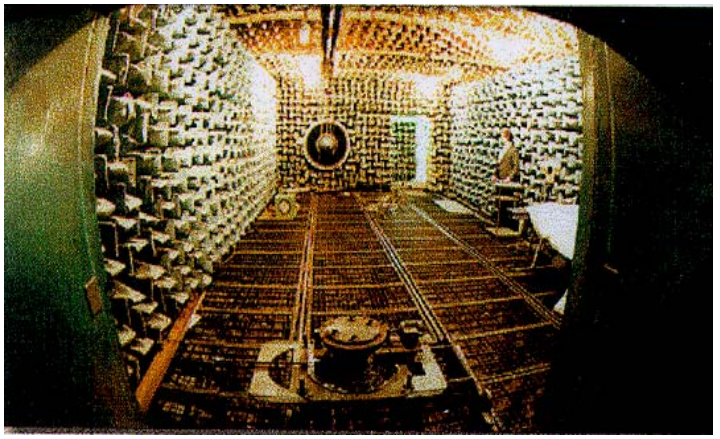

Nozzle exit solutions for intensification of lengthwise vorticity for instability wave control

The main methods of noise control are made on checking some a priory proposed configurations and on experimental search for the optimum. It is obviously, that this optimum substantially depends on the quantity of the models investigated and on the experimenter's luck.

Outline

HF DBD actuators for jet noise reduction (OPENAIR)

- The initial concept. Streamwise vorticity creation.
- Actuator design and characteristics
- HF DBD actuator in external flow
- Jet noise control. Test results.
- Control mechanism.

Instability Wave Control by Plasma Actuators (ORINOCO)

- To develop plasma actuators technologies dedicated to jet noise reduction:
  - surface barrier corona discharge
  - high-current gliding surface discharge
  - high frequency dielectric barrier discharge
- Demonstration of instability wave control

HF DBD actuators for jet noise reduction

Lengthwise vorticity organizing using Surface HF DBD

Surface HF DBD actuator disposes on the inner surface of nozzle.

Transversal flow is organized (steady or periodical) to affect the large scale structures in the initial part of jet shear layer.

This system due to great flexibility in manufacturing and in work (compared chevrons) could be tuning for optimal parameters (in experiment).

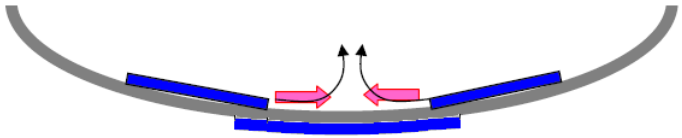

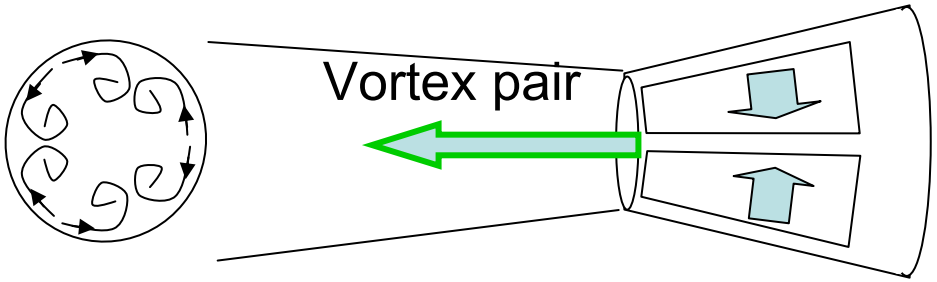

Scheme of plasma actuator

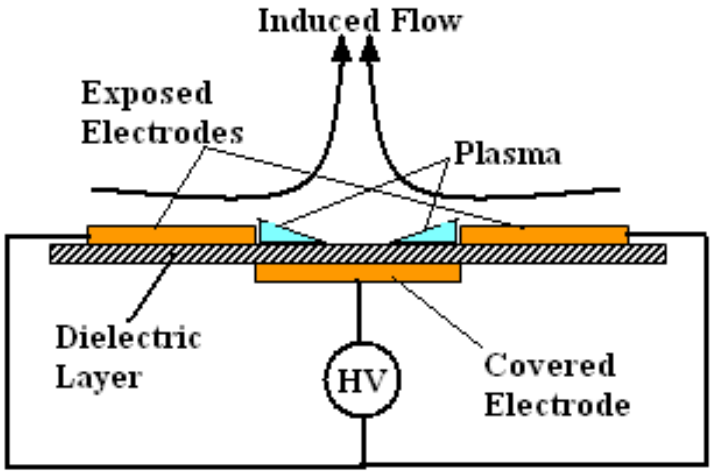

High-frequency power supply parameters

Voltage at discharge	0 - 20 kV
Power	up to 5 kW
Carrier frequency	f =30-300 kHz
Modulation frequency	F=1-30 kHz (depending on f),
Modulation depth	100%.

Two electrodes: creation of normal microjet flow

No flow along the electrodes

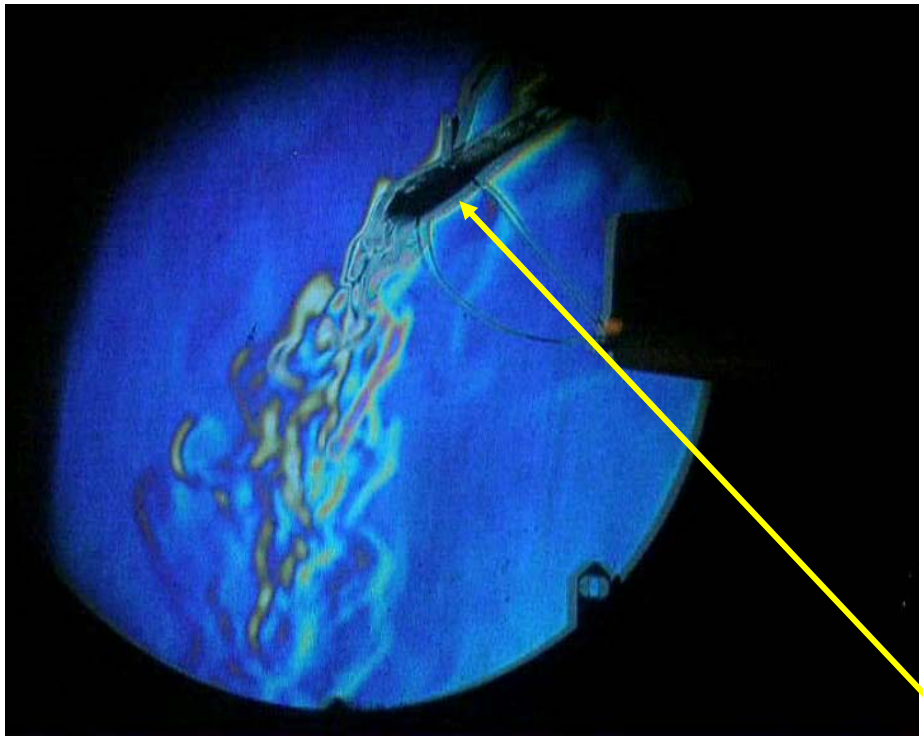

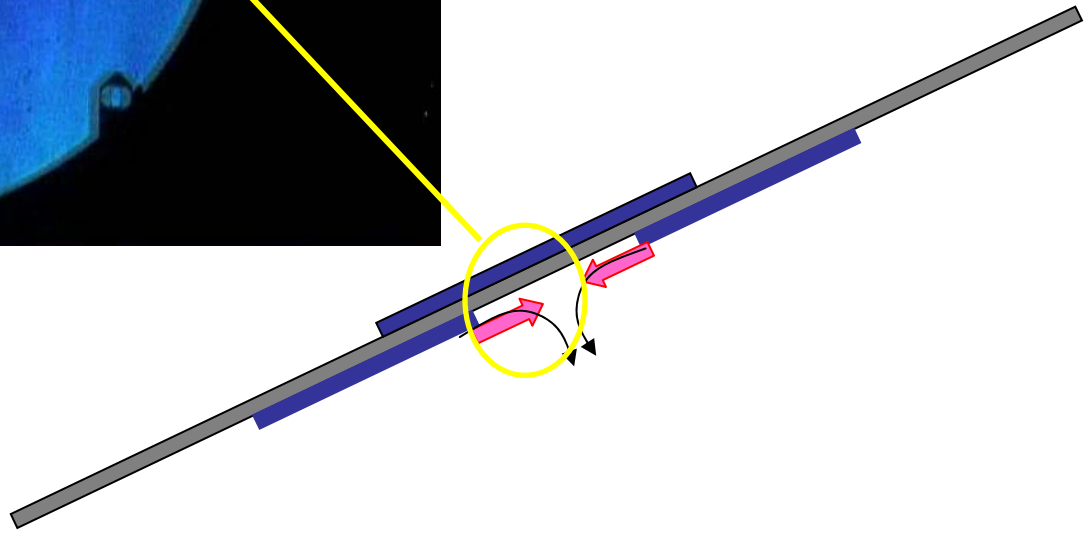

Nozzles with quartz cylinder exit

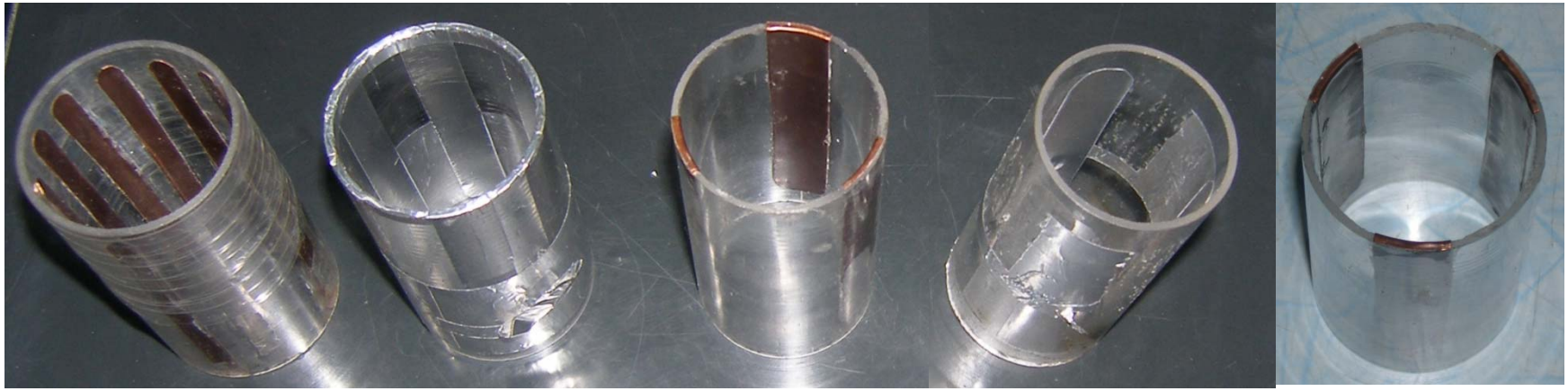

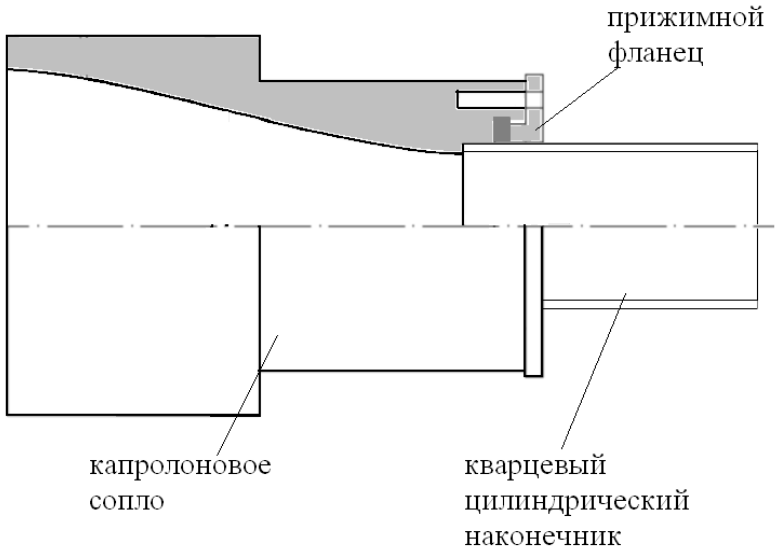

Nozzles with quartz cylinder exit

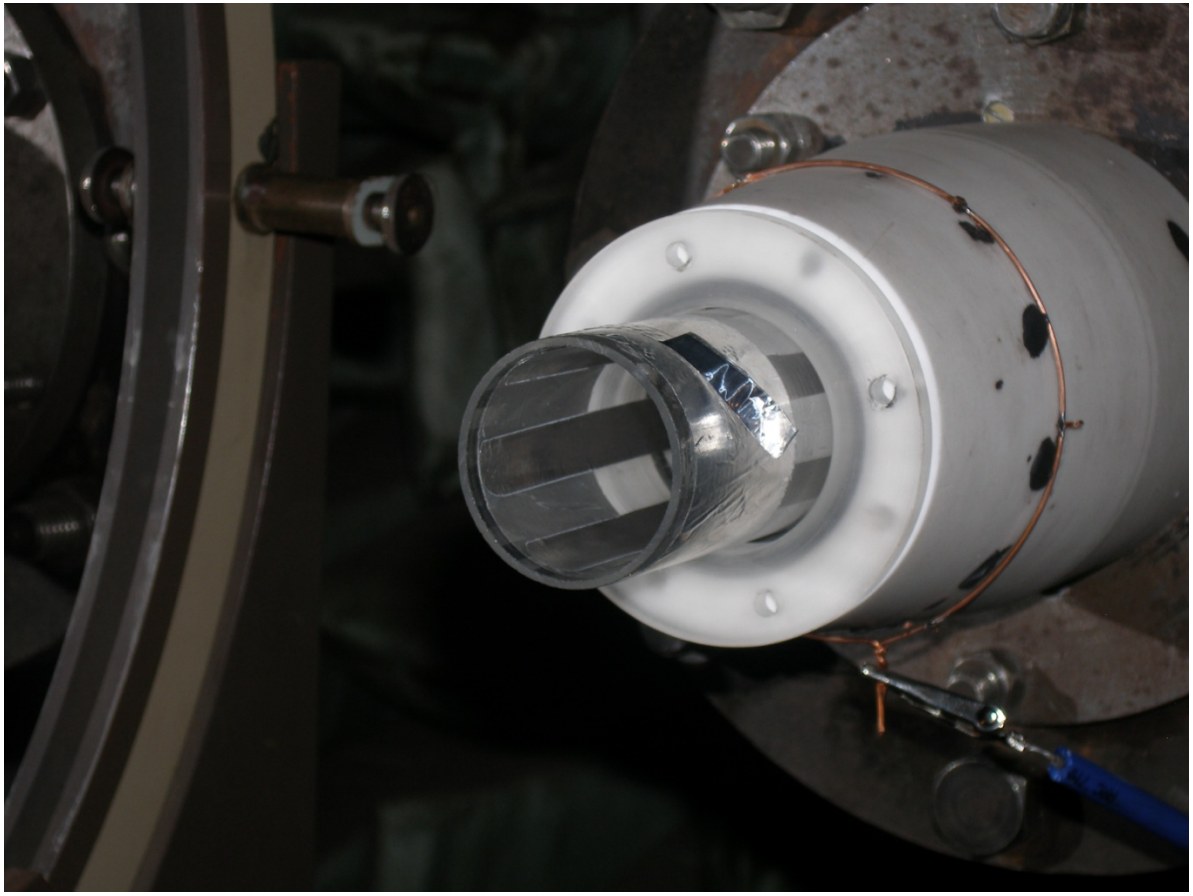

Broadband noise amplification

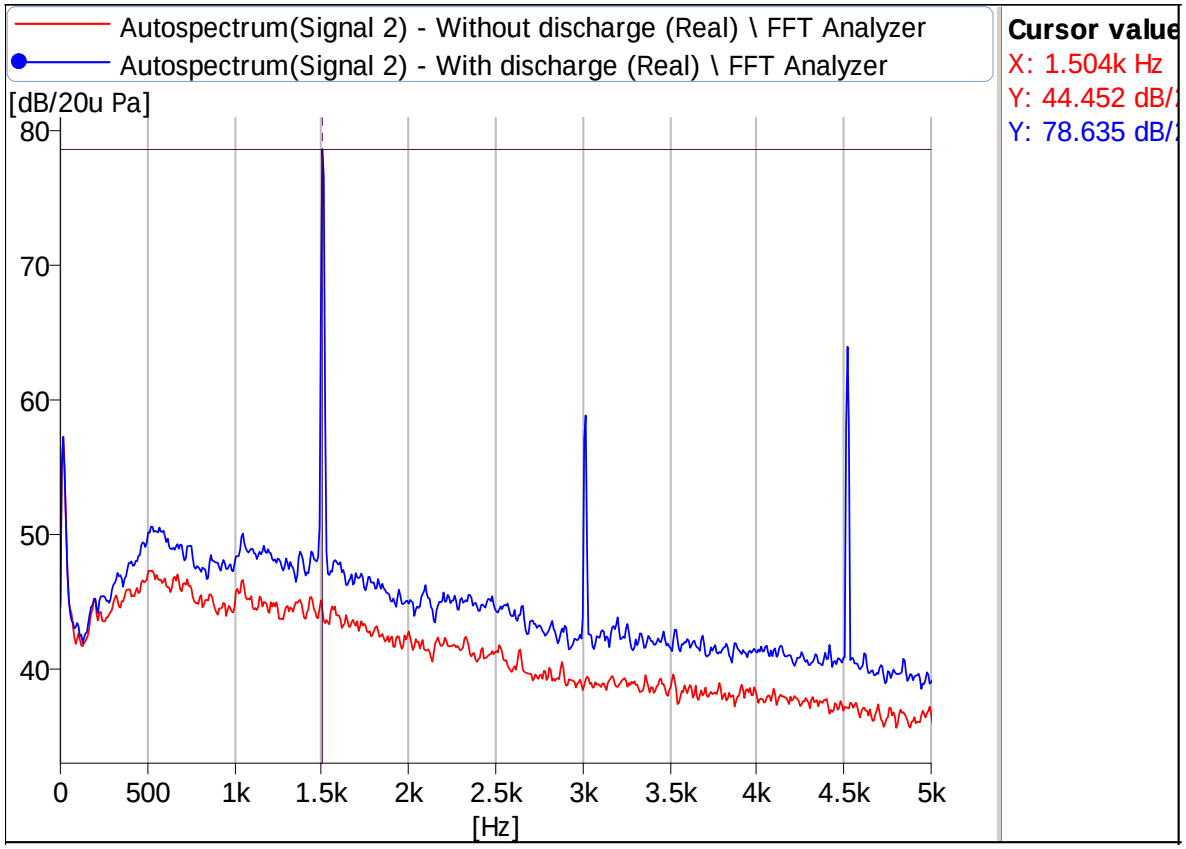

Cylindrical nozzle with 6 electrodes; jet velocity is 100 m/s. The red curve corresponds to the absence of the discharge; the blue curve corresponds to the discharge with the modulation frequency of 1500 Hz.

Broadband noise amplification

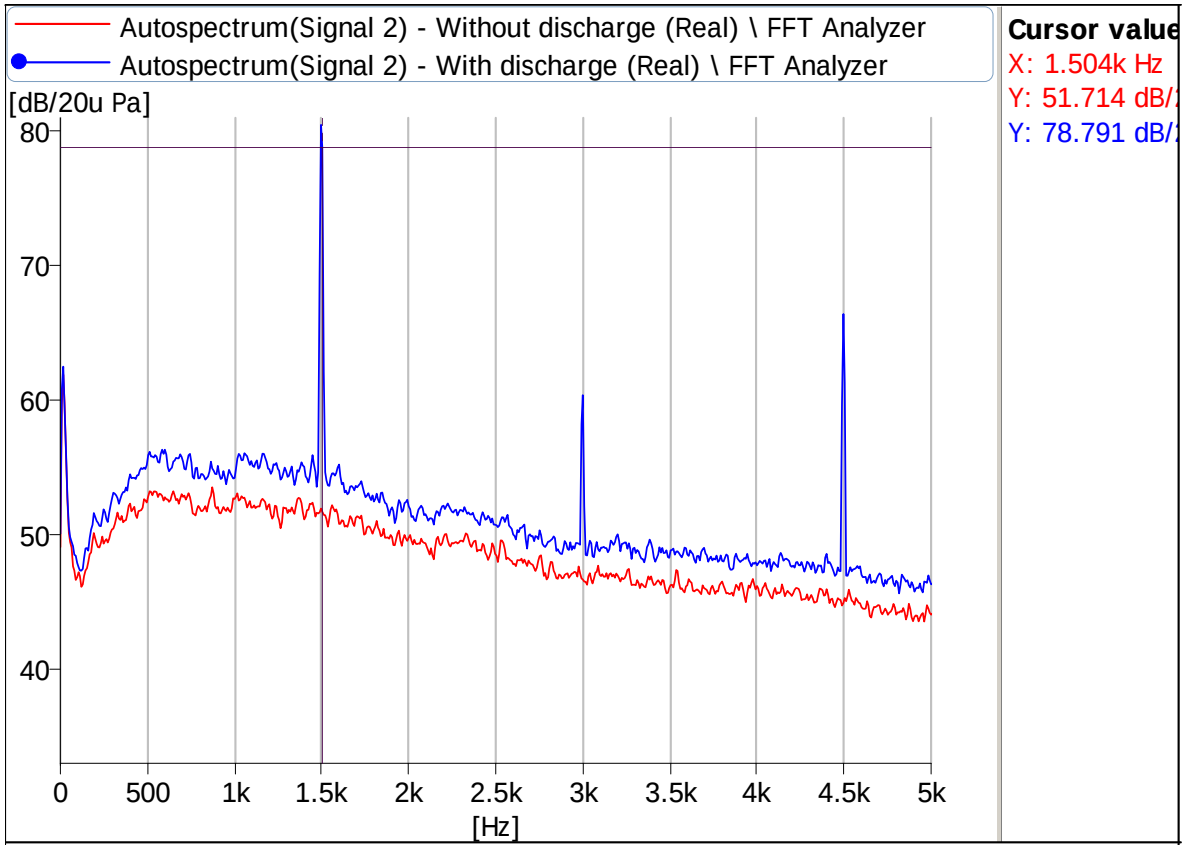

Cylindrical nozzle with 6 electrodes; jet velocity is 120 m/s. The red curve corresponds to the absence of the discharge; the blue curve corresponds to the discharge with the modulation frequency of 1500 Hz.

Conical nozzles with ceramic exit

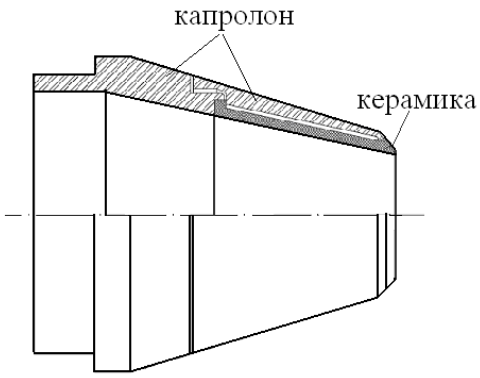

Conical nozzles with ceramic exit

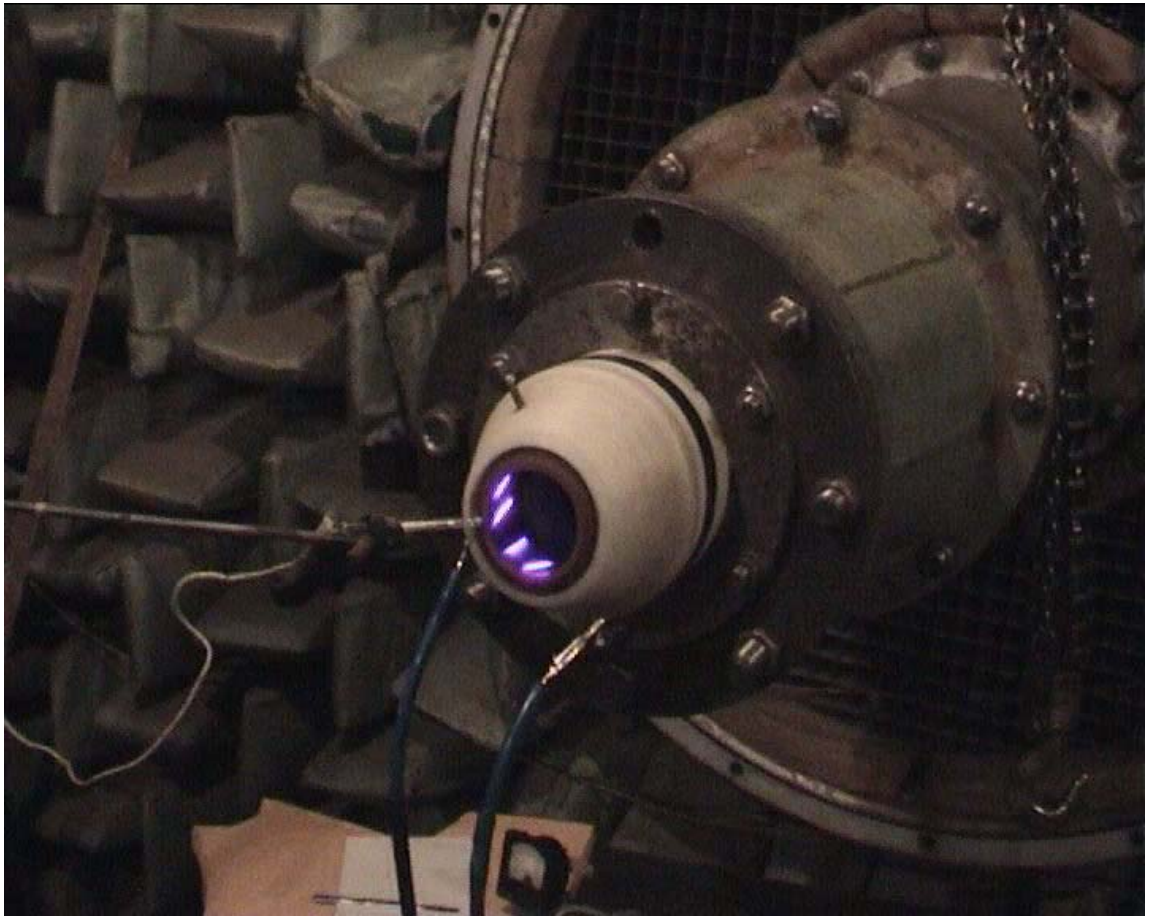

Conical nozzles with ceramic exit

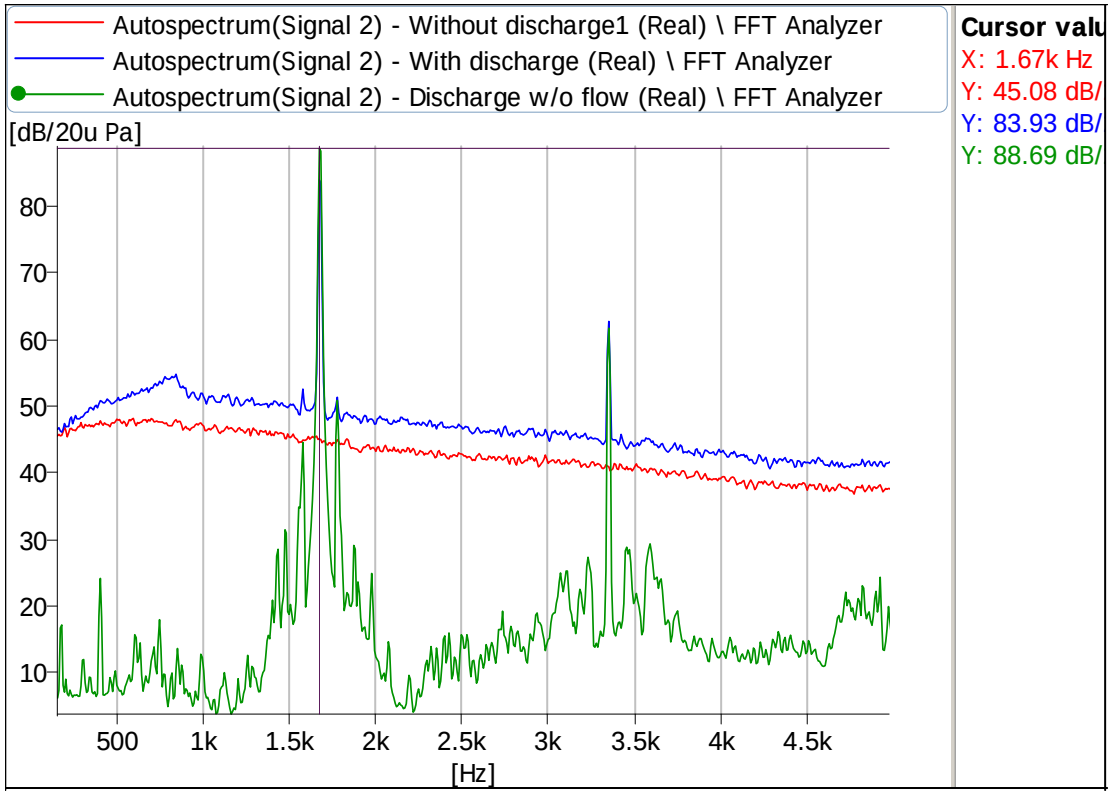

A conical nozzle with 6 electrodes; the jet velocity is 100 m/s. The red curve corresponds to the jet noise with the absence of the discharge; the blue curve corresponds to the jet noise with the discharge with the modulation frequency of 1668 Hz; the green curve corresponds to the discharge with the modulation frequency of 1668 Hz without the mean flow.

PIV measurements

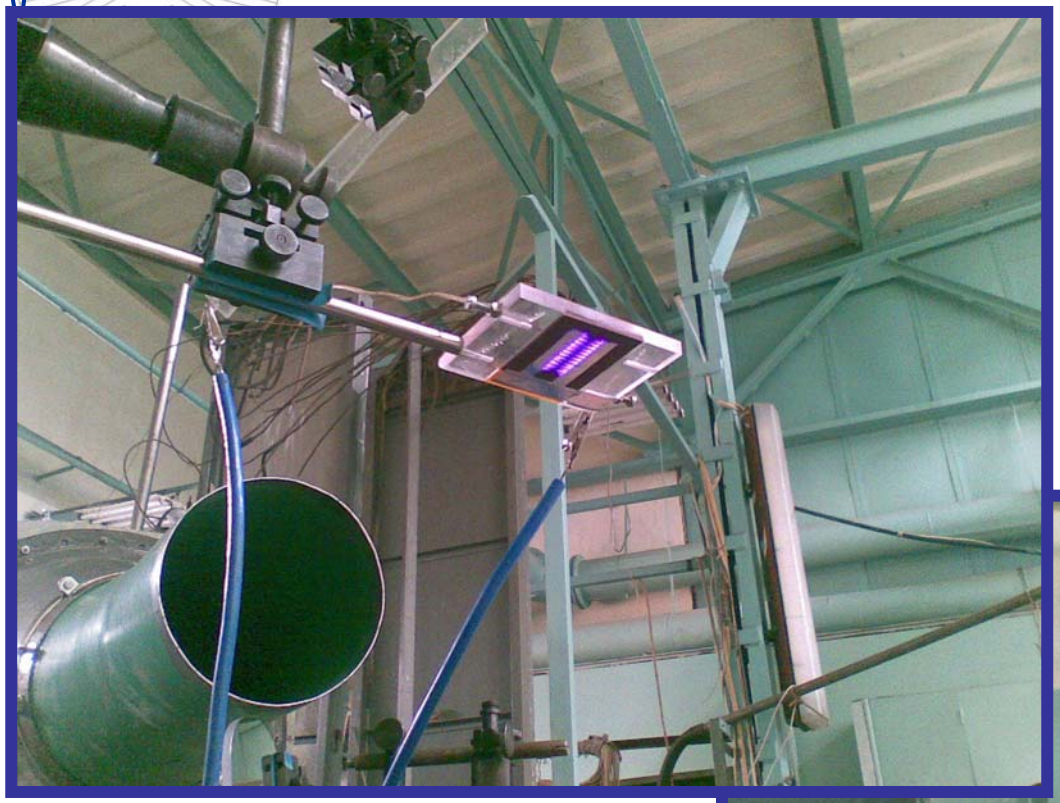

TsAGI

IVTAN

CIAM

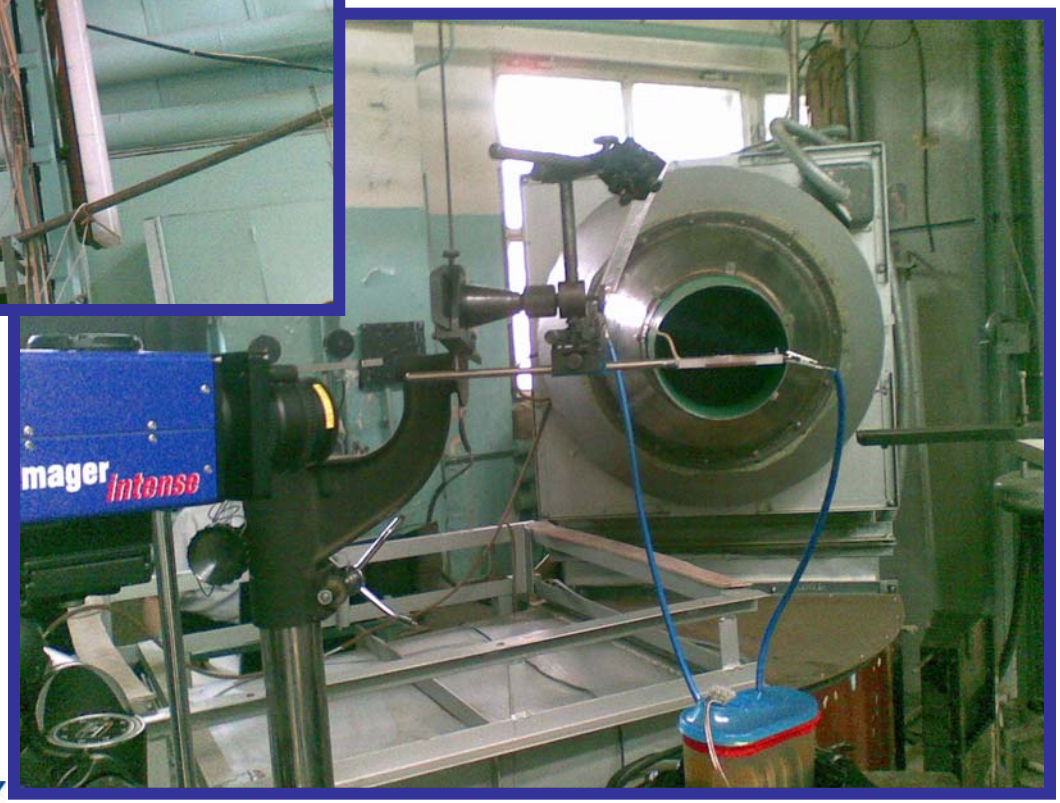

PIV measurements

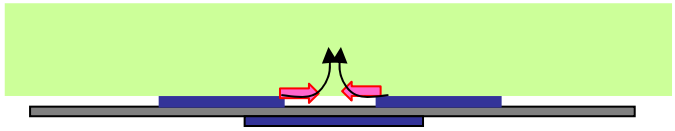

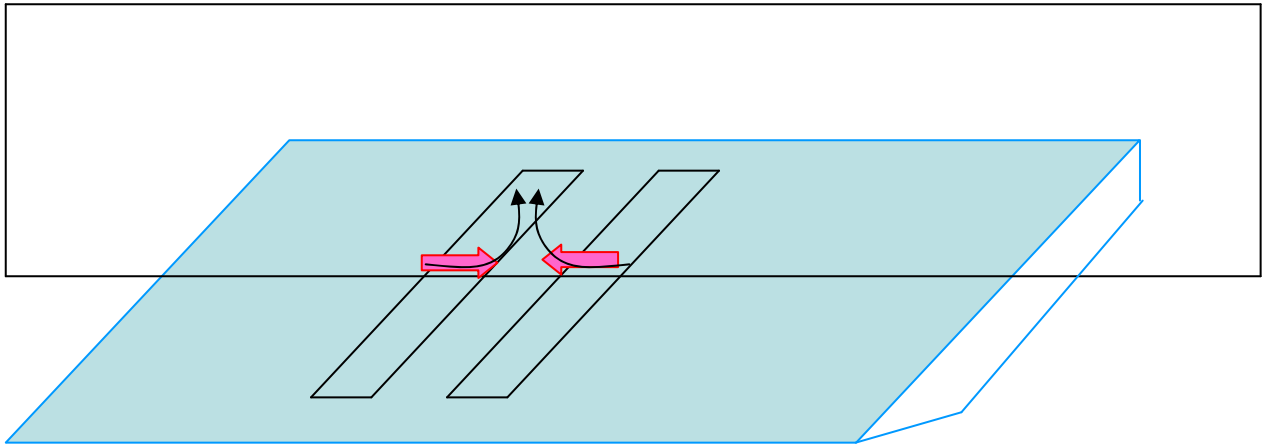

PIV measurements

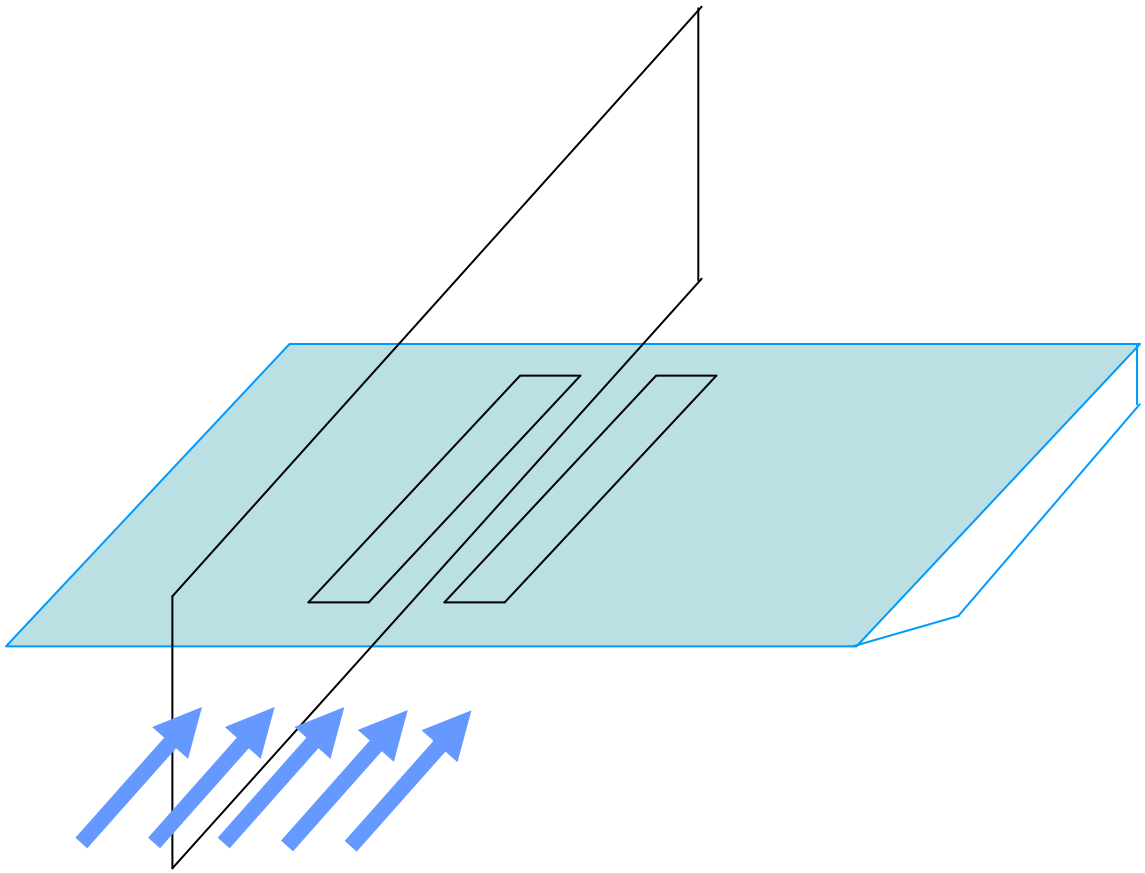

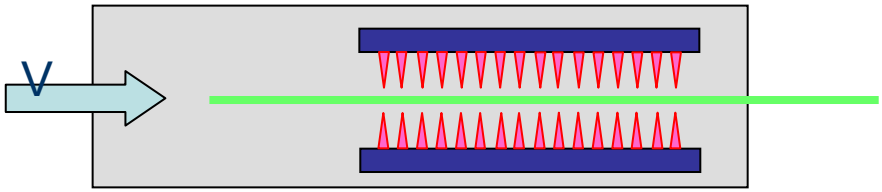

PIV measurements

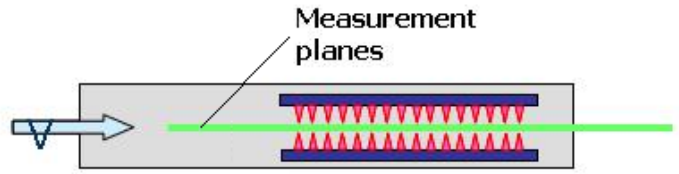

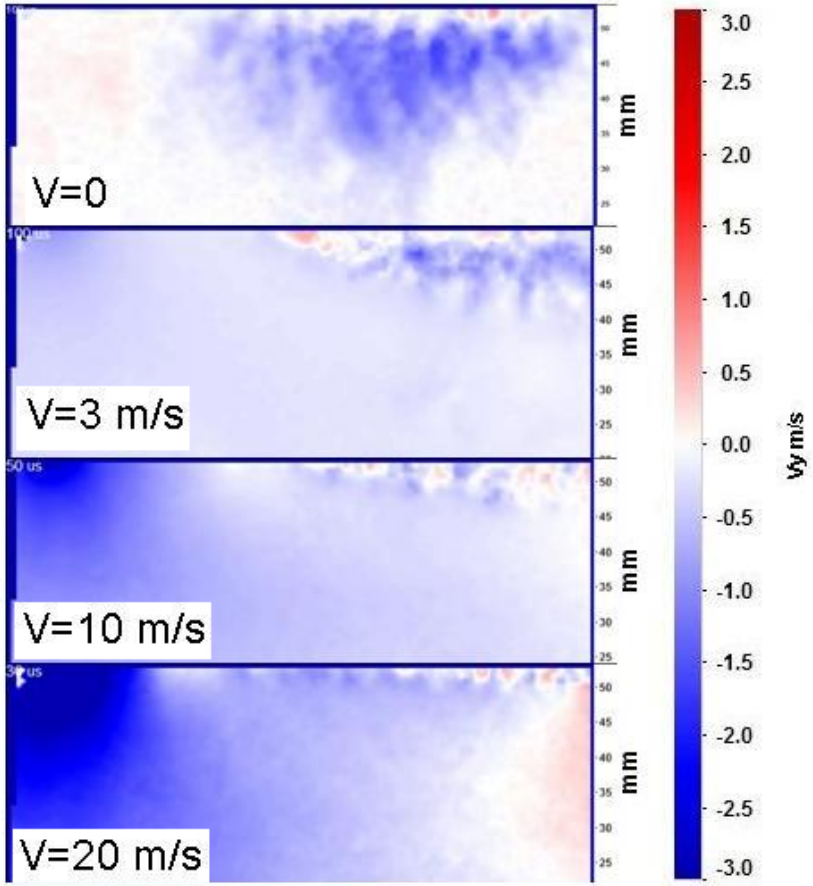

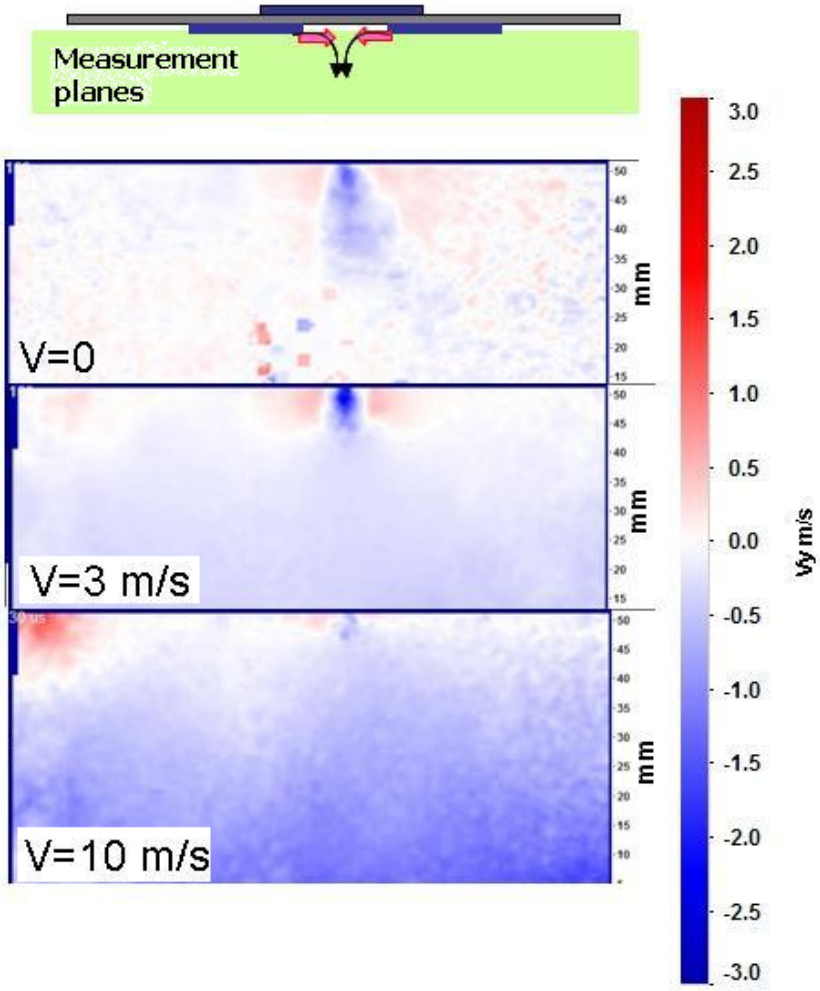

Acoustic excitation

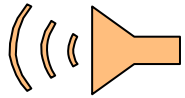

Plasma excitation

(nozzle with quartz cylinder exit)

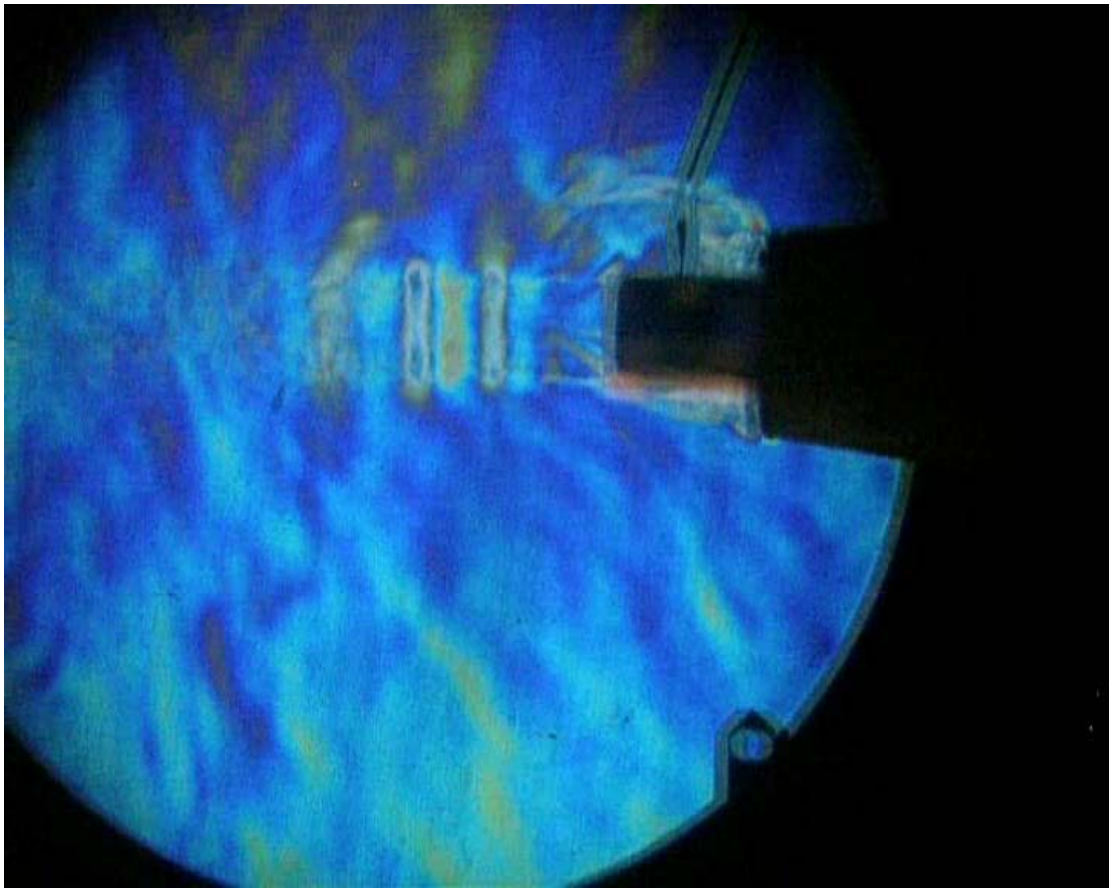

The confirmation of the acoustical nature of the effect was demonstrated by visualization of plasma excited jet and acoustic driver excited jet.

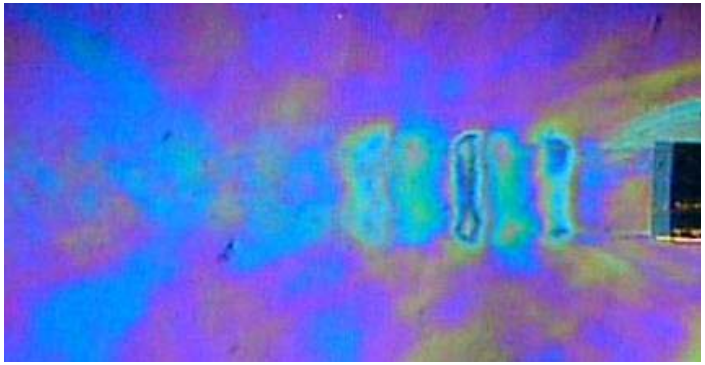

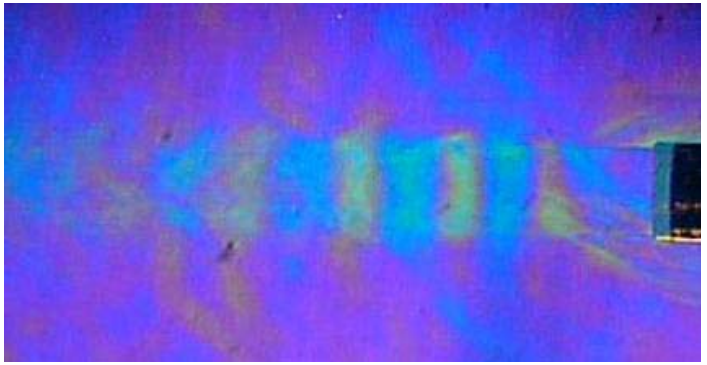

Tone excitation of the jet; a) plasma excitation, b) both plasma and loudspeaker excitation with close frequencies (beating) just before vortex ring disappearing.

The picture of the vortex rings is similar for these cases.

When the jet is excited both by loudspeaker and by plasma with identical frequencies it is easy to obtain the beating effect, when the picture of the vortex rings exist in one period of time and disappear in the other.

Noise control by high frequency excitation

V=100-200 m/s

f=6-12 kHz

D~5cm (conical)

d~5cm (cylindrical)

l=2-5 cm

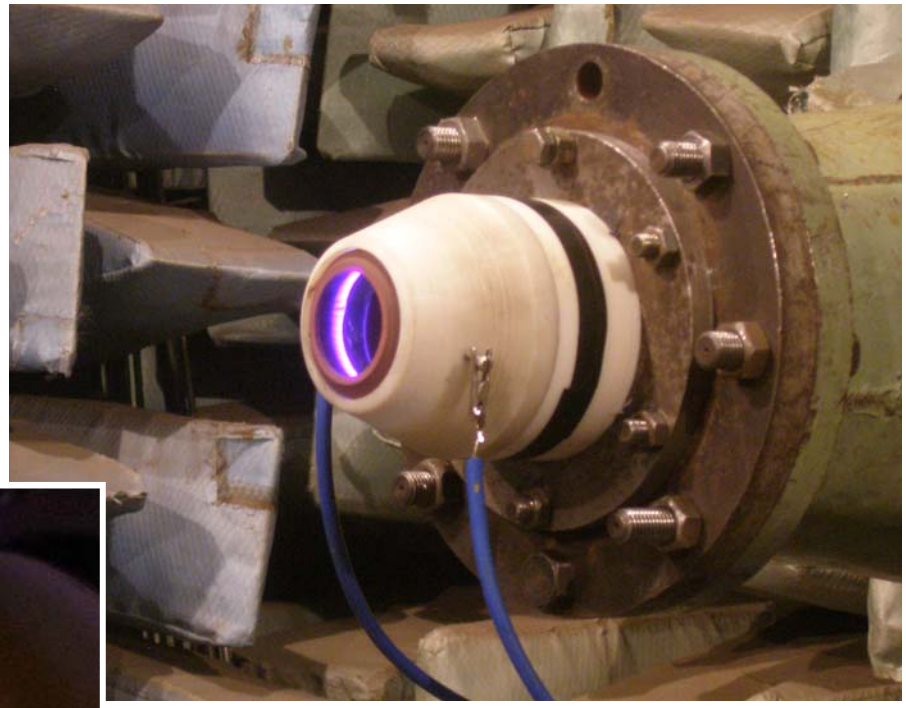

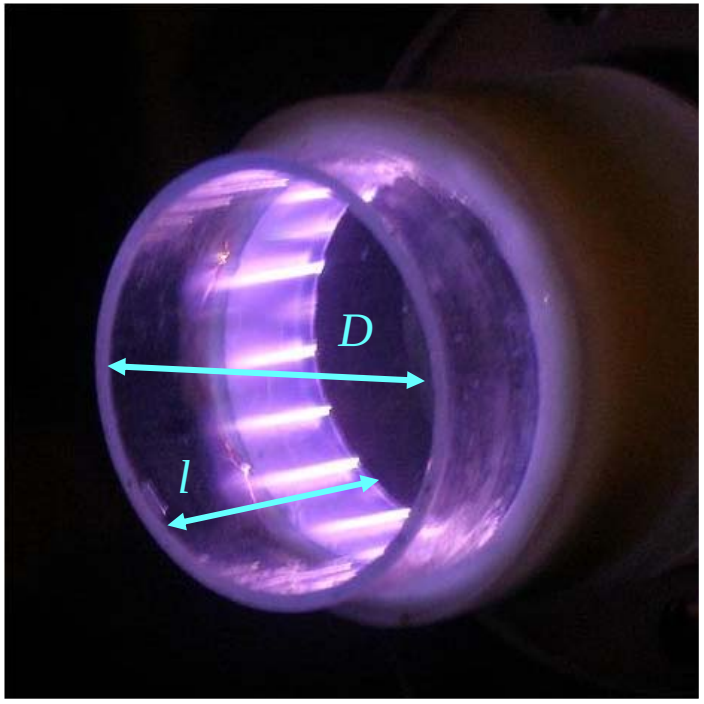

Broadband noise amplification

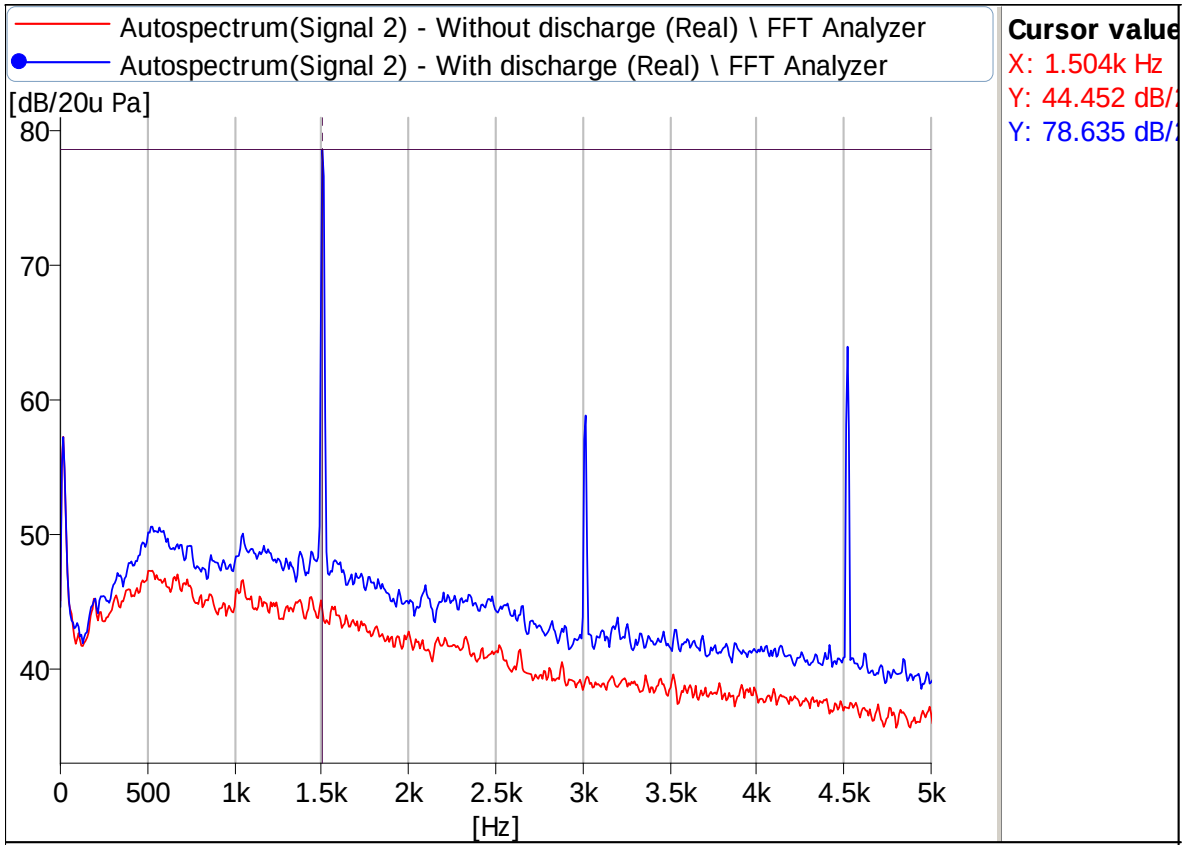

Cylindrical nozzle with 6 electrodes; jet velocity is 100 m/s. The red curve corresponds to the absence of the discharge; the blue curve corresponds to the discharge with the modulation frequency of 1500 Hz.

Noise control by high frequency excitation

V=150 m/s, 30^0

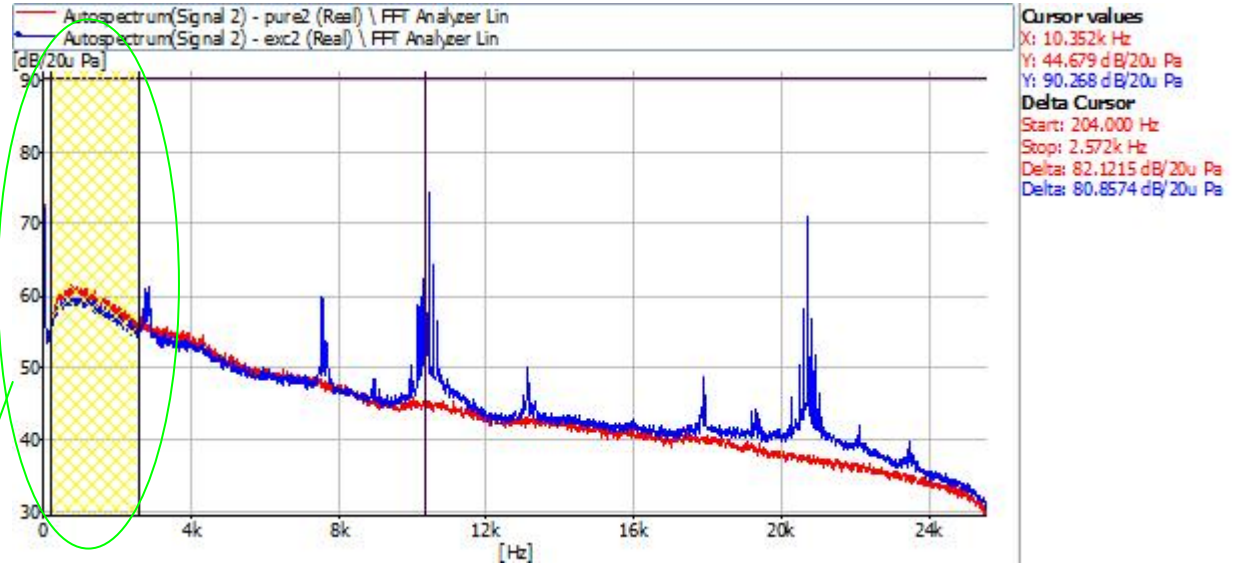

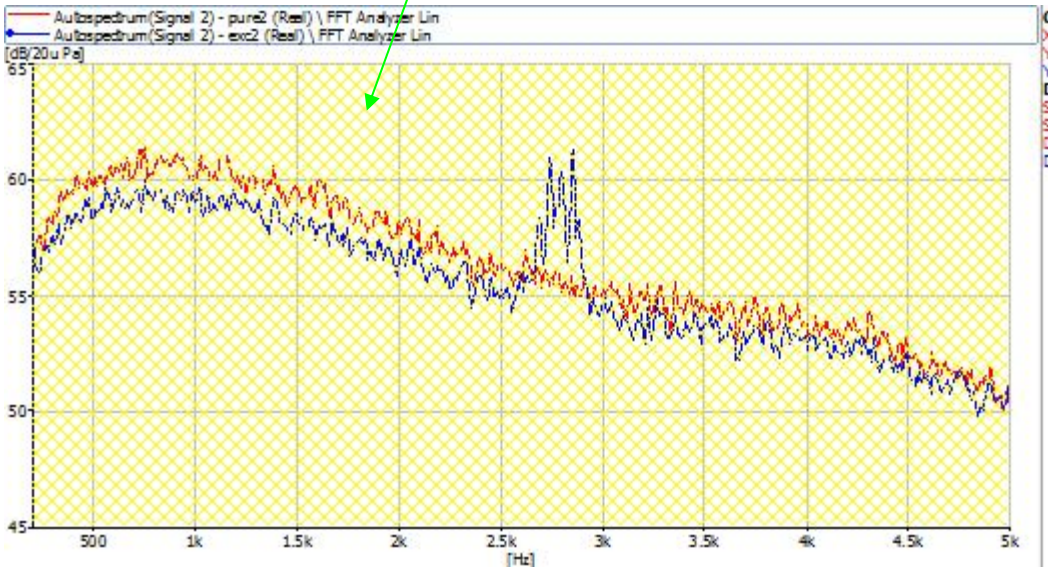

delta – 1.3 dB

Conical nozzle, V=150 м/с,
Excitation f =10.352 kHz (St=3.46),
Electrode location l=5 cm to nozzle exit,
Microphone at the angle 30° to jet axis at the distance L=2 m.

Noise control by high frequency excitation

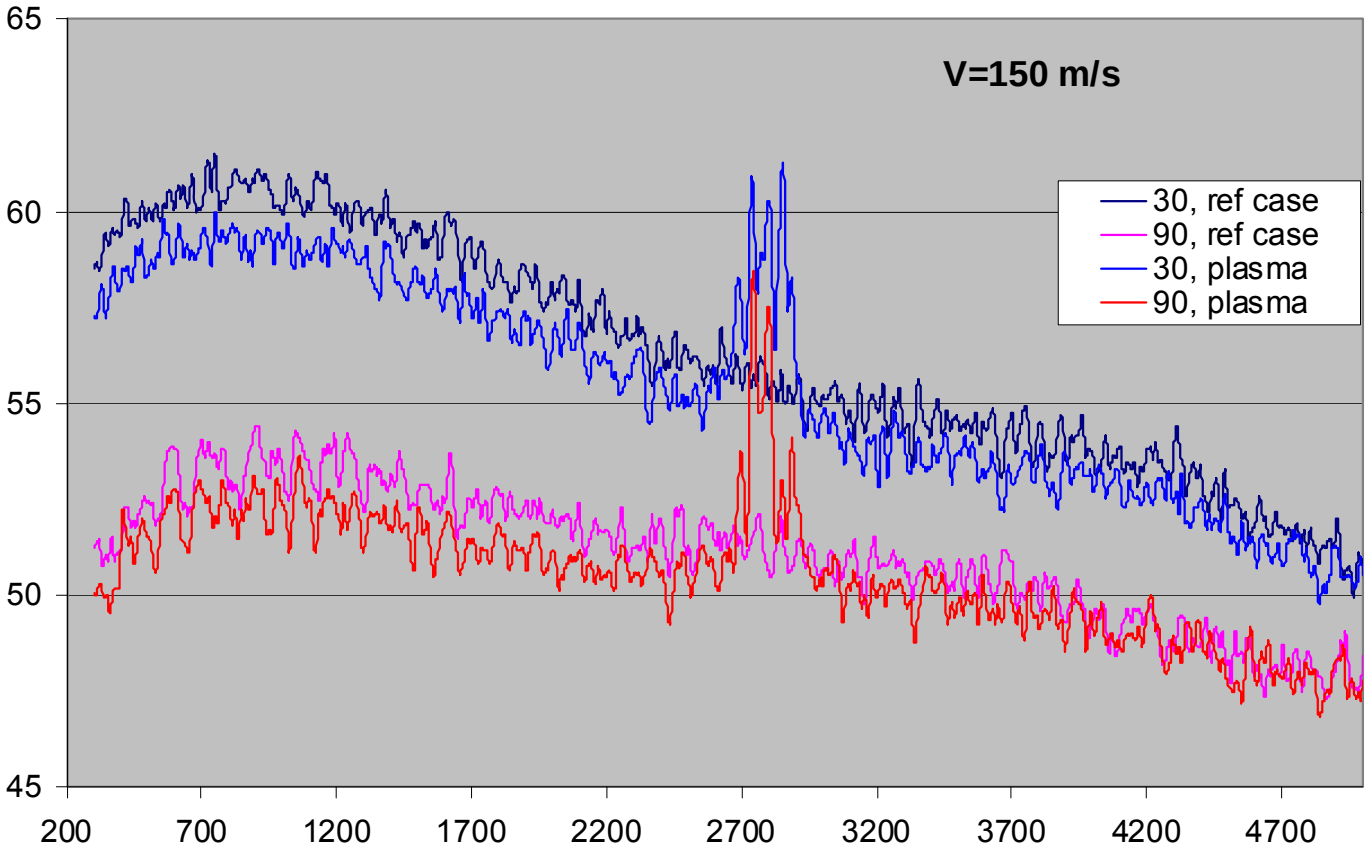

Noise control by high frequency excitation

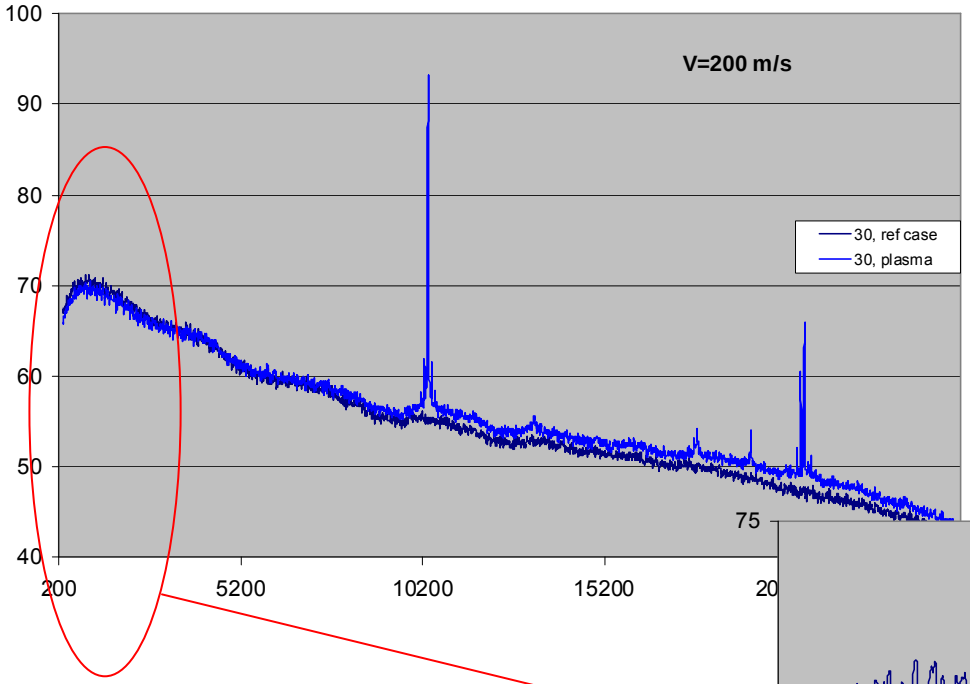

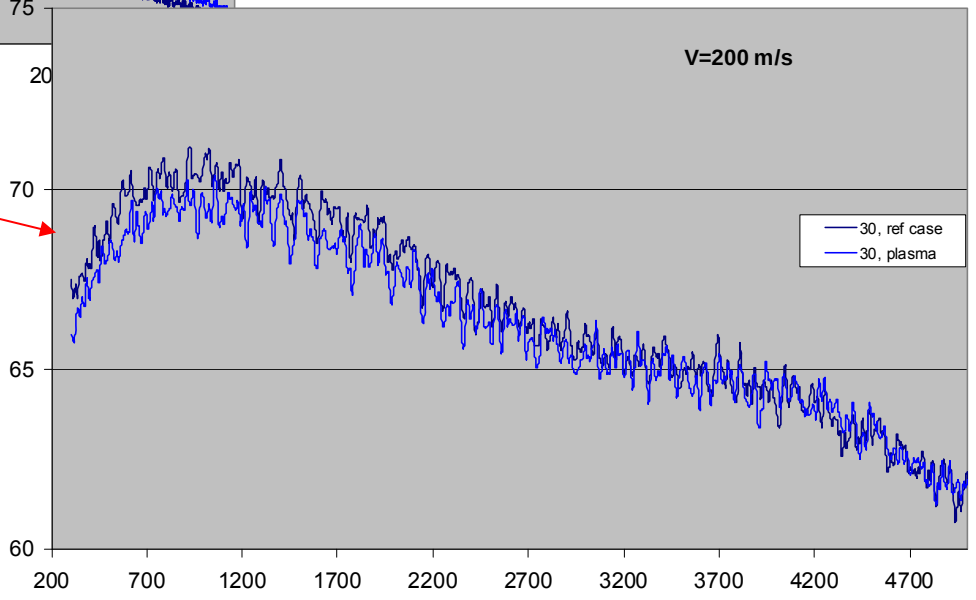

V=200 m/s, 30^0

Saturation character of the effect of noise suppression

High frequency control of jet noise
(Vlasov-Ginevsky effect)

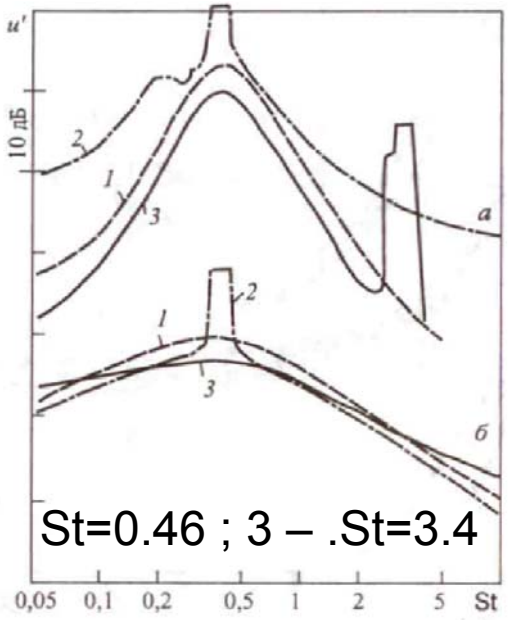

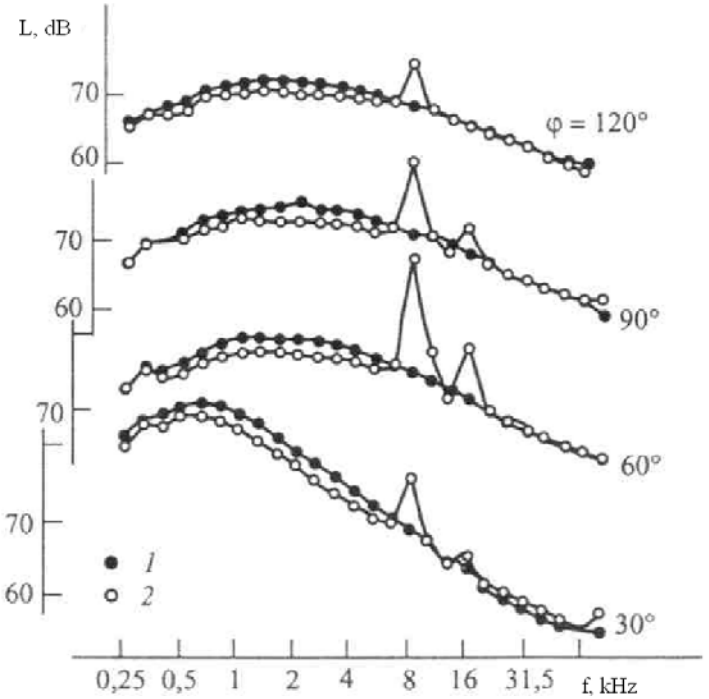

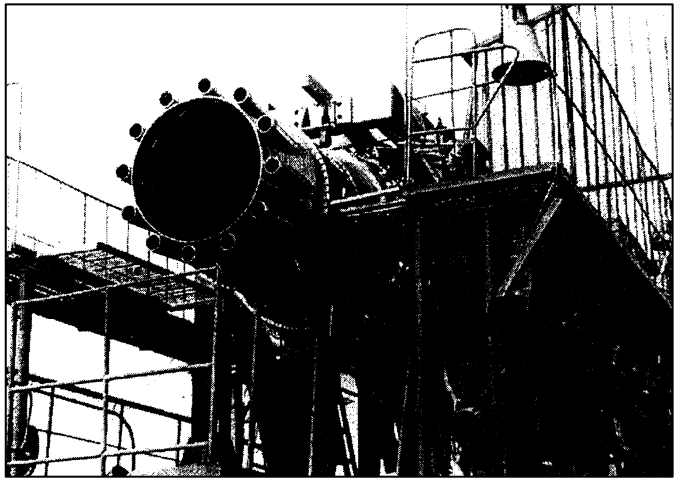

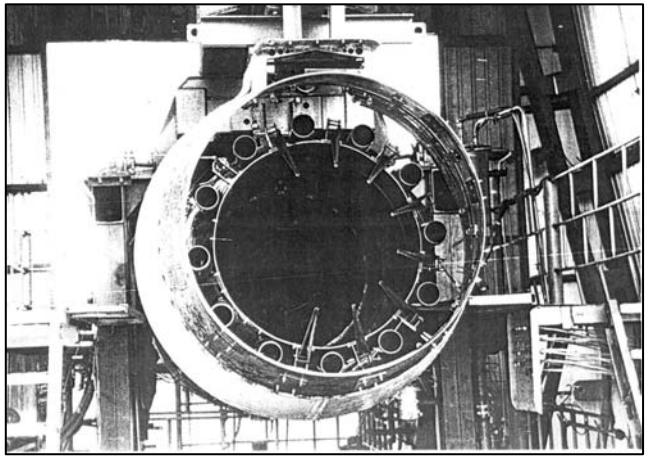

ЦАГИ & ONERA

Pproposed plasma actuator configurations can induce at the nozzle inner surface an electric wind with the speed up to 3-4 m/s in the direction normal to the nozzle surface.

The effectiveness of actuator decreases if there is a mean flow along the electrode edge

The effect of HF DBD actuator on the jet for the used configuration is related with the acoustic radiation of the discharge and is in many ways similar to the Ginevsky-Vlasov effect:

The jet excitation at St~0.5 results in the broadband amplification of jet noise.

High frequency plasma excitation (St~2-3) leads to low frequency band noise suppression;

However, high frequency broadband extra penalty would be higher the low frequency noise reduction.

AMCT (Azimuthal Mode Coupling Technique)

Experiments on jet noise reduction by corrugated nozzles

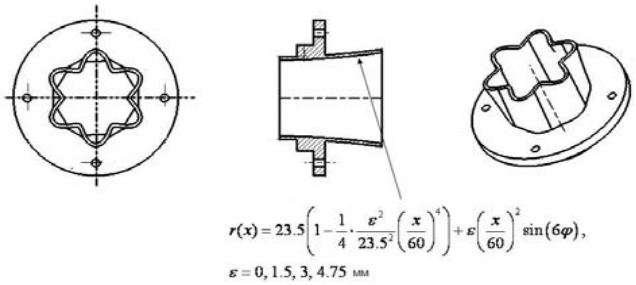

$$r(x) = 23.5\left(1 - \frac{1}{4}\cdot\frac{\varepsilon^2}{23.5^2}\left(\frac{x}{60}\right)^4\right) + \varepsilon\left(\frac{x}{60}\right)^2 \sin(6\varphi),$$

$\varepsilon = 0, 1.5, 3, 4.75$ мм

Experimental conditions:

Cold jet, *V*=240 *m/s,* Venturi tube for measuring flow rate

Microphones Bruel&Kjaer type 4189C

R= 2m, 90, 60 deg.

Noise power density spectra, 60 deg.

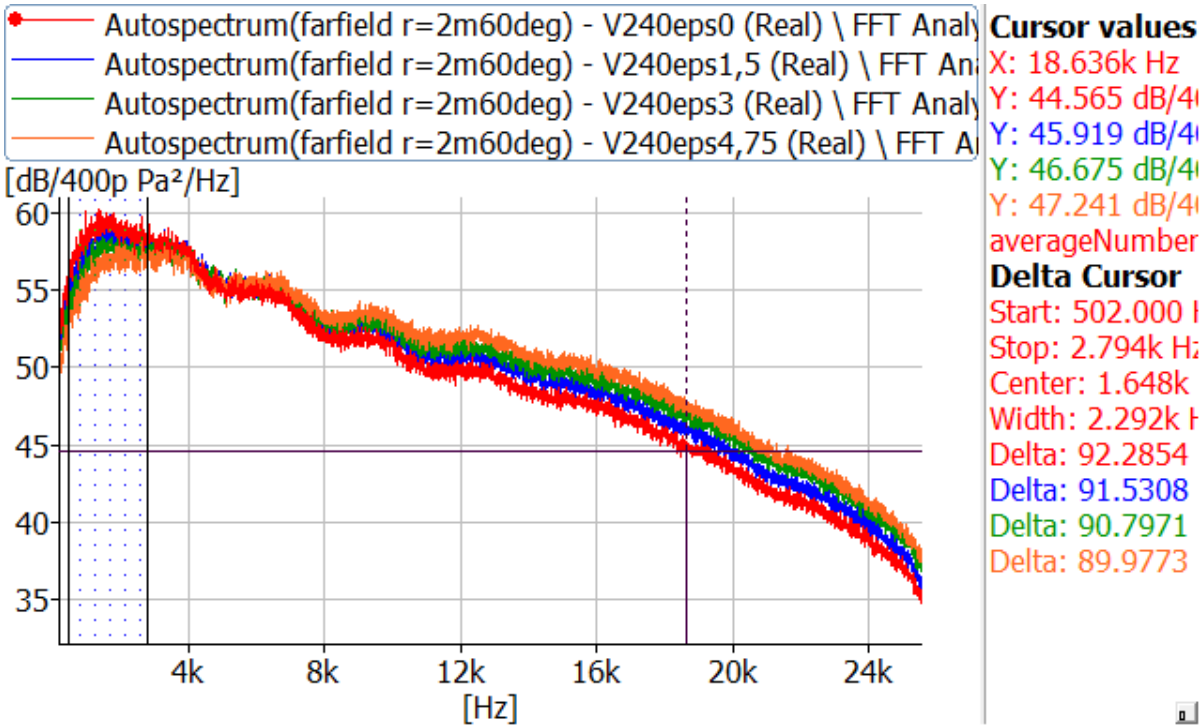

It is shown that the increase in corrugation amplitude (the area of the nozzle cross sections being fixed) leads to remarkable decrease in the far field noise levels around the spectral peak (0,1<St<0,7) and weak increase at high frequencies.

The total noise attenuation (in the band 0,16–25,6 kHz) was measured to be 2.3dB

Modification of jet mean flow for instability wave coupling

1st stage – corrugated nozzle

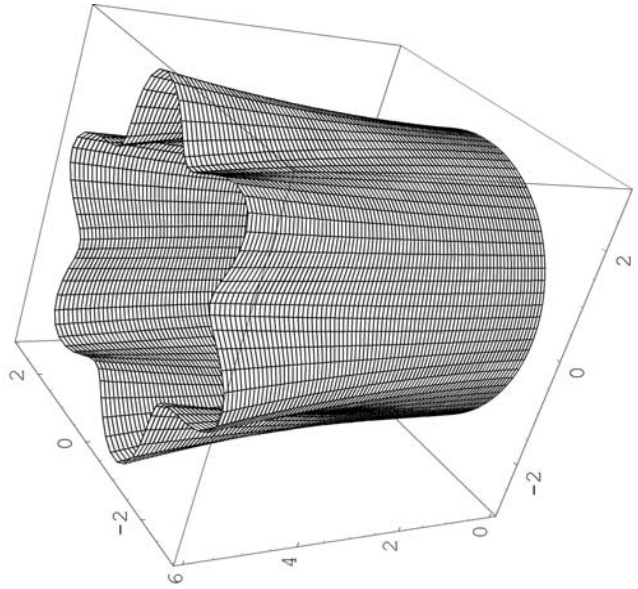

2nd stage – steady plasma

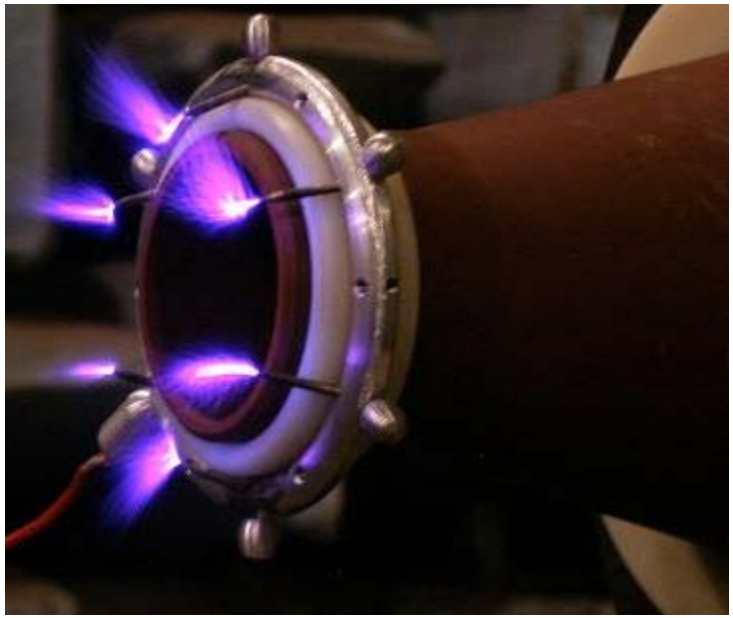

Quasistationary plasma actuator based on HF DBD

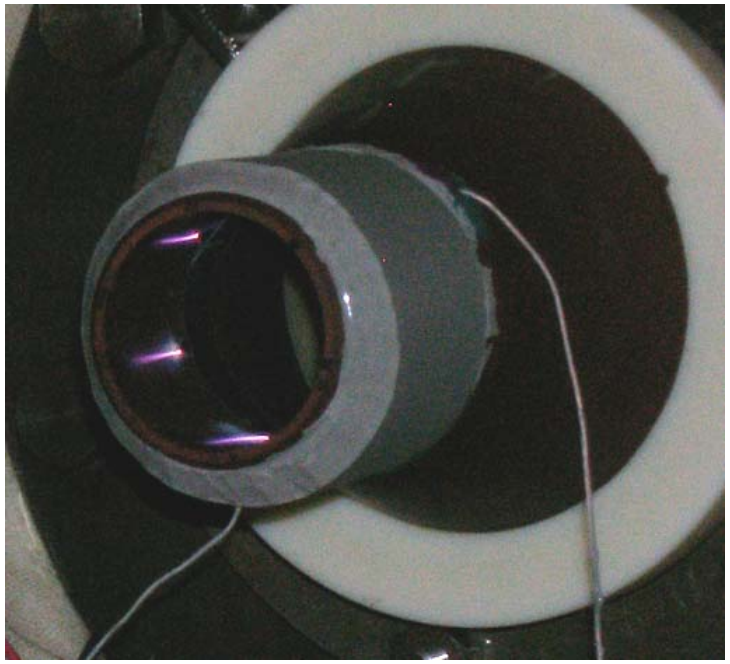

Discharge parameters:

High voltage	16 kV
Oscillation frequency	160 kHz
Modulation frequency	without modulation
Power	about 1kWt

Noise spectra of jet (100m/s)

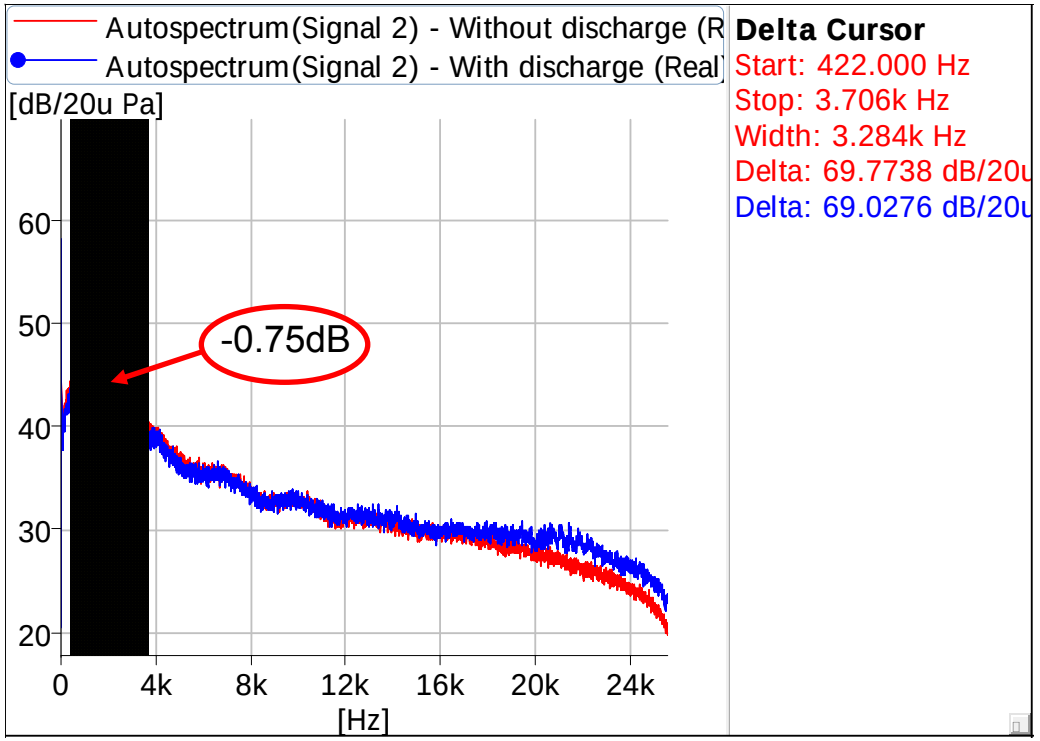

Red curve – actuator off
Blue curve – actuator on

Direct Instability Wave Control

ORINOCO project

Statement: For high speed jets the mechanism of noise generation is related to a considerable degree with ***Kelvin-Helmholtz instability waves*** evolving downstream from the nozzle edge

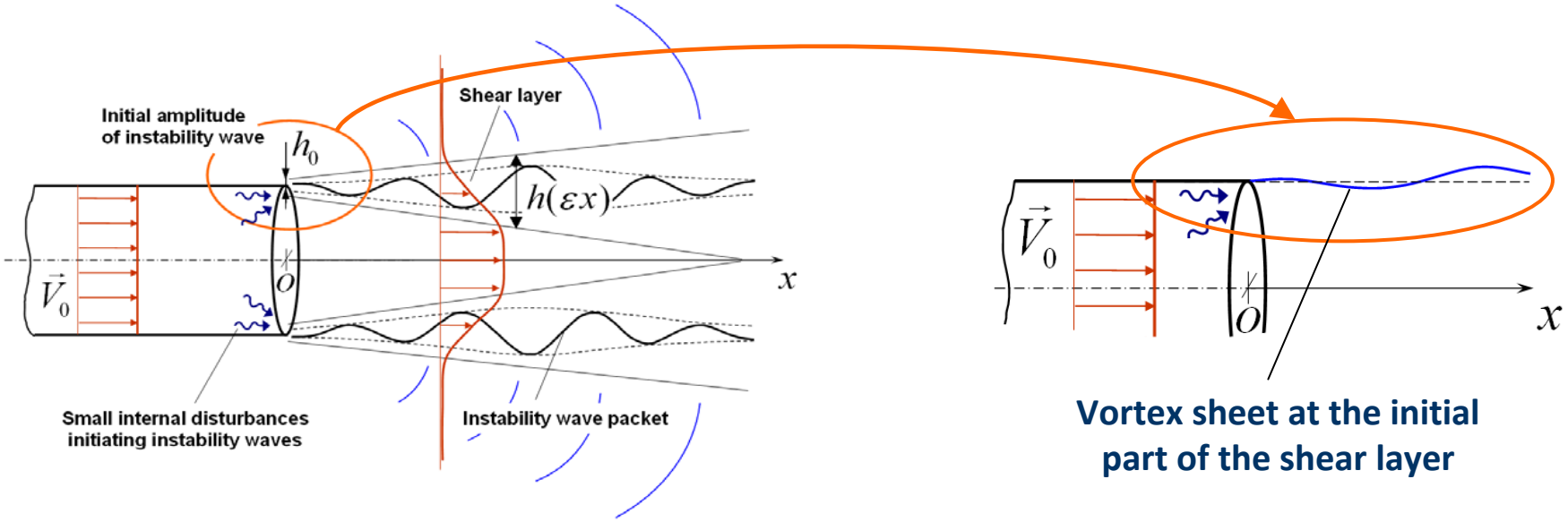

Re ~ 10^5... 10^6

Instability waves – suitable objects for active control

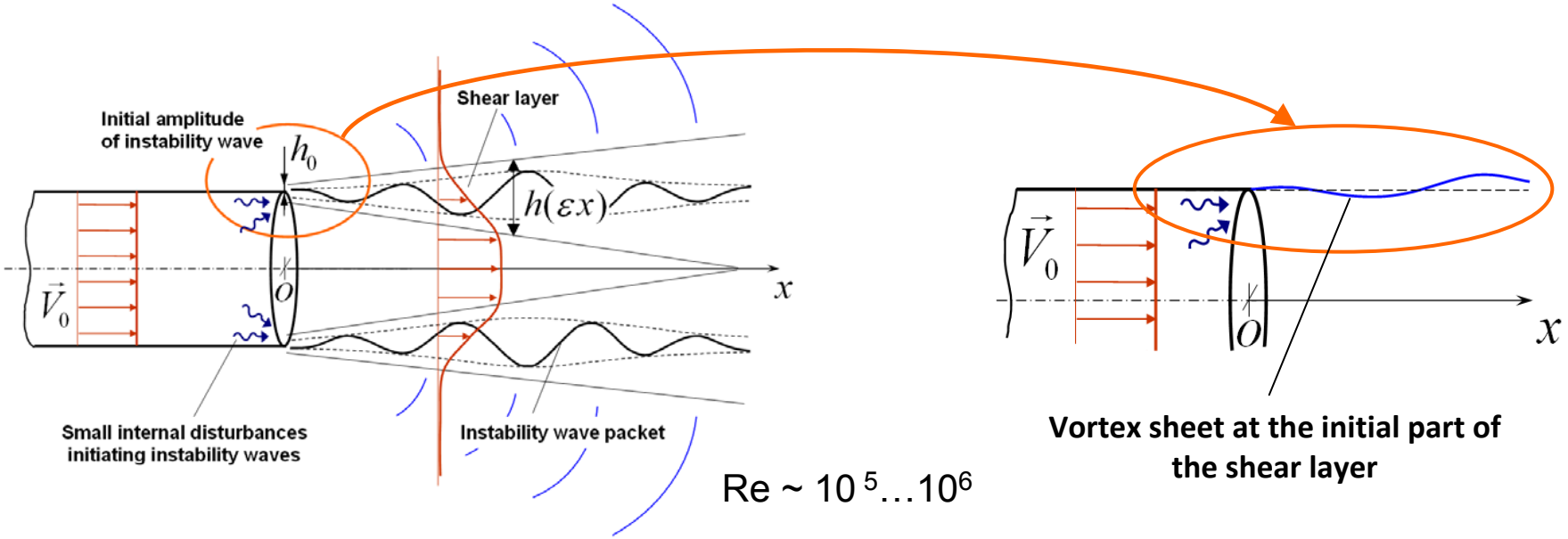

$\mathrm{Re} \sim 10^5 \ldots 10^6$

Sedel'nikov T.K. The frequency spectrum of the noise of a supersonic jet // Phys. Aero. Noise Moscow: Nauka. 1967. (Trans. 1969. NASA TTF-538. P.71-75.)

Tam C.K.W., Burton D.E. Sound generated by instability waves of supersonic flows // J. Fluid Mech. 1984. V.138. P.249-295.

Crighton D.G., Huerre P. Shear-layer pressure fluctuations and superdirective acoustic sources // J. Fluid Mech. 1990. V.220. P.355-368.

Suzuki, T., Colonius, T., "Instability waves in a subsonic round jet detected using a near-field phased icrophone array," J. Fluid Mech., 2006, Vol. 565, pp. 197-226.

Zaitsev M.Yu., Kopiev V.F., Chernyshev S.A. Experimental investigation of the role of instability waves in noise radiation by supersonic jets // Fluid Dynamics. 2009. V.44, N.4, P.587-595.

Morris P.J. The instability of high speed jets // Int. J. Aeroacoustics. 2010. V.9. N.1-2. P.1-50.

Plane wave incidence on the trailing edge

Wiener-Hopf technique

Kutta-Zhukovsky condition

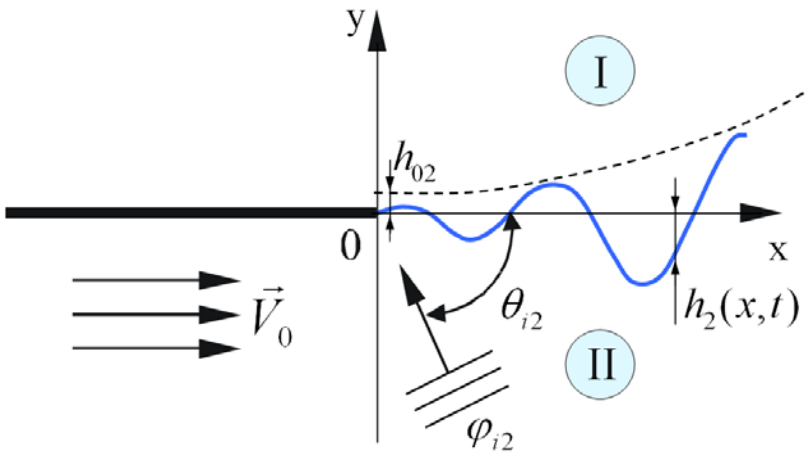

Full solution contains the incident wave and diffraction field that along with instability wave satisfy the Kutta condition near the edge. Therefore the instability wave initial amplitude is determined by the incident wave properties only.

Governing Eqs for 2D problem

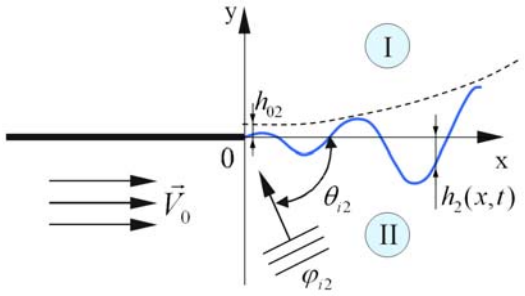

$$\begin{cases} \Delta\varphi_I + k^2\varphi_I = 0, & y > 0 \\ \Delta\varphi_{II} - \left(-ik + M\dfrac{\partial}{\partial x}\right)^2 \varphi_{II} = 0, & y < 0 \end{cases}$$

$$\varphi \sim exp\left(i\alpha x - ikct\right)$$

$$\varphi \sim exp\left(-\gamma y\right)$$

$$\varphi \sim exp\left(\beta y\right)$$

$$\gamma = \sqrt{\alpha^2 - k^2}$$

$$\beta = \sqrt{\left(\alpha(1+M)+k\right)\left(\alpha(1-M)-k\right)}$$

$$\Phi(\alpha, y, k) = \int_{-\infty}^{+\infty} \varphi(x, y, k)\exp(i\alpha x)dx$$

$$\varphi(x, y, t) = A \cdot e^{-ikct} \int_C \Phi(\alpha, y, k) e^{-i\alpha x} d\alpha$$

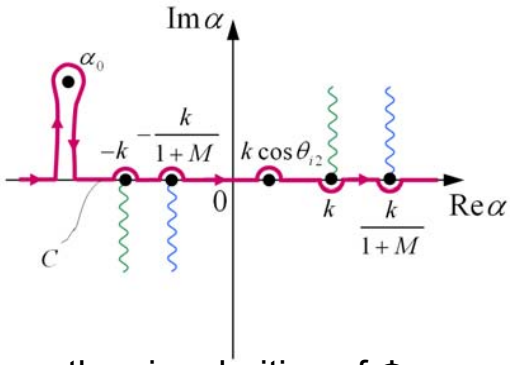

$$\Delta\left(k, \alpha\right) \equiv k^2\beta + (k + M\alpha)^2\gamma = 0$$ ← Roots of this Eq. are the singularities of Φ

Governing Eqs for 2D problem

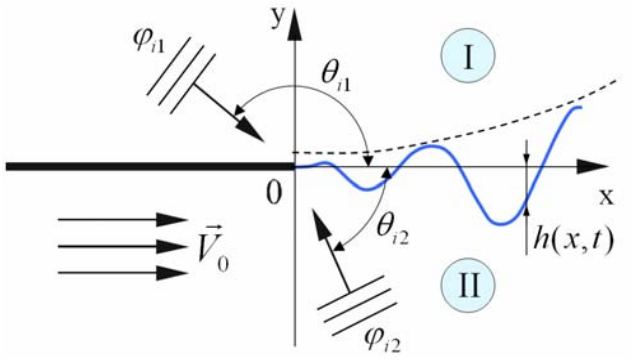

Internal disturbance

$$\varphi_{i2} = B\exp\left(-ikct - i\frac{k\cos\theta_{i2}}{1-M\cos\theta_{i2}}x + i\frac{k\sin\theta_{i2}}{1-M\cos\theta_{i2}}y\right)$$

Control action

$$\varphi_{i1} = A\exp\left(-ikct - ik\cos\theta_{i1}x - ik\sin\theta_{i1}y\right)$$

We require the instability waves to suppress each other

$$h(x,t) = h_1(x,t) + h_2(x,t) = 0$$

integration over the entire path
along the axis $Re\,\alpha$

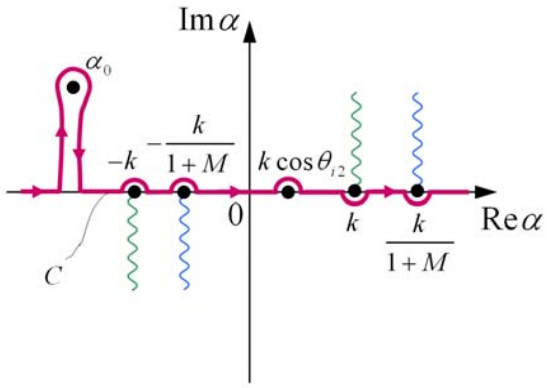

$$p_{inner}(\vec{r},t) = B \cdot e^{-i\omega t} \int_C f_{inner}(\alpha, y) e^{-i\alpha x} d\alpha$$

loop around the root α_0
(residual input)

shear layer

Jet

$$p_{inner}(\vec{r},t) = B \cdot e^{-i\omega t} \int_{-\infty}^{+\infty} f_{inner}(\alpha, y) e^{-i\alpha x} d\alpha$$

Acoustic part

$$p_{inner}(\vec{r},t) = B \cdot e^{-i\omega t} \int_{C} f_{inner}(\alpha, y) e^{-i\alpha x} d\alpha$$

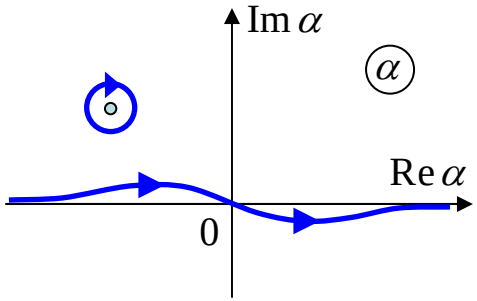

$$p_{iw2}(\vec{r},t) = B \cdot \hat{f}_{inner} e^{-i\omega t - i\alpha_0 x - \gamma_0 y}$$

Hydrodynamic part

shear layer

Jet

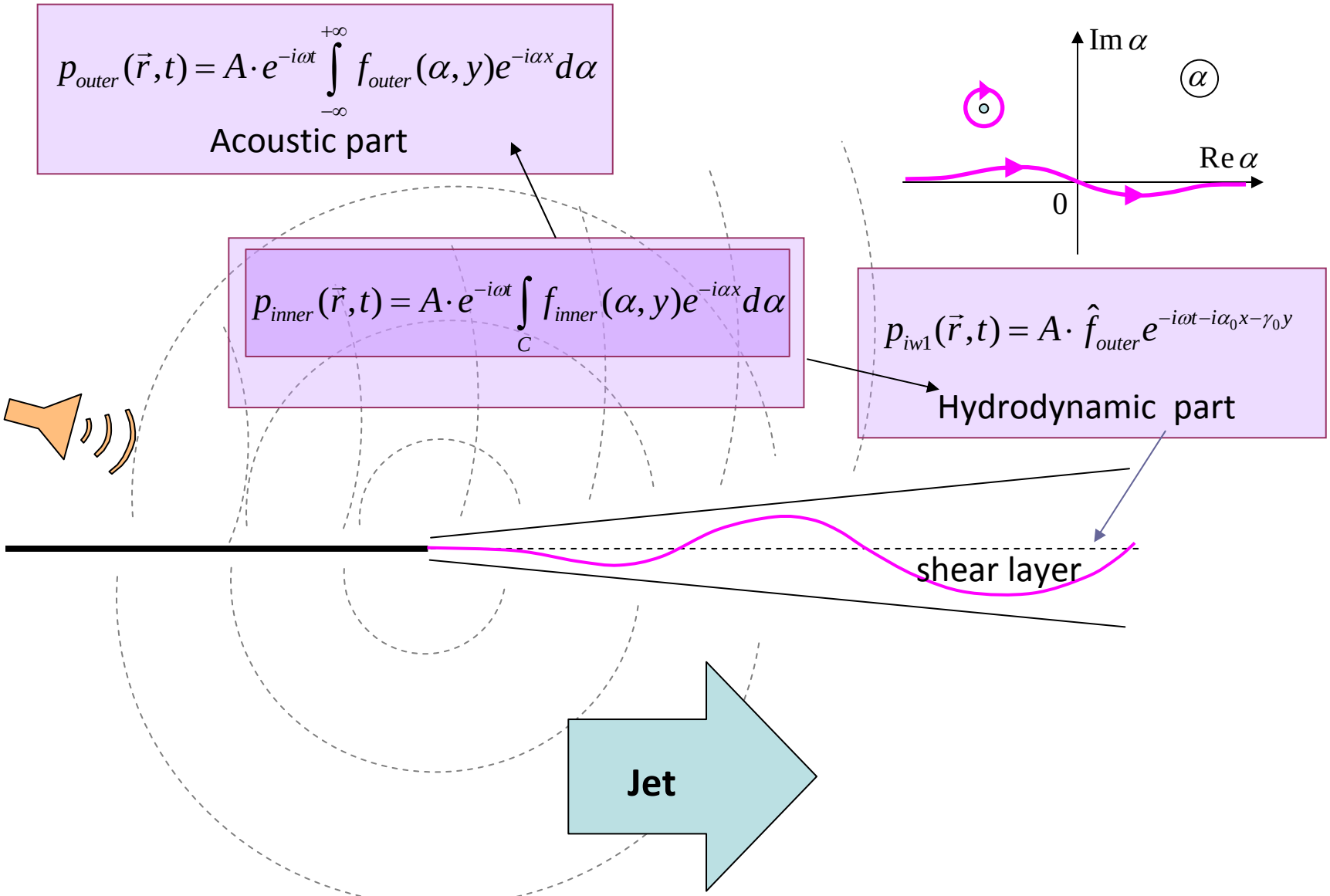
$p_{outer}(\vec{r},t) = A \cdot e^{-i\omega t} \int_{-\infty}^{+\infty} f_{outer}(\alpha, y) e^{-i\alpha x} d\alpha$
Acoustic part
$p_{inner}(\vec{r},t) = A \cdot e^{-i\omega t} \int_{C} f_{inner}(\alpha, y) e^{-i\alpha x} d\alpha$
$p_{iw1}(\vec{r},t) = A \cdot \hat{f}_{outer} e^{-i\omega t - i\alpha_0 x - \gamma_0 y}$
Hydrodynamic part
Im α
α
Re α
0
shear layer
Jet

$$p(\vec{r},t) = e^{-i\omega t}\int_{-\infty}^{+\infty}\left(A\cdot f_{outer}(\alpha,y) + B\cdot f_{inner}(\alpha,y)\right)e^{-i\alpha x}d\alpha$$

Acoustic part

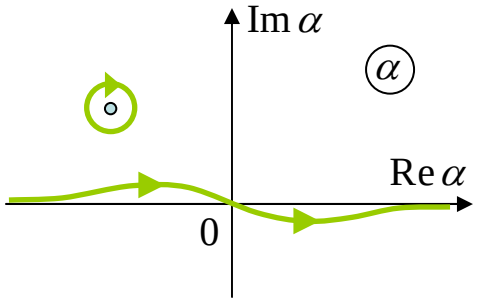

$$p_{iw}(\vec{r},t) = \left(A\cdot \hat{f}_{outer} + B\cdot \hat{f}_{inner}\right)e^{-i\omega t - i\alpha_0 x - \gamma_0 y}$$

Hydrodynamic part

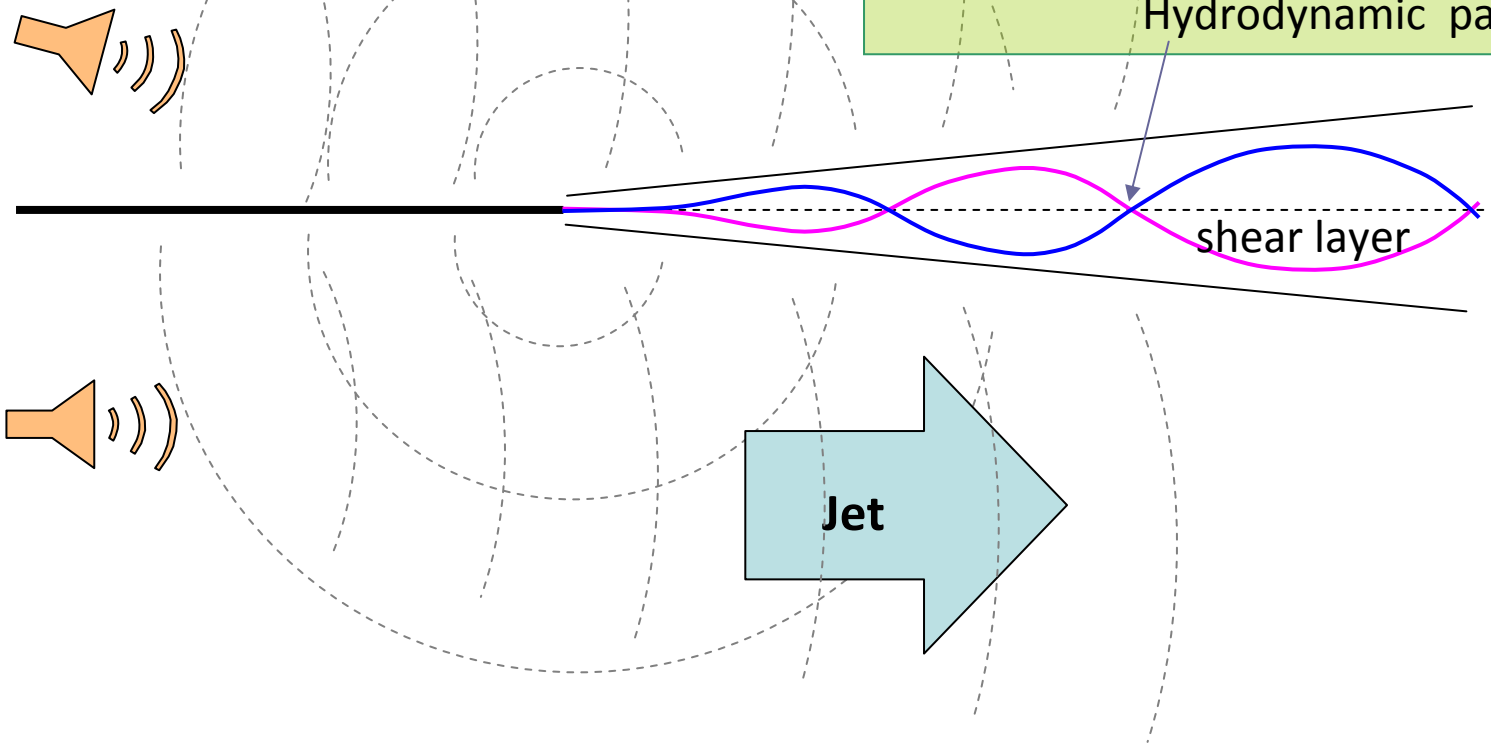

$$p(\vec{r},t) = e^{-i\omega t}\int_{-\infty}^{+\infty}\left(A\cdot f_{outer}(\alpha,y) + B\cdot f_{inner}(\alpha,y)\right)e^{-i\alpha x}d\alpha$$

Acoustic part ≠ 0

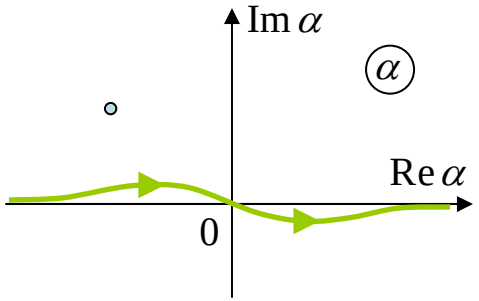

$$p_{iw}(\vec{r},t) = 0, \quad A = -B\cdot \hat{f}_{inner} / \hat{f}_{outer}$$

Hydrodynamic part = 0

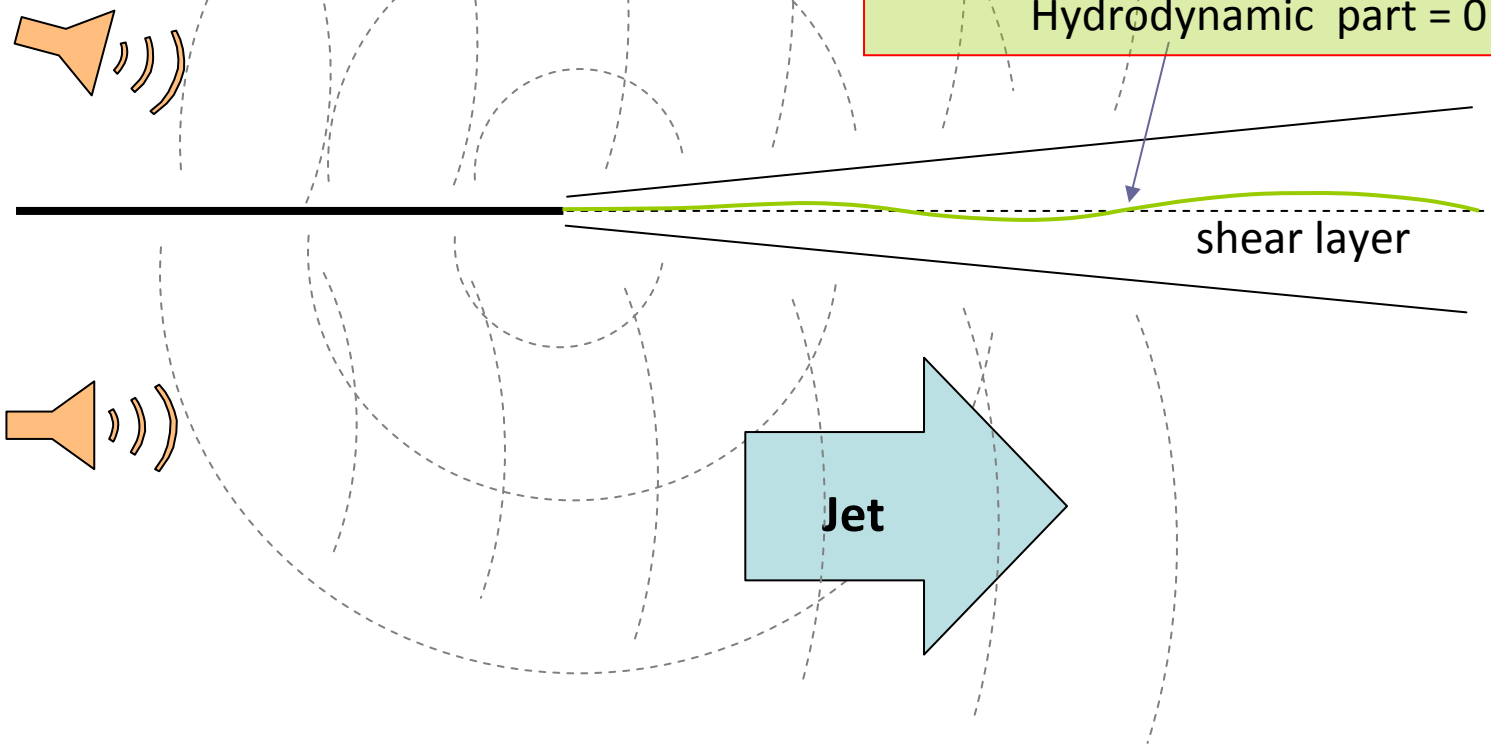

Theory for the axisymmetric jet (3D)

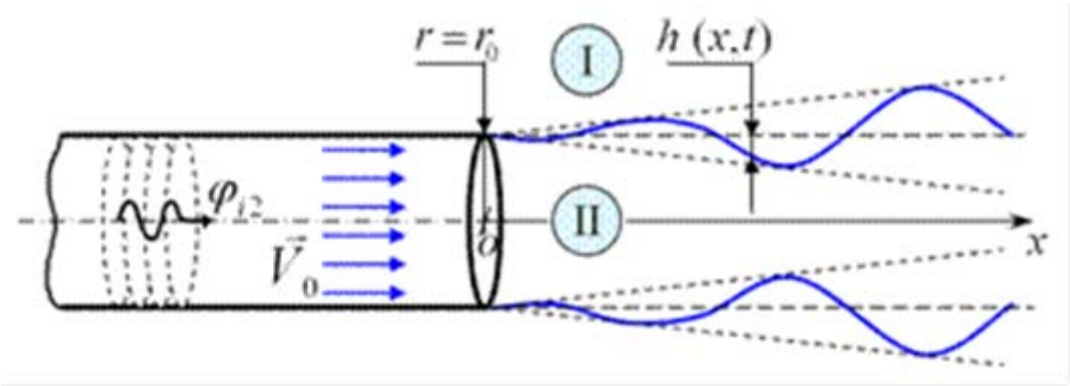

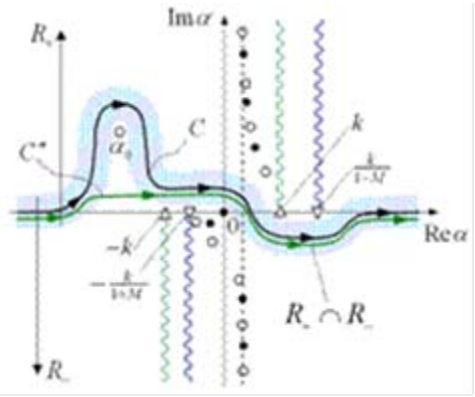

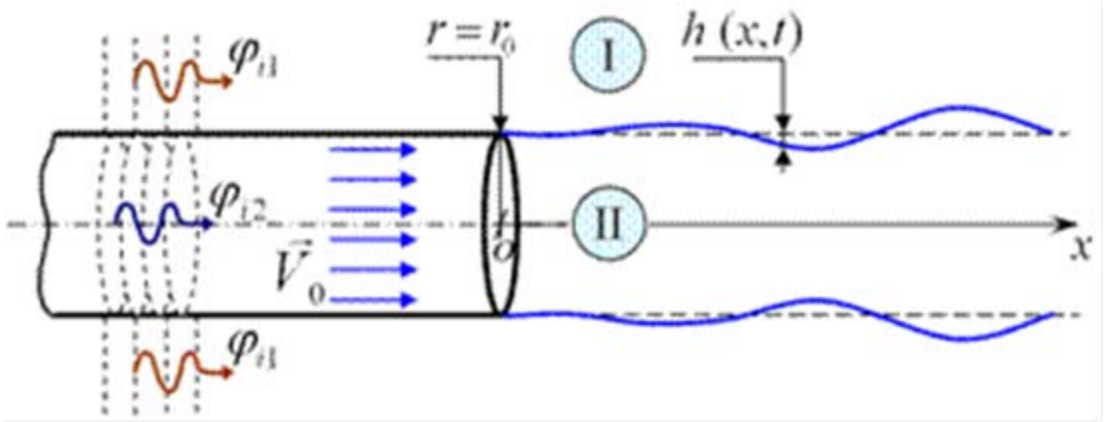

Theory for the axisymmetric jet (3D)

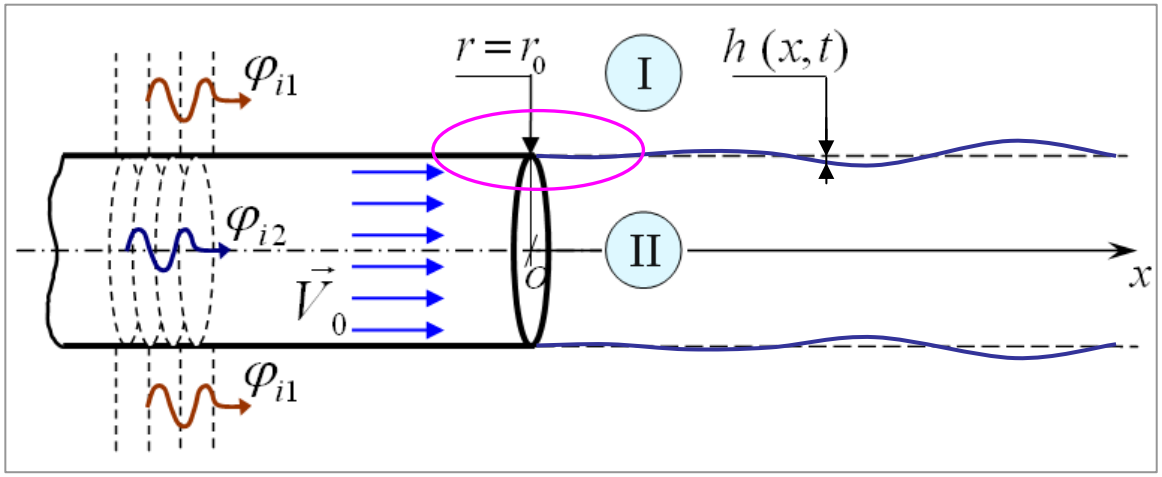

Internal disturbance

$$\varphi_{i2} = B\exp\left(-ikct + i\frac{k}{1+M}x\right)$$

Control action

$$\varphi_{i1} = A\exp\left(-ikct + kx\right)$$

We require the instability waves to suppress each other

$$h(x,t) = h_1(x,t) + h_2(x,t) = 0$$

Relation between the control action and internal disturbance parameters

$$A = \frac{icH_-(-k)(\alpha_0 + k)}{k\lim\limits_{\alpha\to\alpha_0}\frac{\alpha-\alpha_0}{H_+(\alpha)}}\cdot h_{02} = \frac{1}{1+M}\frac{H_-(-k)}{H_-(-\frac{k}{1+M})}\frac{\alpha_0 + k}{\alpha_0 + \frac{k}{1+M}}\cdot B$$

Measurement setup: one excitation and two excitations

Control of artificially excited jet

Sketch of the experiment

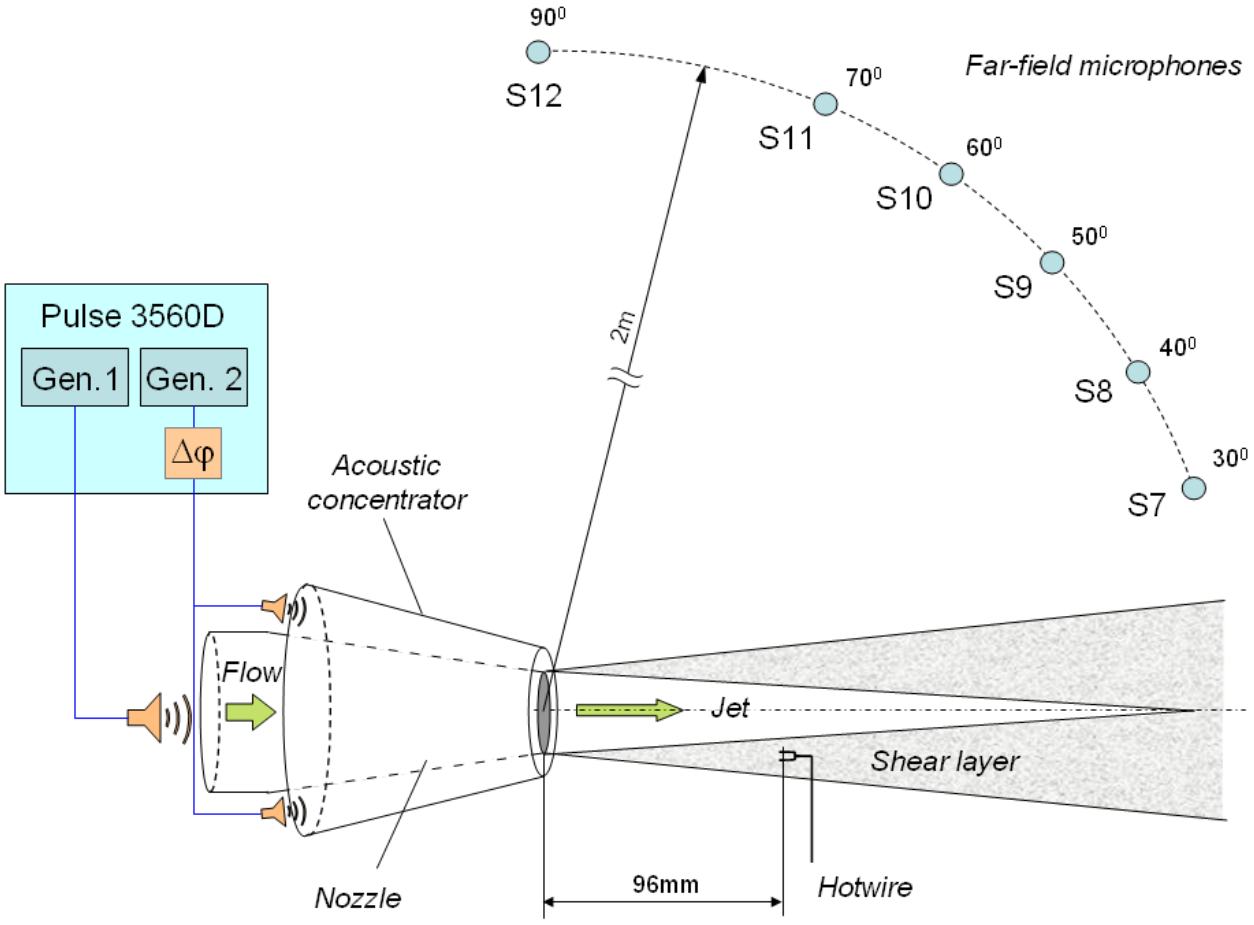

Experimental setup

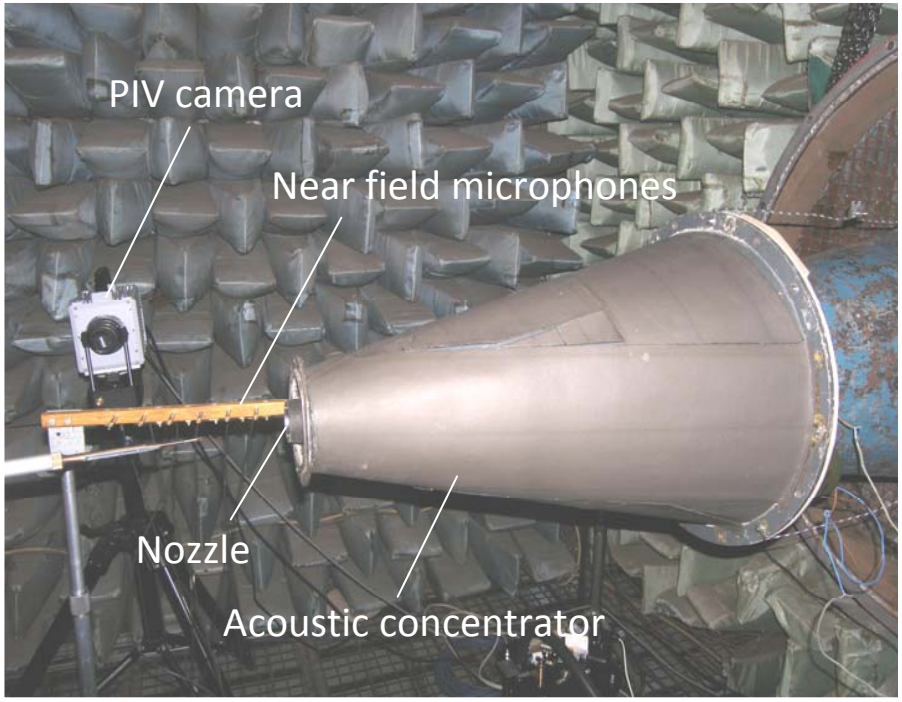

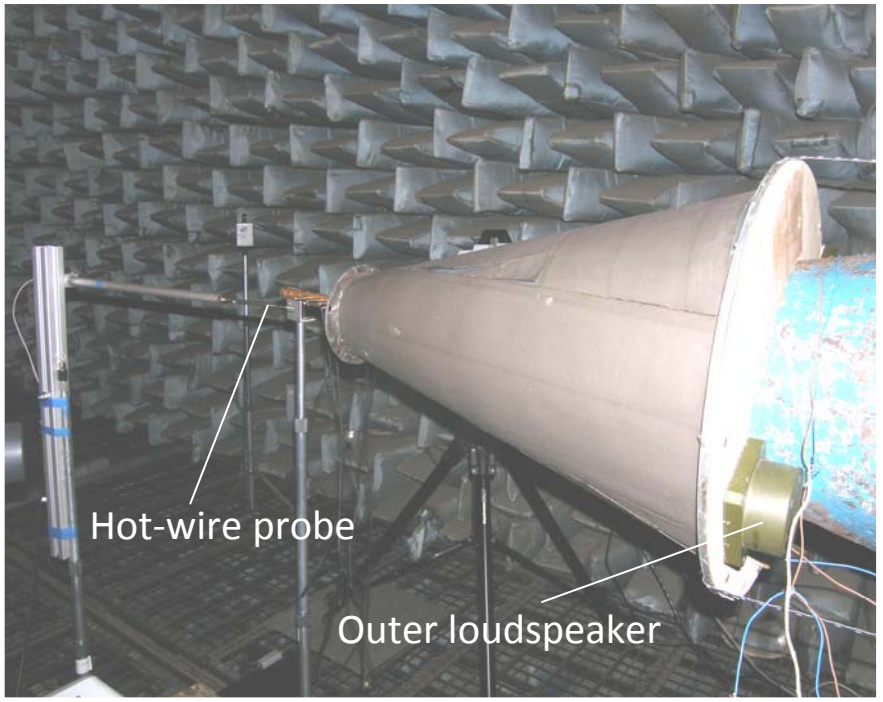

Hotwire probe	Dantec 55P01
Near field microphones	¼'' 4935 Bruel&Kjaer
Far field microphone	½'' 4189C Bruel&Kjaer
TR PIV	FlowMaster HS-PIV by LaVision©

Azimuthal structure of the field produced by the external sources

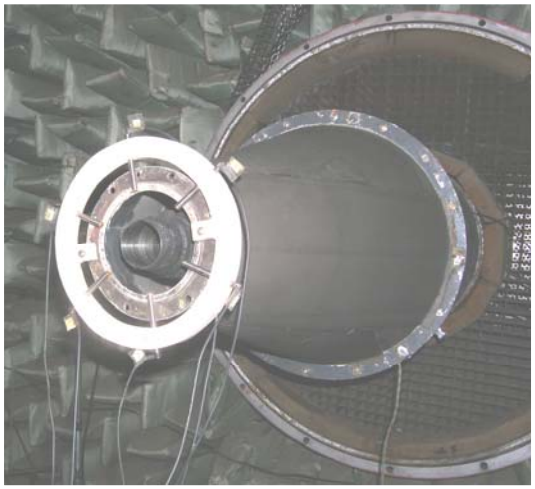

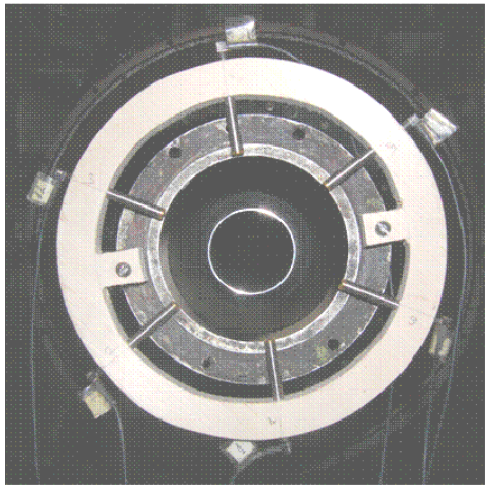

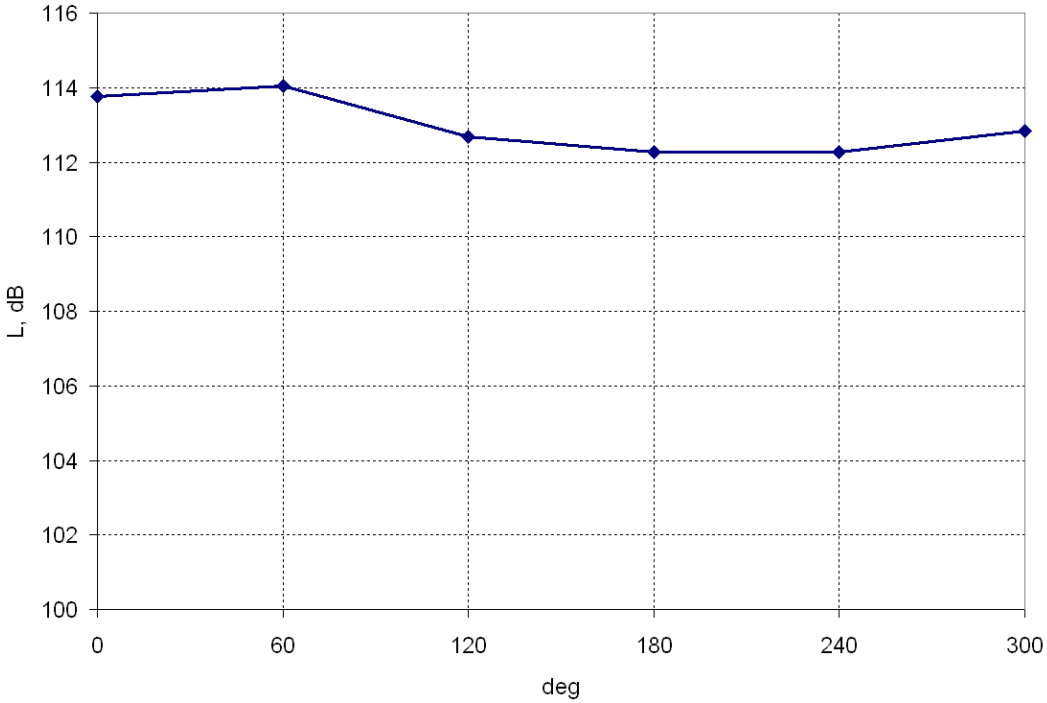

This system of external excitation provided azimuthal uniformity of the near field with the error about ±0.9dB

Hot-wire measurements

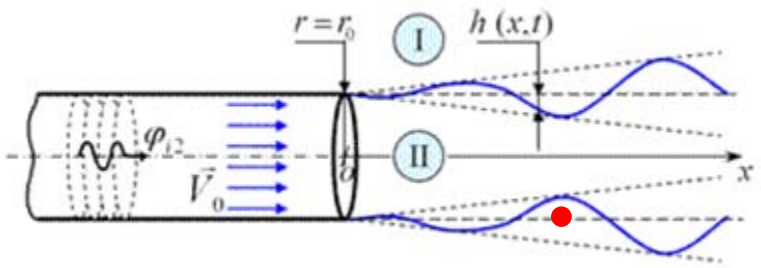

V=50 m/s, at f=1kHz

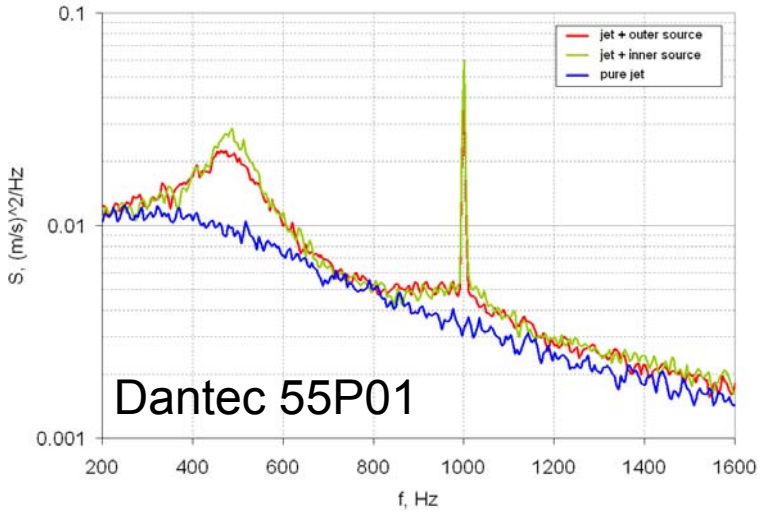

V=280 m/s, at f=2.5kHz

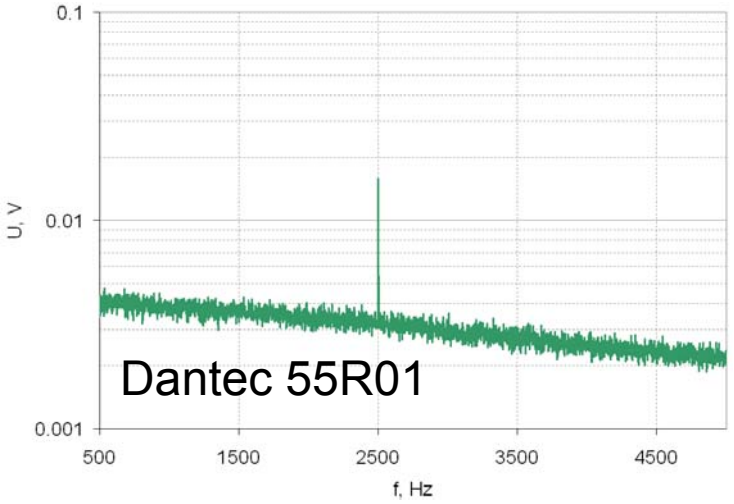

Hot-wire measurements

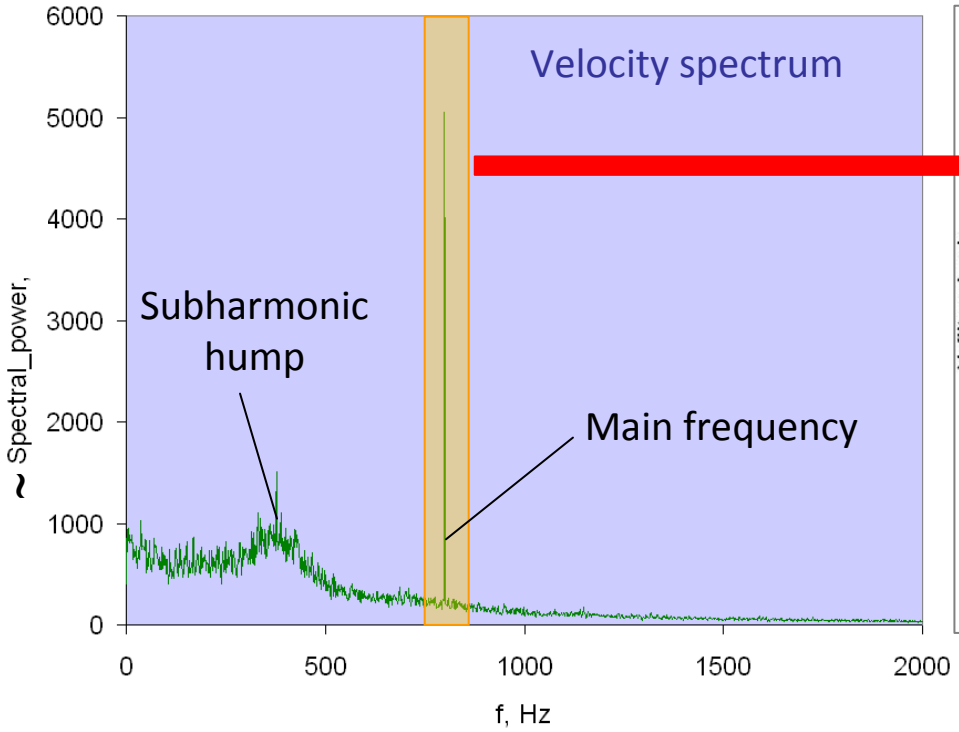

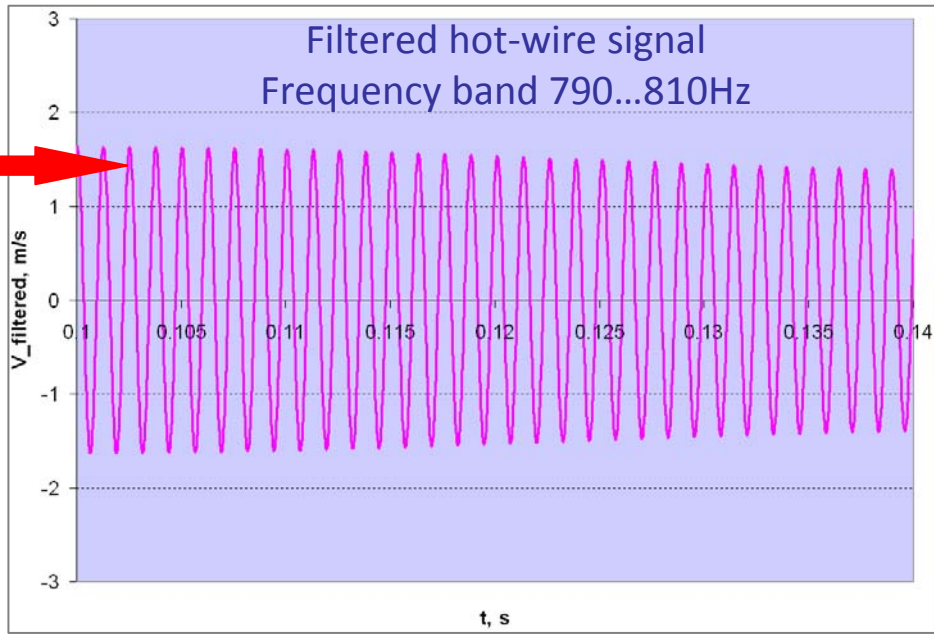

ADT measurements: axisymmetrical mode in local frequency band near tone

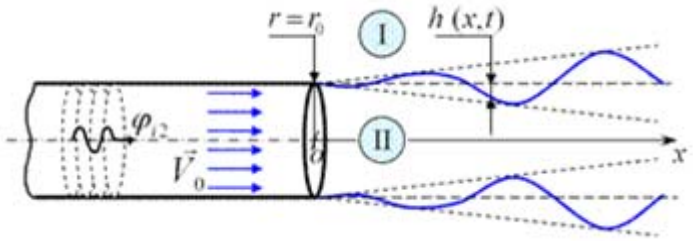

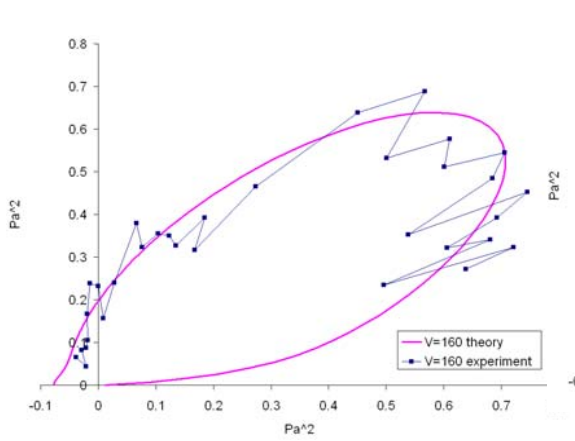

160 m/s

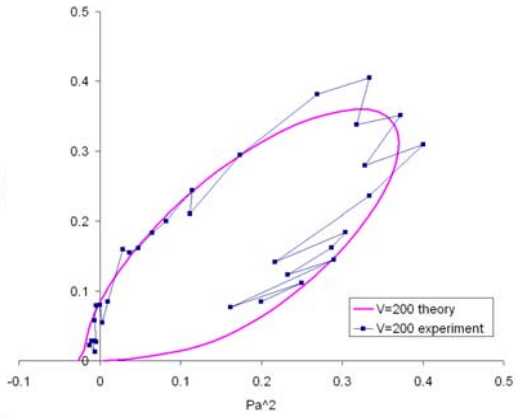

200 m/s

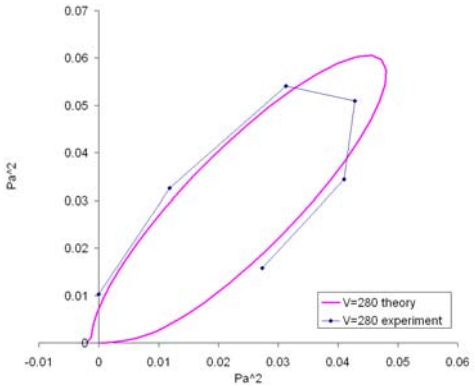

280 m/s

PIV measurements , $f_{exc}=f_{samp}$ =1kHz

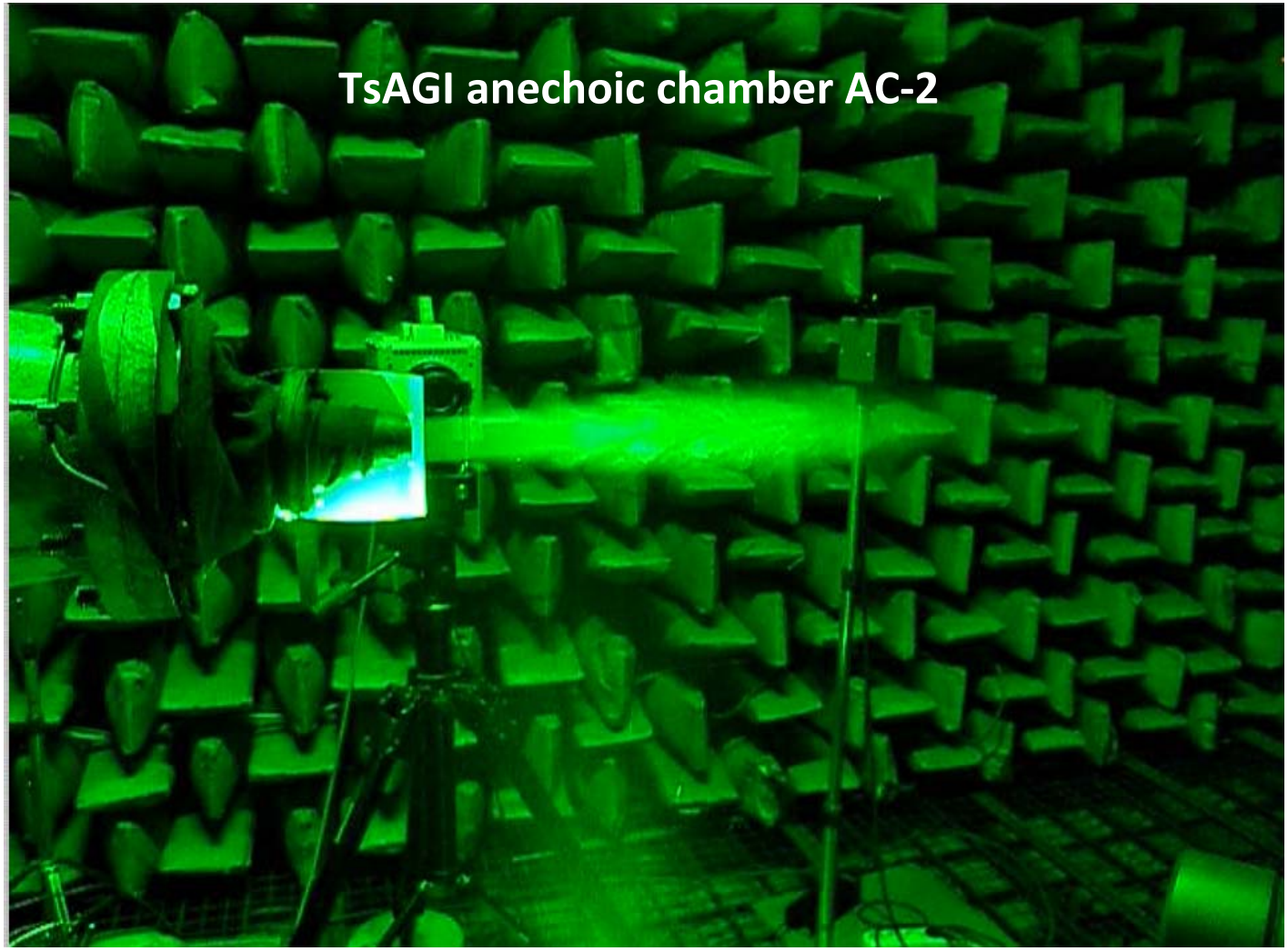

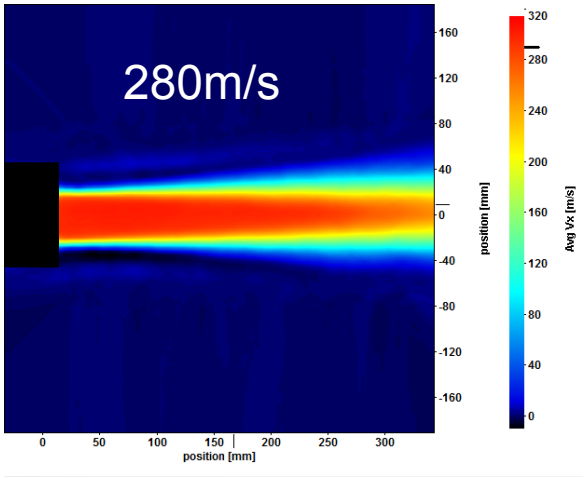

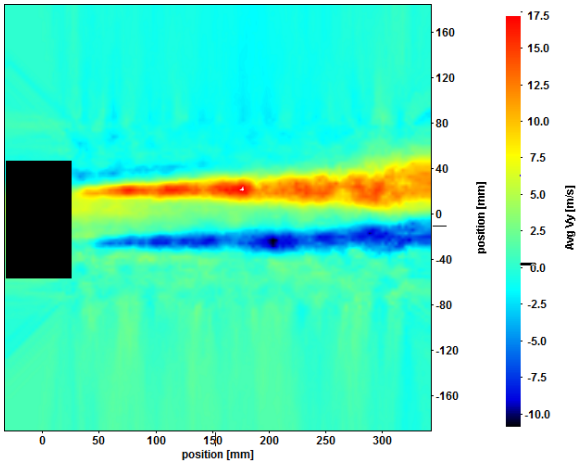

Average V_x (a) and V_y (b) velocity fields for the unforced jet

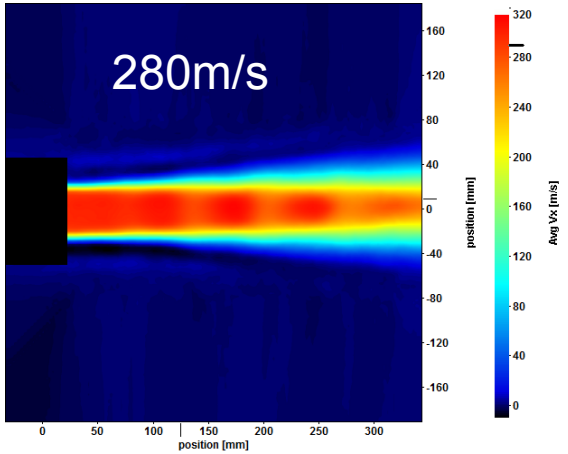

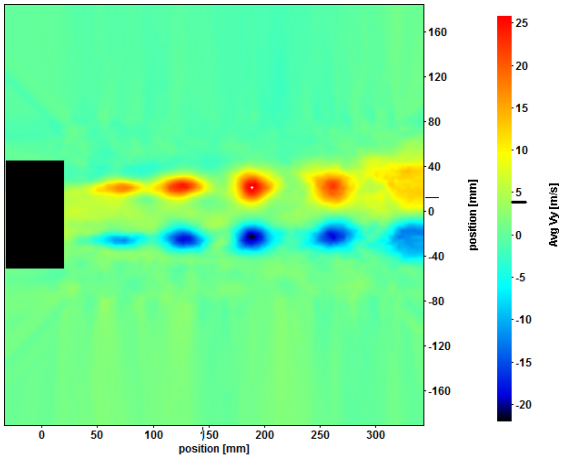

Average V_x and V_y velocity fields for the acoustically forced jet

Excitation frequency 3000 Hz; sampling rate is also 3000 fps

Time resolved PIV measurements of turbulent disturbances

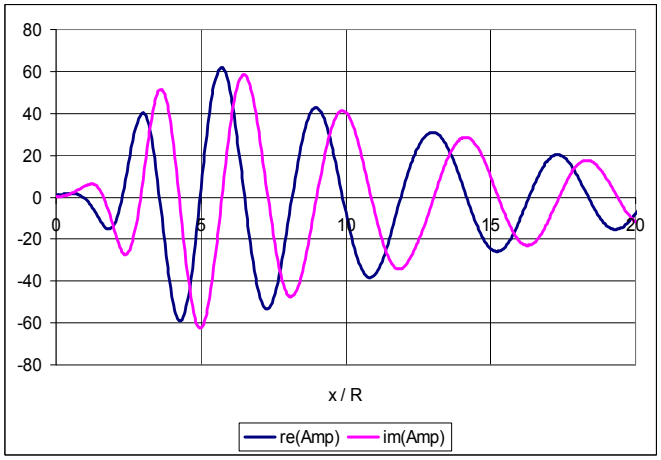

Wave pocket Tam inviscid

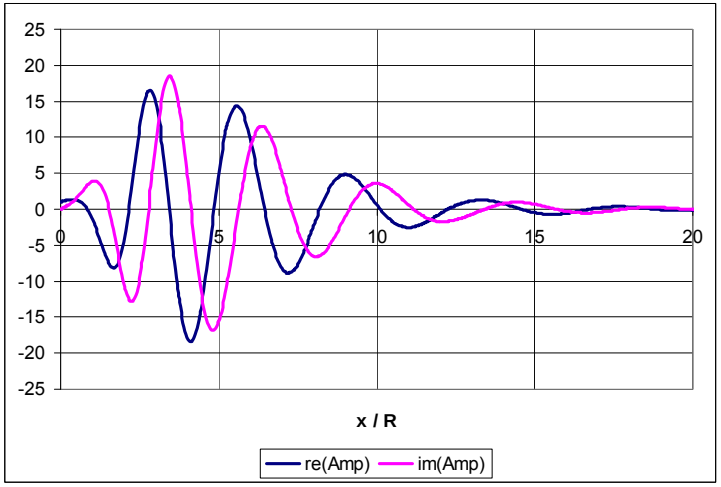

Wave pocket Tam viscous

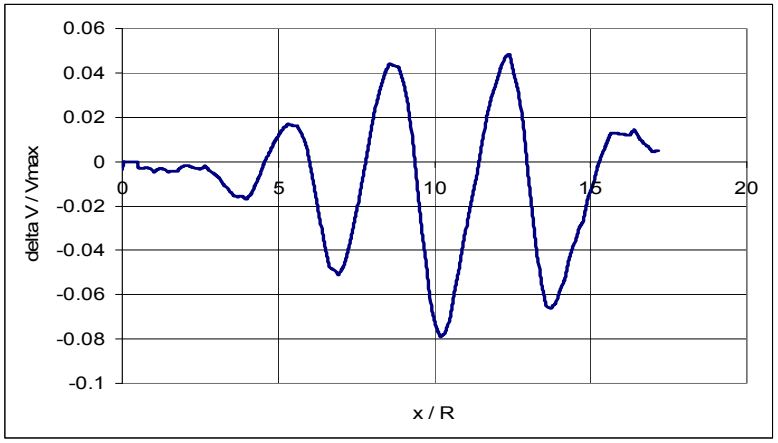

PIV measurements

V_y velocity field for the jet acoustically forced at the frequency 3000 Hz, jet velocities are: (a) 150 m/s, (b) 200 m/s, (c) 250 m/s.

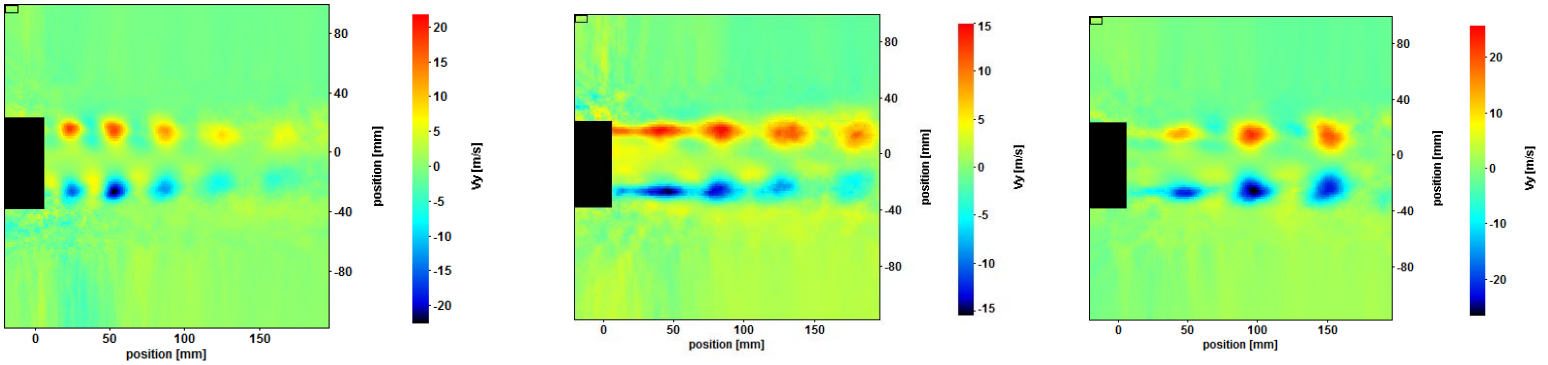

normalized Vx and Vy, 150 m/s

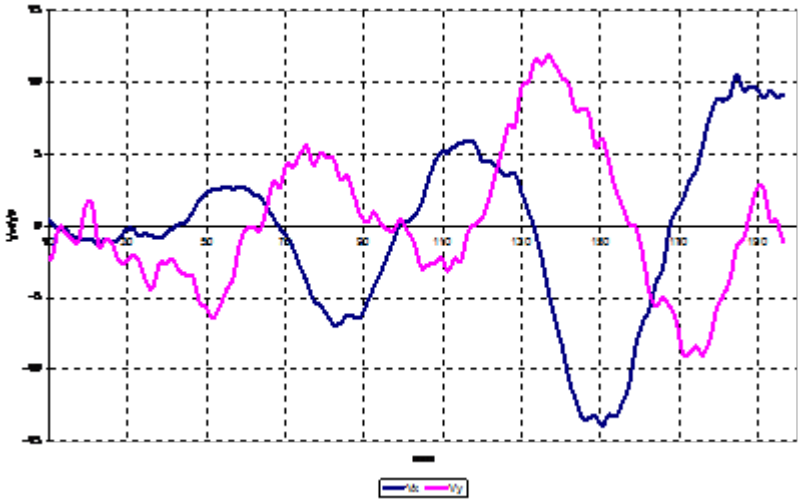

150 m/s (blue), 200 m/s (magenta), 250 m/s (green), 300 m/s (orange)

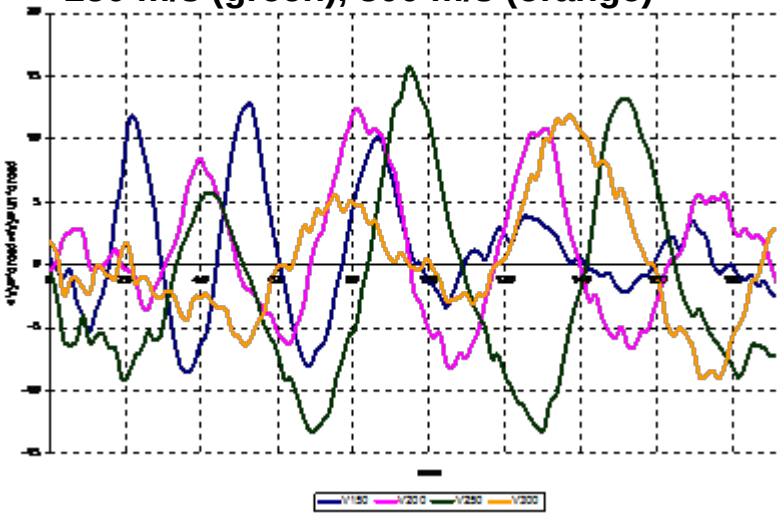

Demonstration of instability wave control: hot-wire

Hot-wire measurements, f_{exc}=1kHz

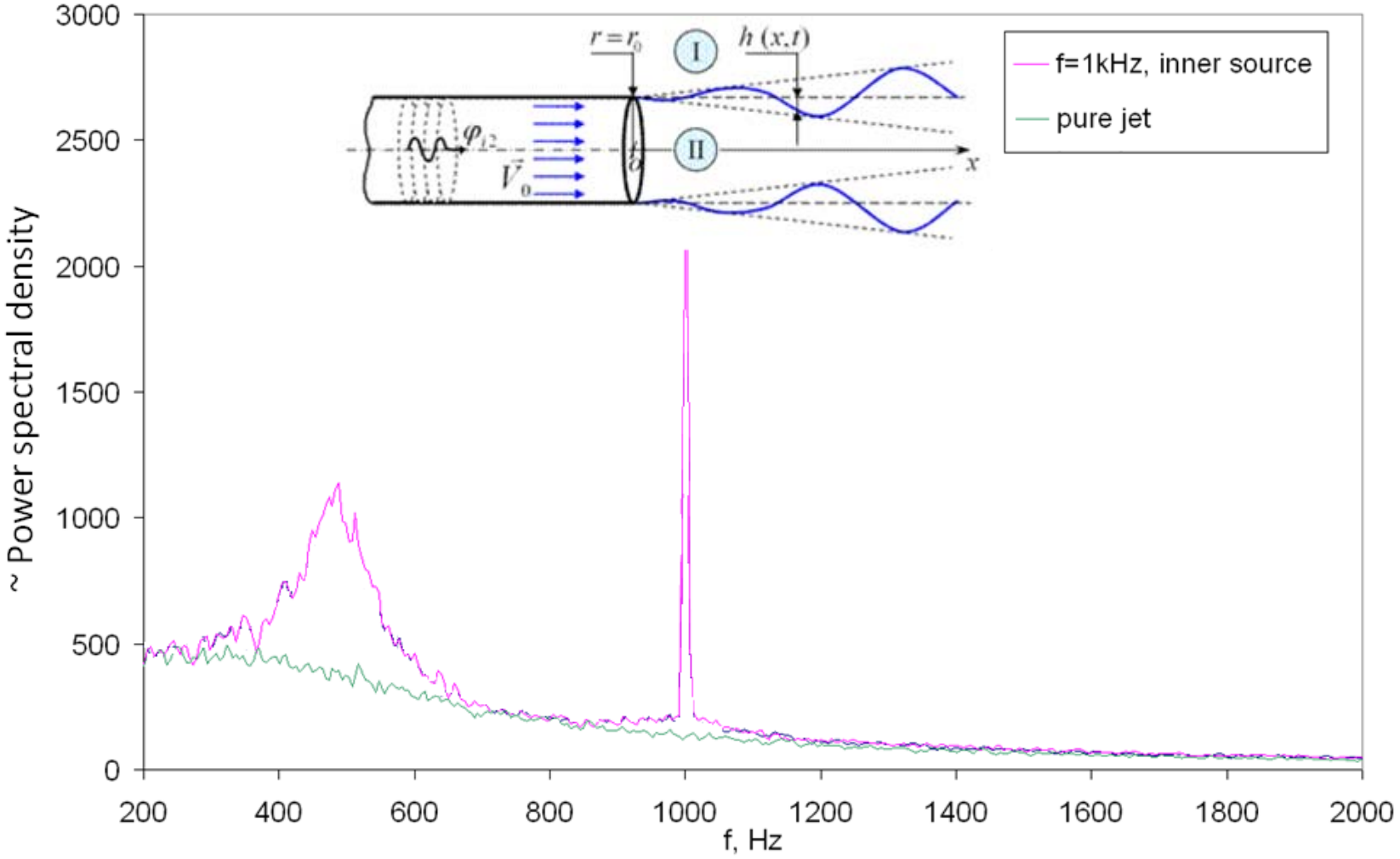

Hot-wire measurements, f_{exc}=1kHz

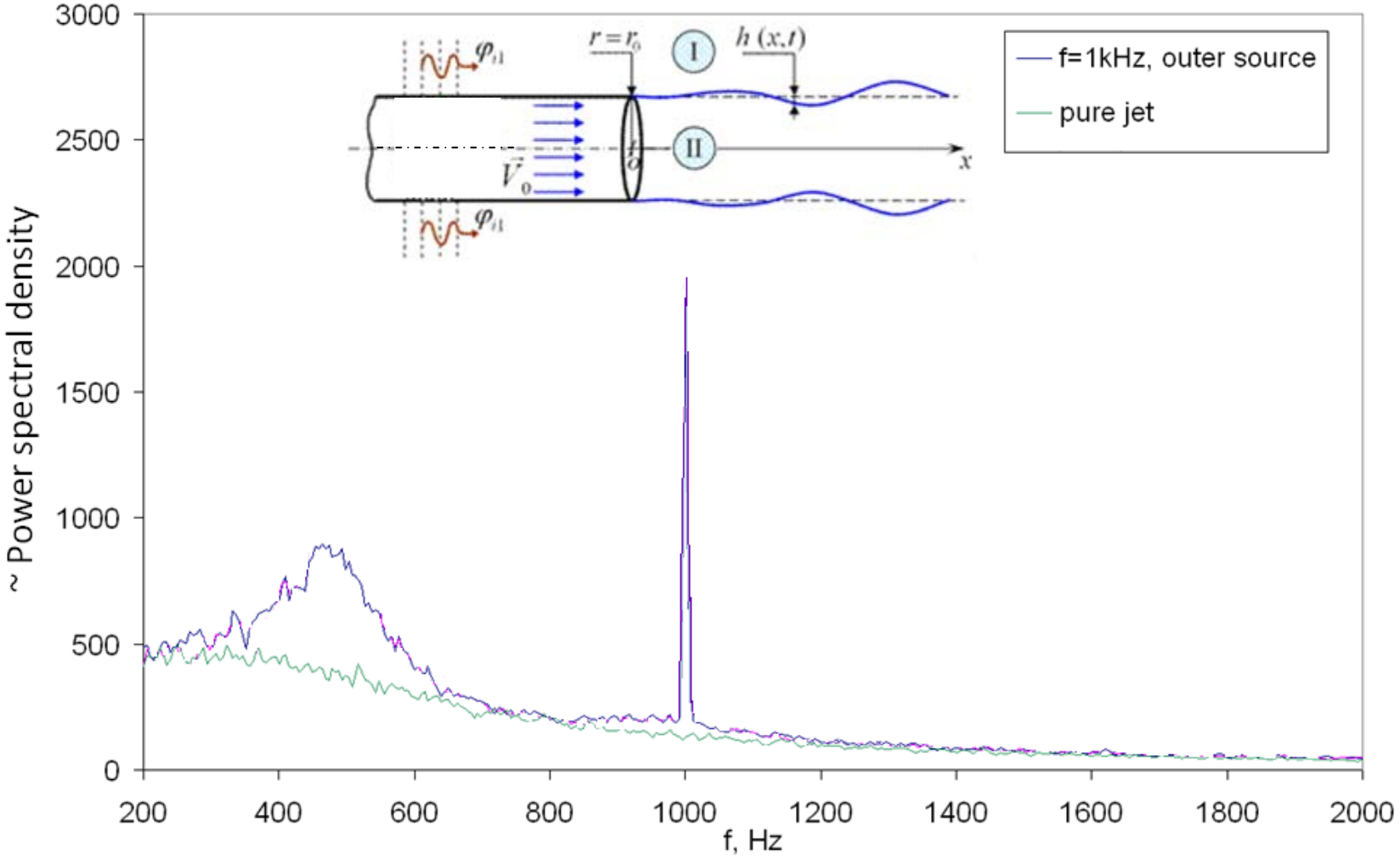

Hot-wire measurements, f_{exc}=1kHz

Variation of phase shift

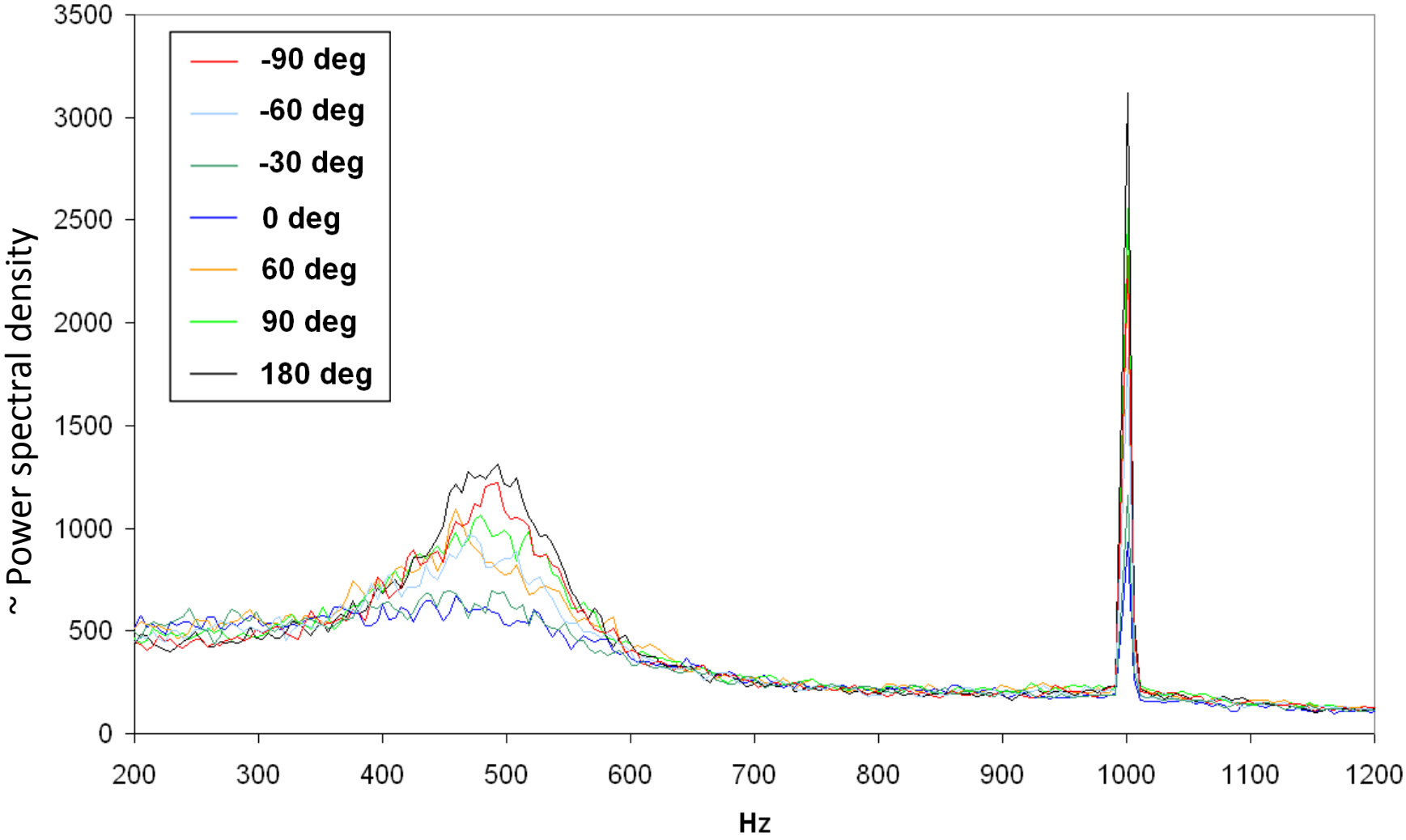

Hot-wire measurements, f_{exc}=1kHz

Variation of phase shift

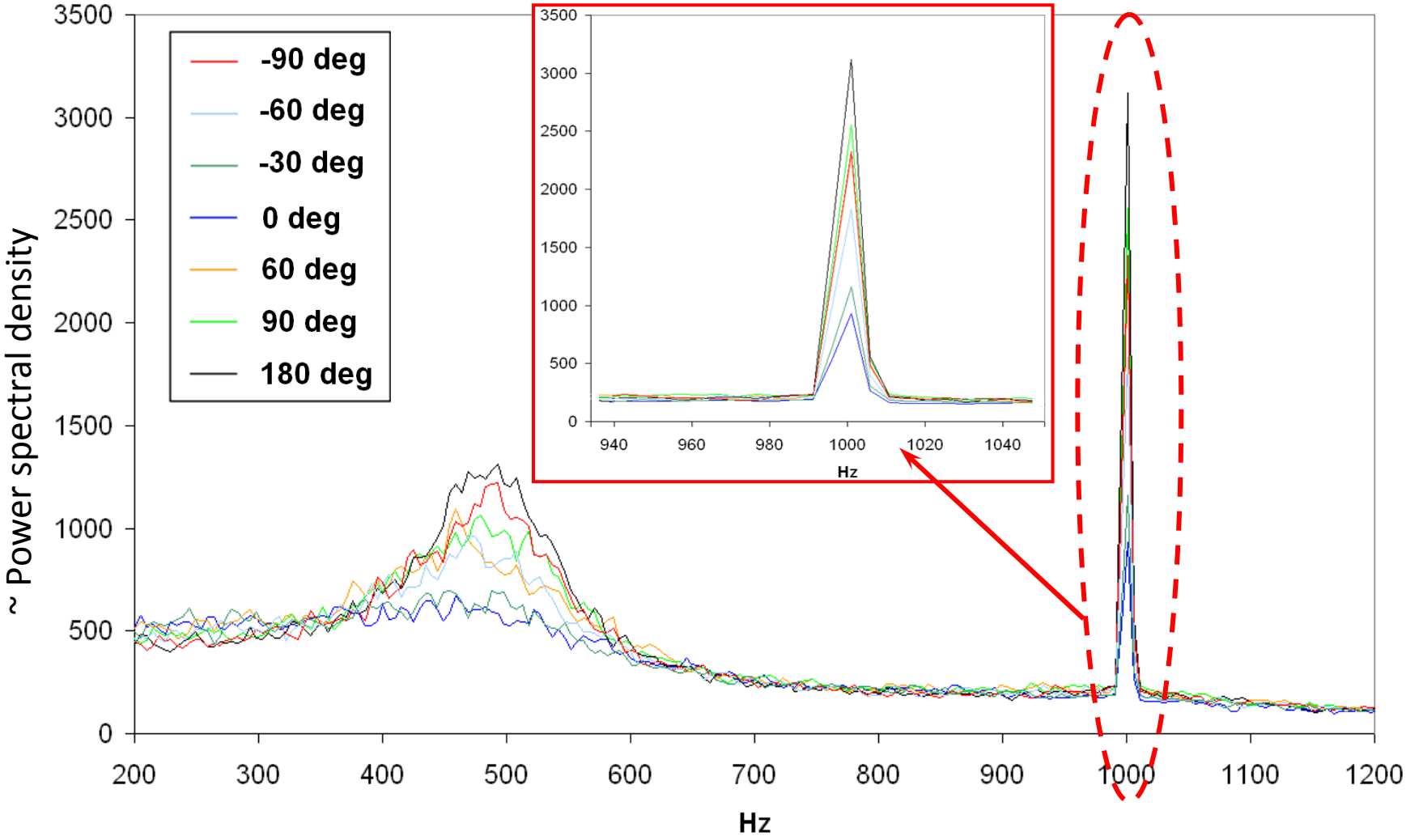

Jet velocity 280 m/s

Hot-wire measurements, f_{exc}=2.5kHz

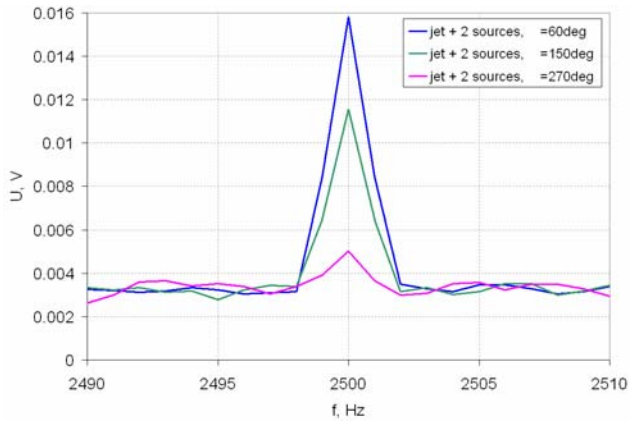

Evolution of hot-wire measured spectrum with variation of signals phase shift

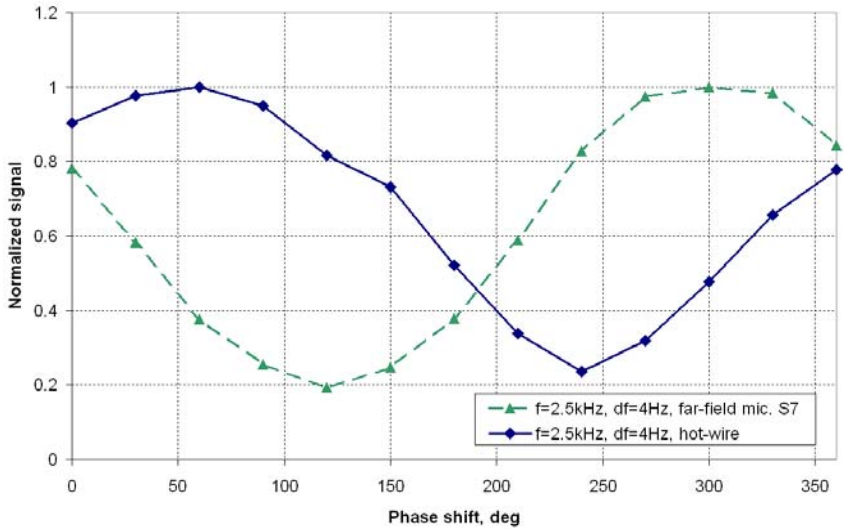

Variation of harmonic peak intensity for hot-wire and far field microphone (direction 30^0 to jet axis) with phase shift, each peak value being normalized to the corresponding maximum value.

Demonstration of instability wave control: PIV

PIV measurements , $f_{exc}=f_{samp}$ =1kHz

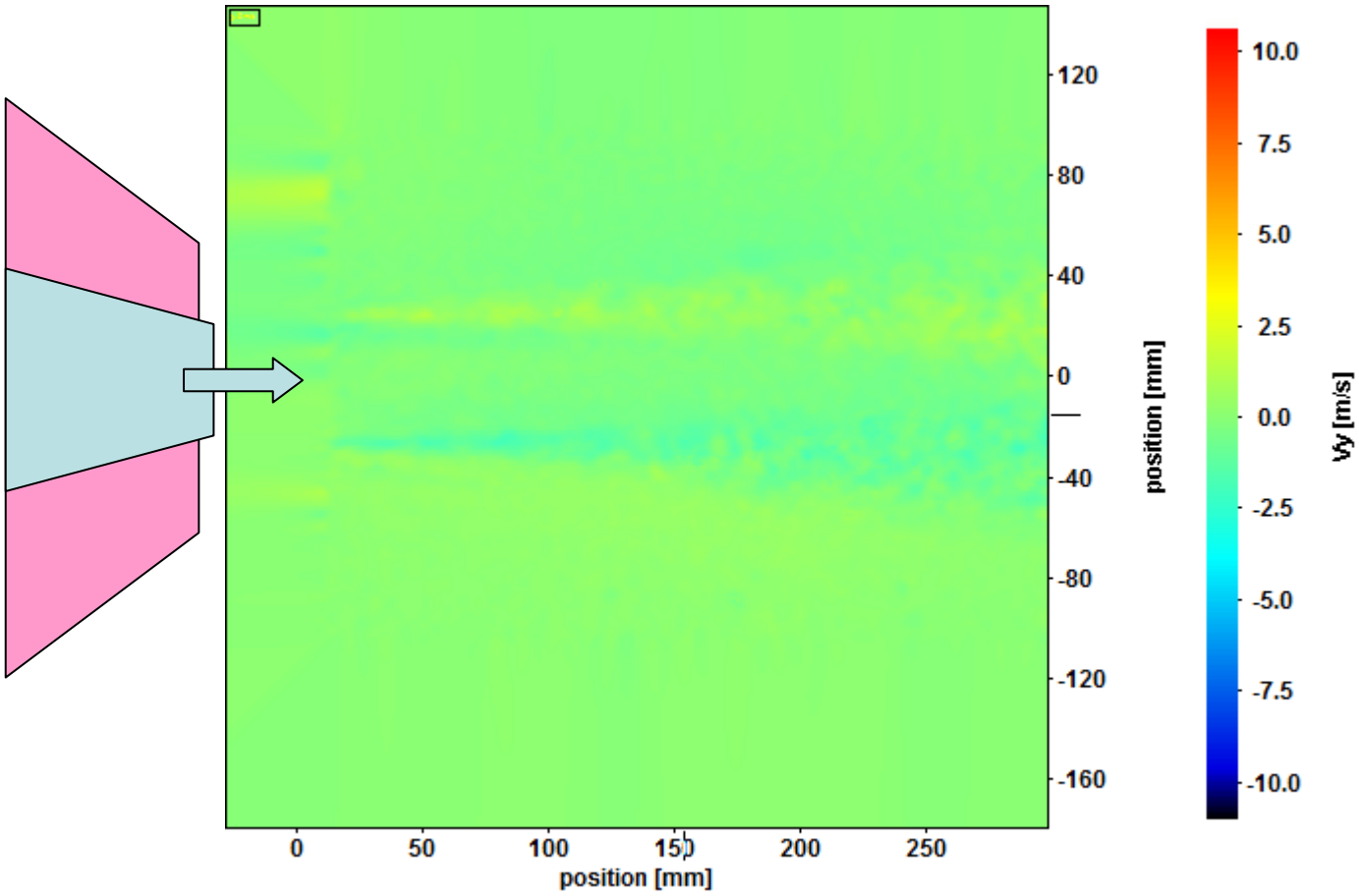

V_y -<V_y>

Pure jet

PIV measurements , $f_{exc}=f_{samp}$ =1kHz

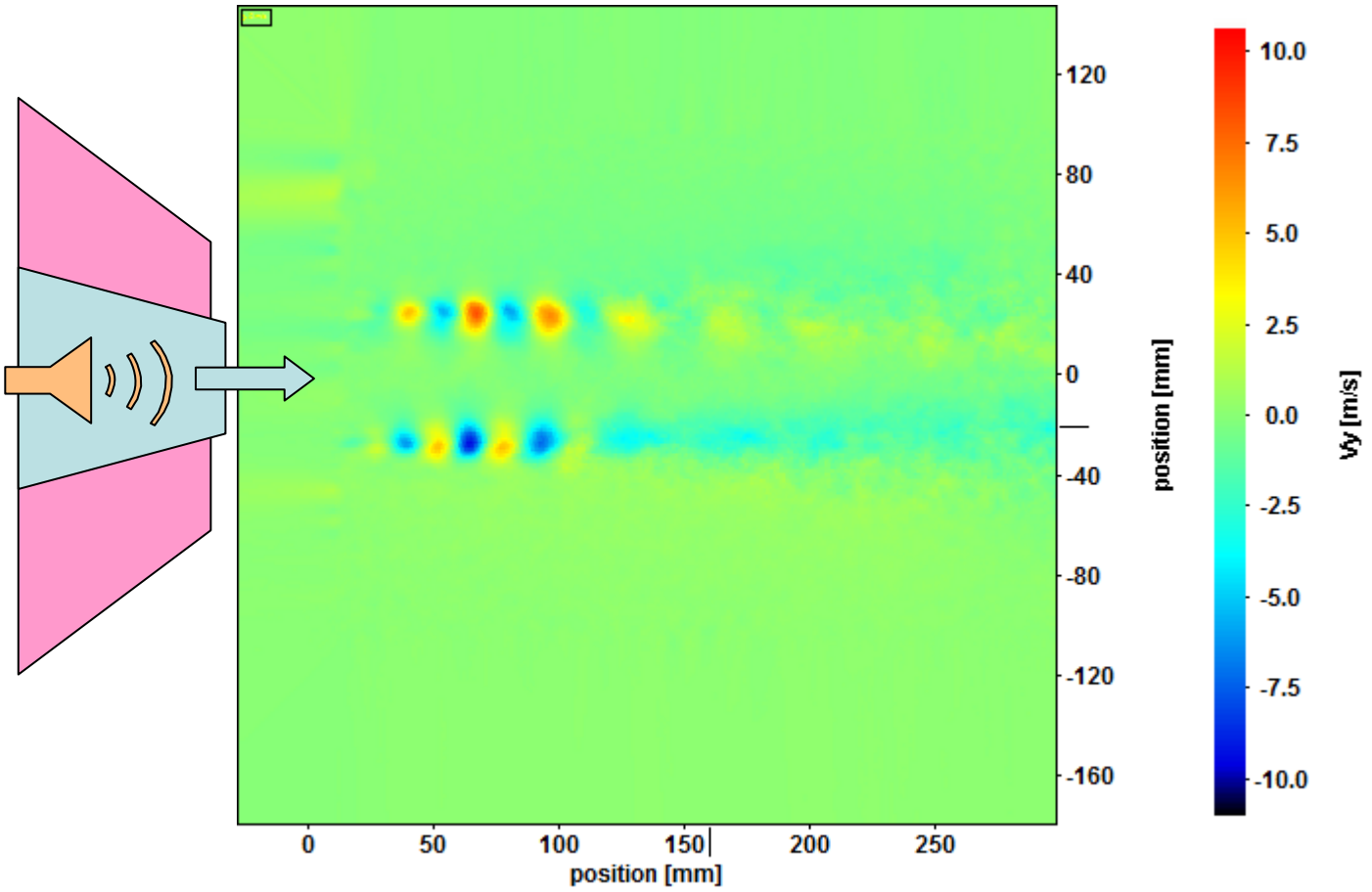

V_y -<V_y>

Inner source

PIV measurements , $f_{exc}=f_{samp}$ =1kHz

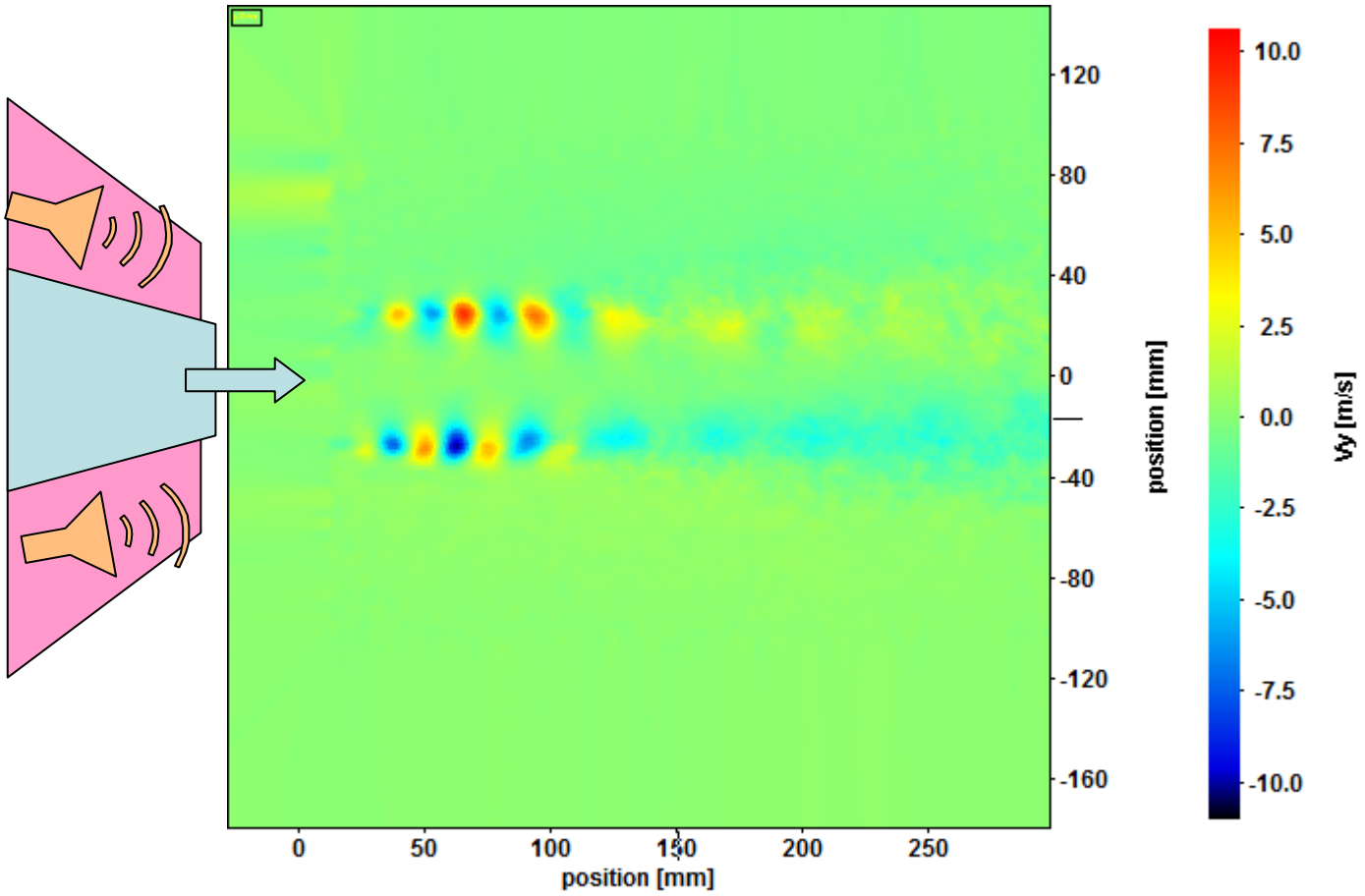

V_y -<V_y>

Outer source

PIV measurements , $f_{exc}=f_{samp}$ =1kHz

$V_y - \langle V_y \rangle$

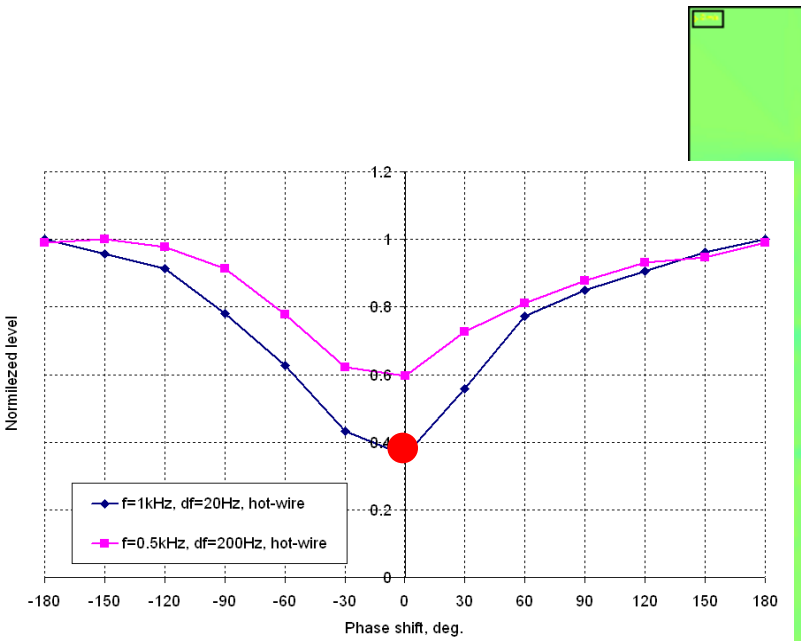

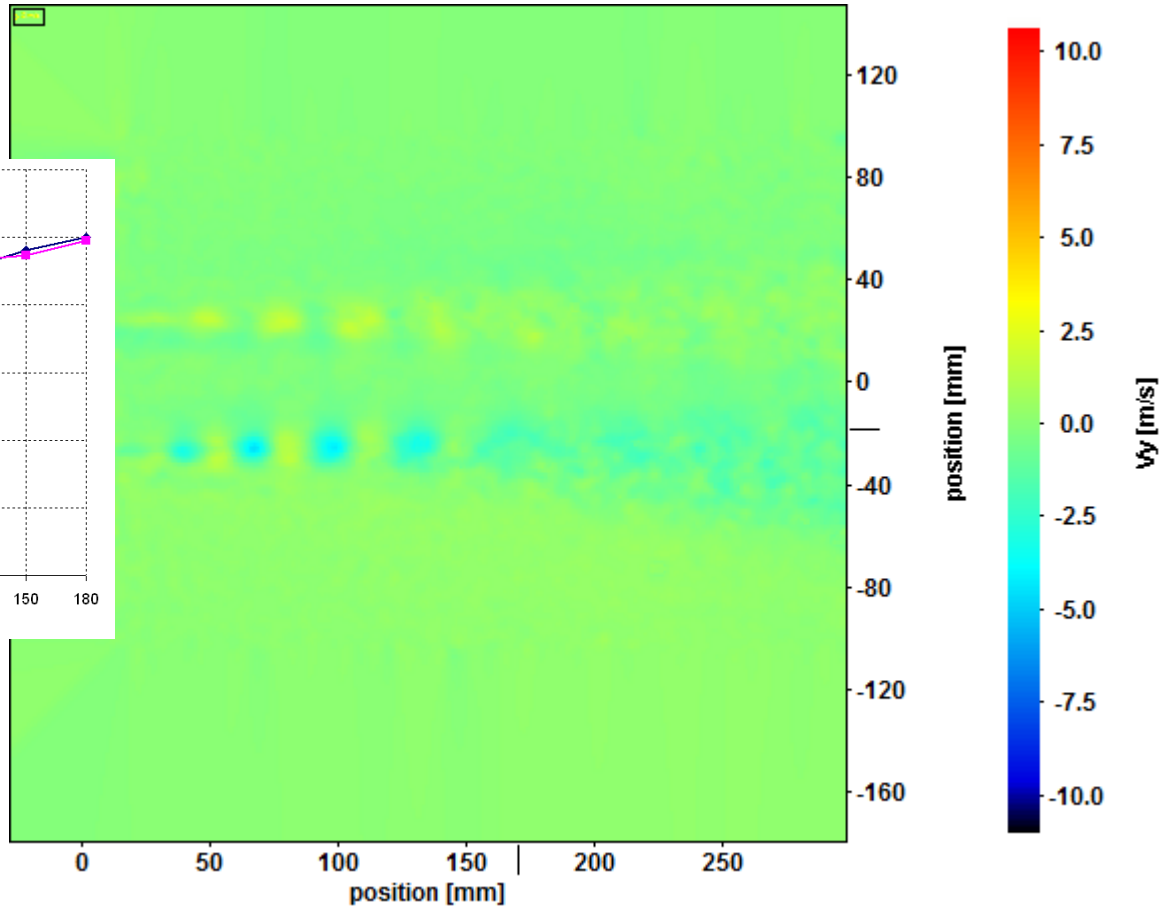

$\Delta\varphi = -60^0$

PIV measurements, $f_{exc}=f_{samp}$ =1kHz

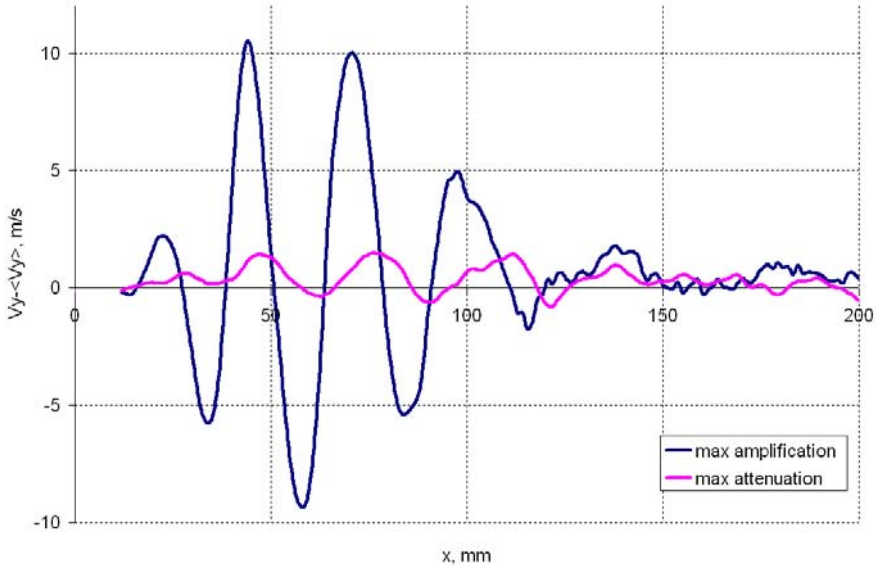

Profile of V_y-<V_y> along the lip-line

Jet velocity 280 m/s

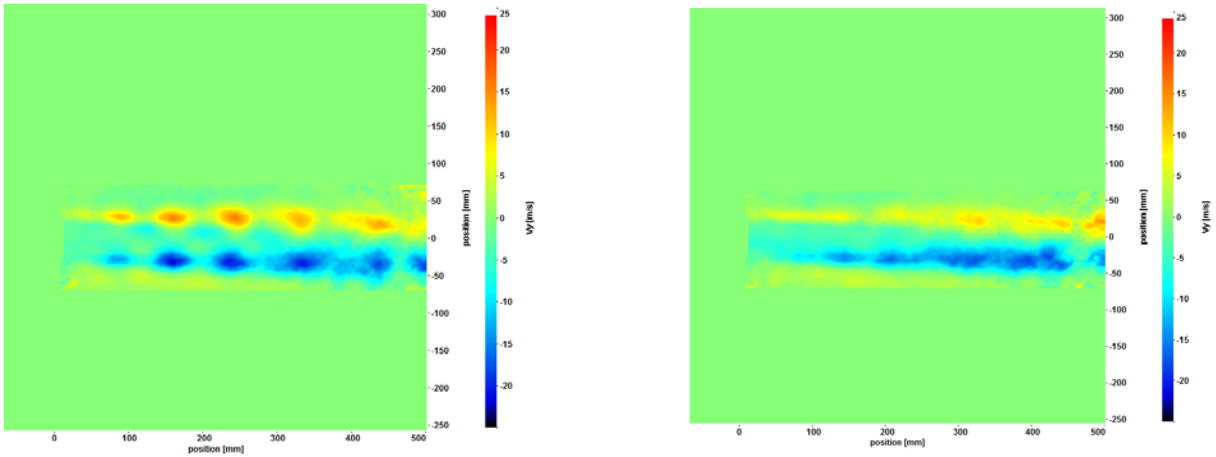

Radial velocity field for the phase shift corresponding to maximal amplification (left, phase shift 90^0) (right, phase shift 270^0).

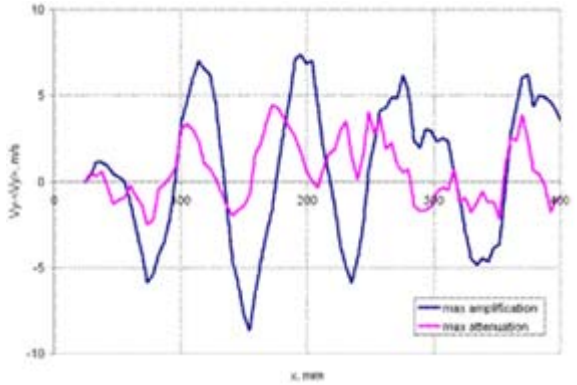

Profile of V_y-$\langle V_y \rangle$ along the lip-line

IW generated by an acoustic sound driver located in the stilling chamber, and by plasma actuators in jet shear layer.

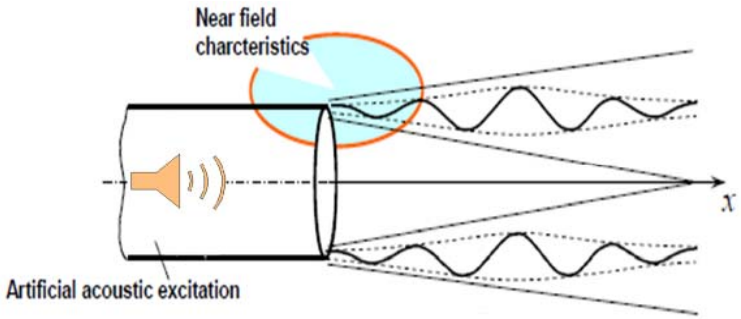

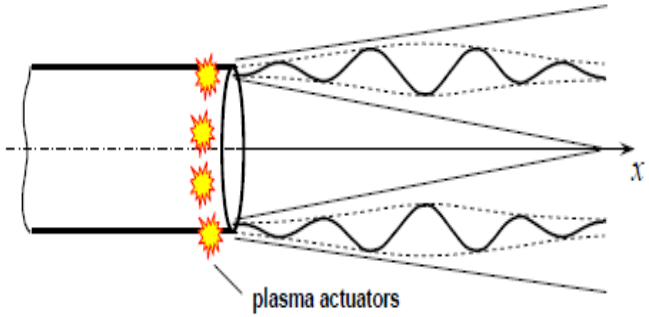

Witoszynski ceramic nozzles

$$r(x) = \frac{r2}{\sqrt{1 - \left(1 - \left(\frac{r2}{r1}\right)^2\right) \frac{\left(1 - \frac{x^2}{L^2}\right)^2}{\left(1 + \frac{x^2}{L^2}\right)^3}}}$$

Plasma Actuators

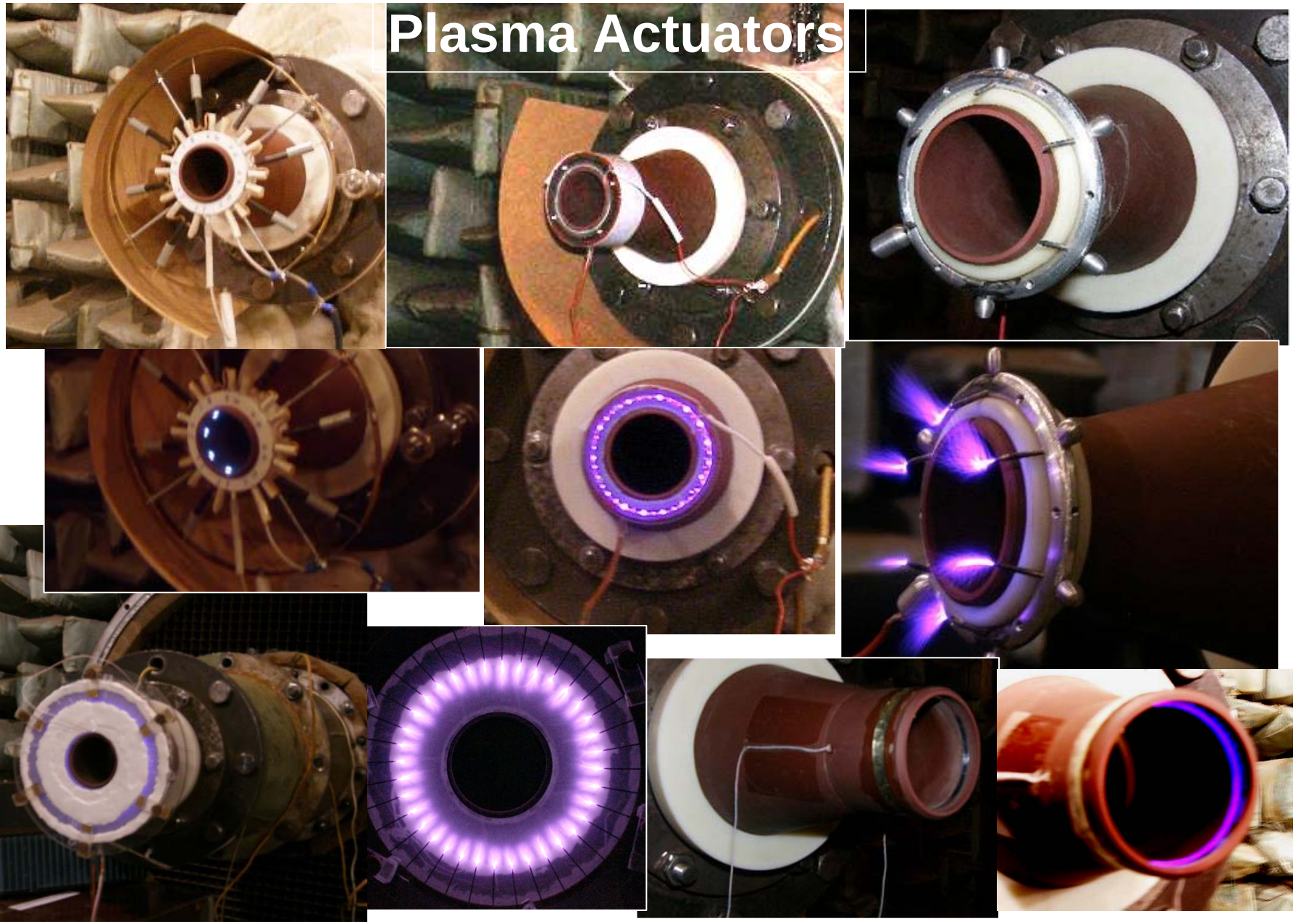

Plasma actuator IW suppression

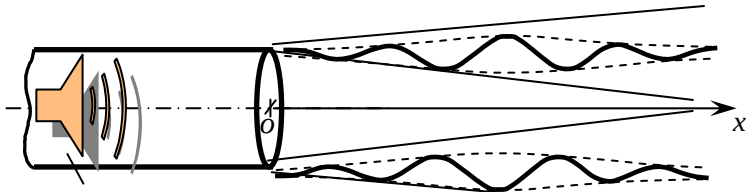

Artificial acoustic excitation characterized by amplitude and phase at given frequency

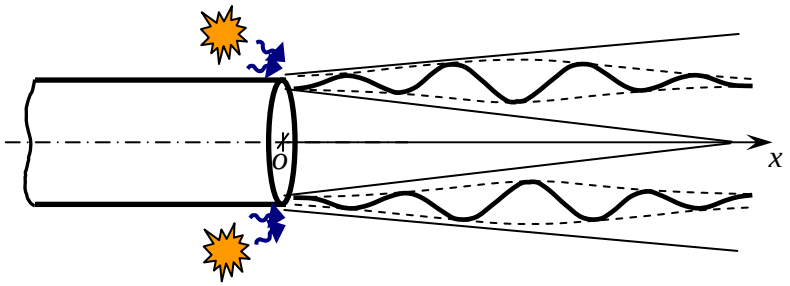

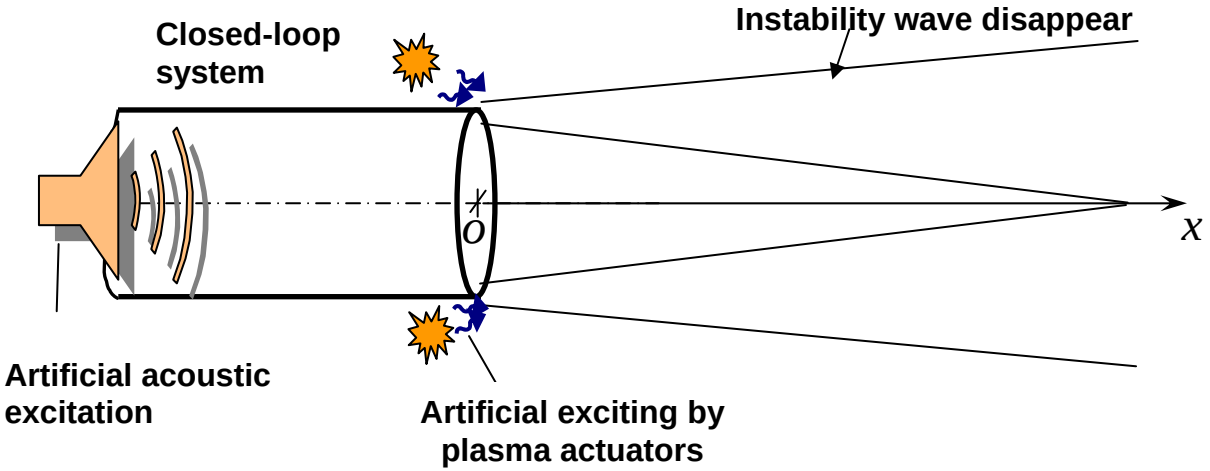

HF DBD actuator

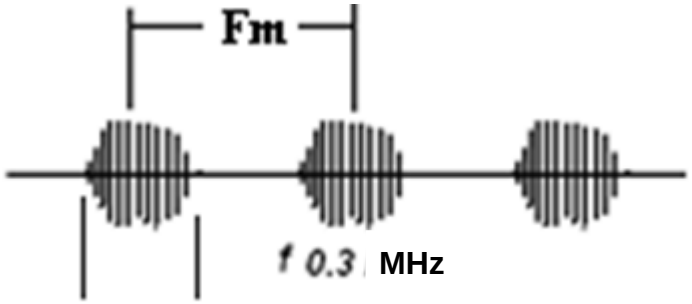

Ceramic layer-
1-4mm

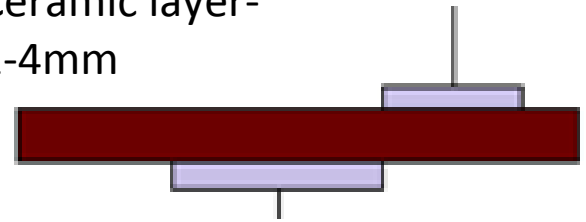

Carrying frequency f	100-400kHz
Modulation frequency F_m	1-3kHz
Typical power consumption	100-500W

Plasma actuators based on surface barrier corona

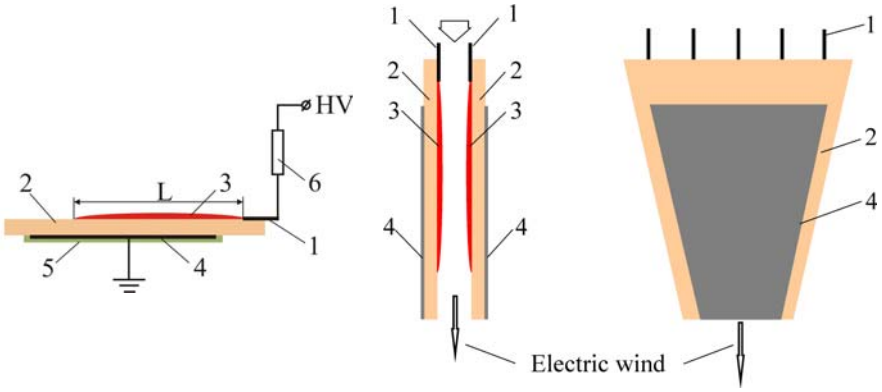

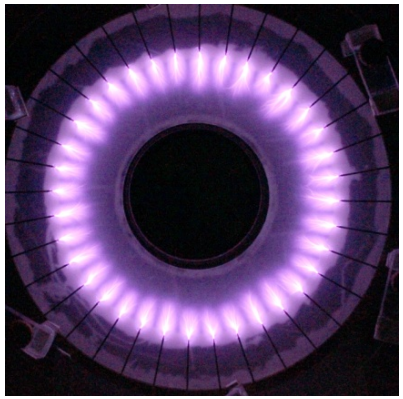

The image of the surface corona discharge actuator with a single disk at operating condition

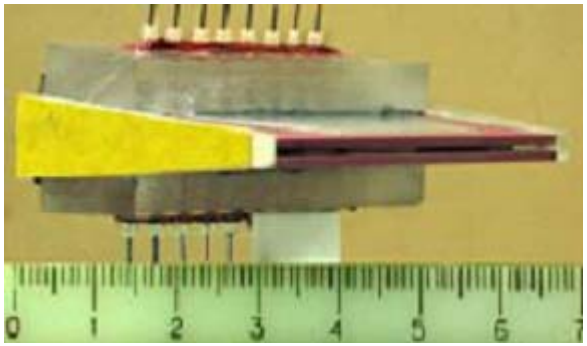

Scheme and photo of barrier corona actuator.

1 - High-Voltage pin electrodes typical for corona discharge; 2 - dielectric plate (dielectric barrier); 3 - surface streamers; 4 - grounded electrode; 5 - insulation; 6 – ballast resistor

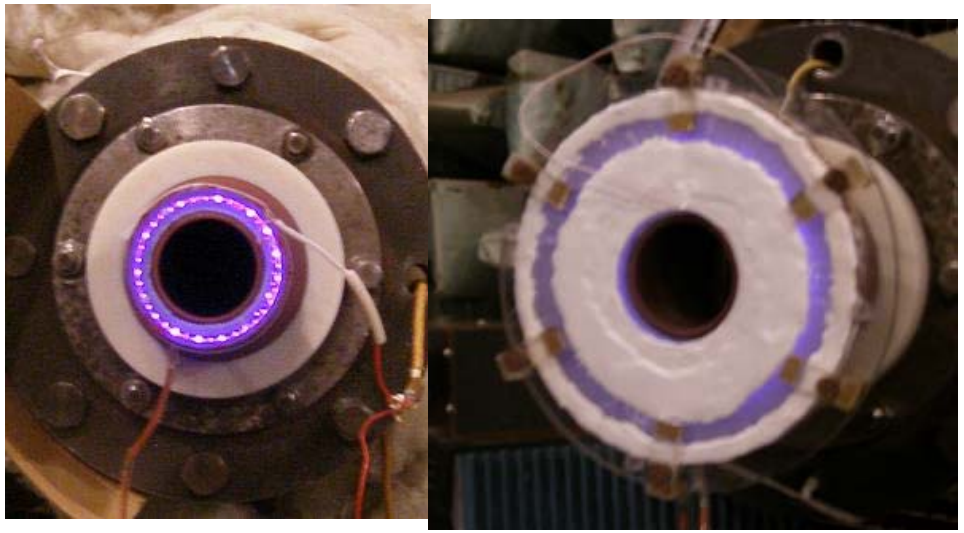

Images of a closed barrier corona actuators

Multispark Actuator Based on the High-Current Gliding Surface Discharge

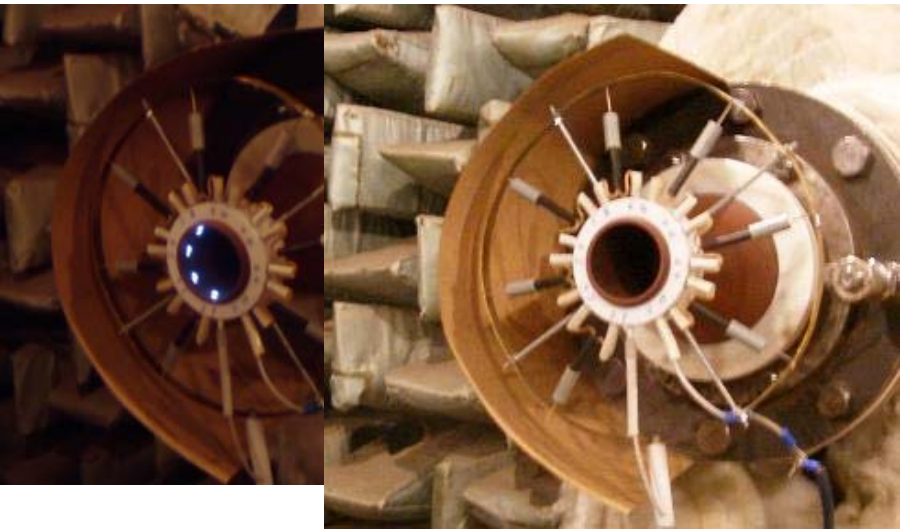

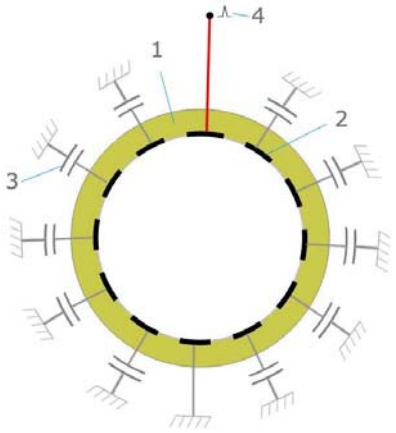

Principle electric scheme of actuator. 1-dielectric ring; 2-electrodes; 3-lumped capacities; 4-high-voltage pulse

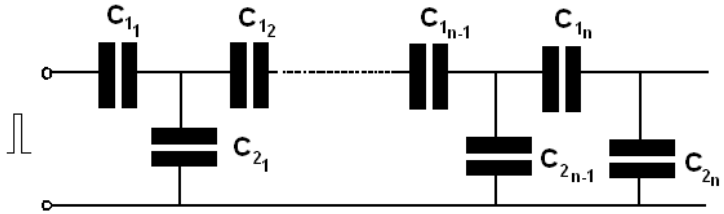

Equivalent electric scheme of discharger

$C_{2i} >> C_{1i}$

Electrical parameters of discharge :

High voltage	15 kV
Current pulse	150A
Pulse duration	~1μs
Repetition frequency	1 kHz
Mean power	< 200 Wt

Instability waves excitation by plasma actuators

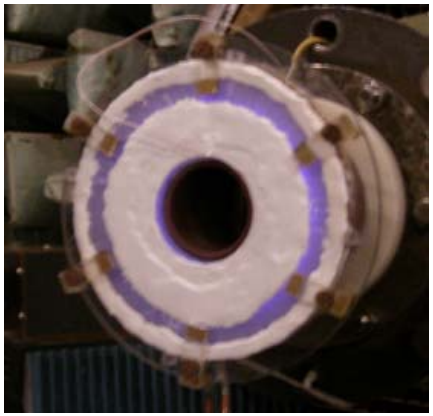

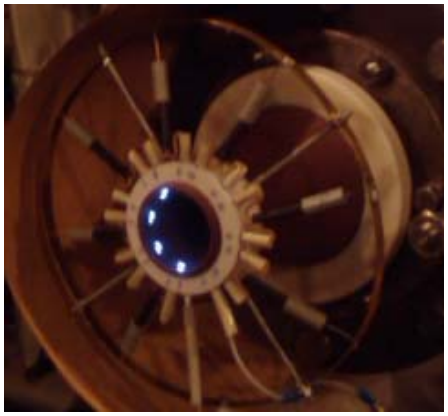

Unforced jet

HF dielectric barrier discharge actuator

Surface barrier corona actuator

Gliding surface discharge actuator

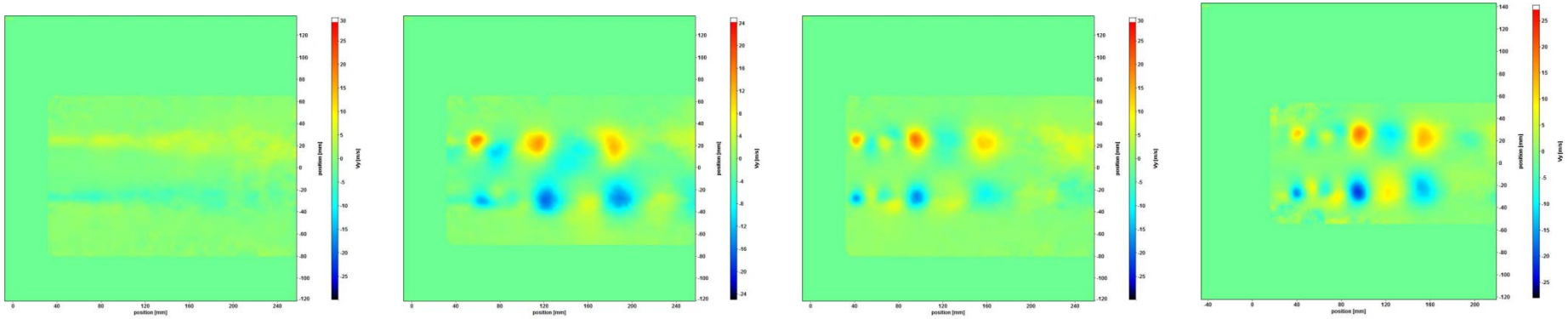

Average radial velocity field for 100 m/s velocity jet

PIV measurements , $f_{exc}=f_{samp}$ =1kHz

Control of instability waves in excited jet

Sketch of the experimental system for instability wave control with plasma actuators

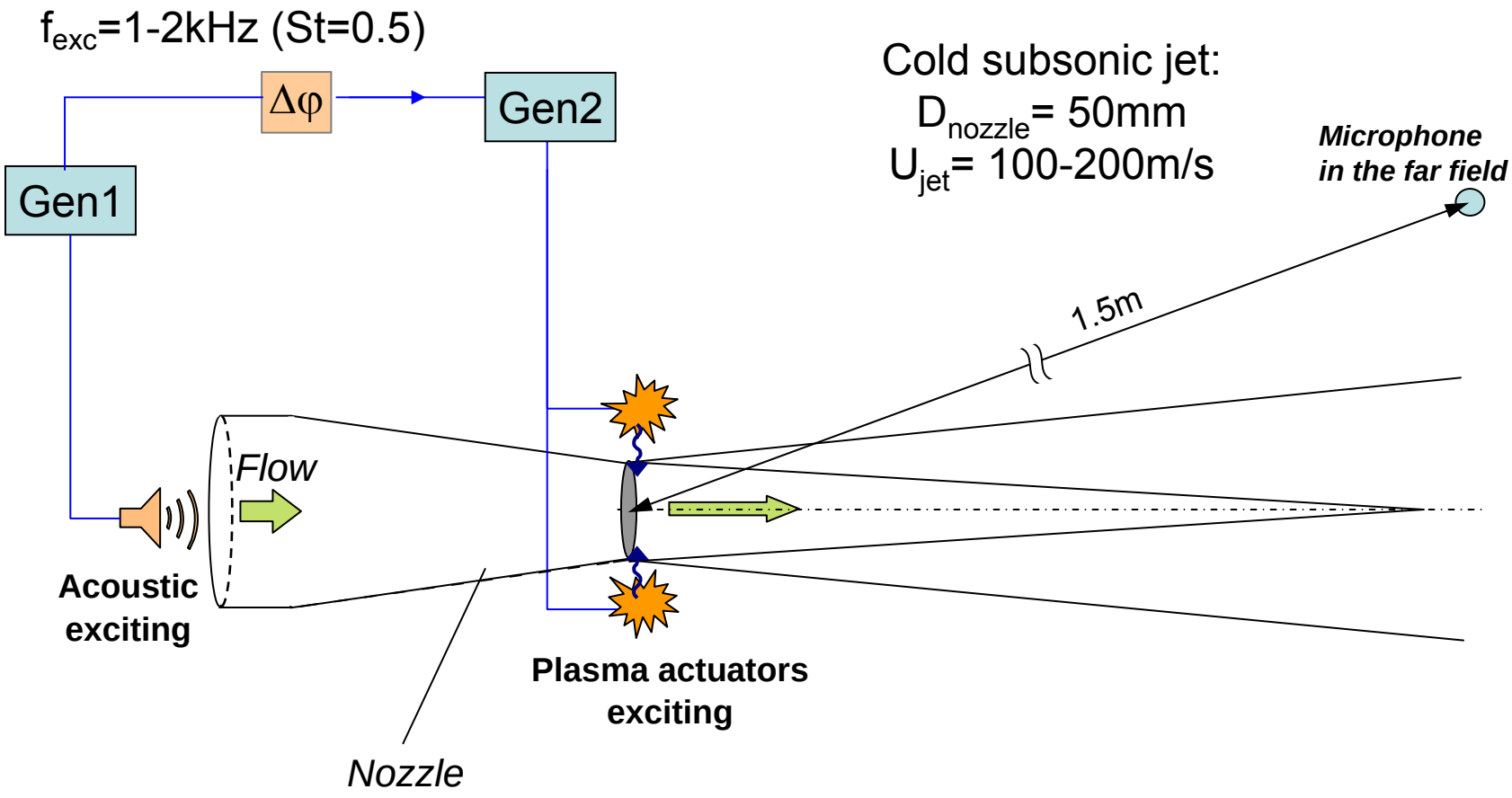

Instability waves suppression by plasma actuator

Average radial velocity component field in the jet (200 m/s) for different phase shift

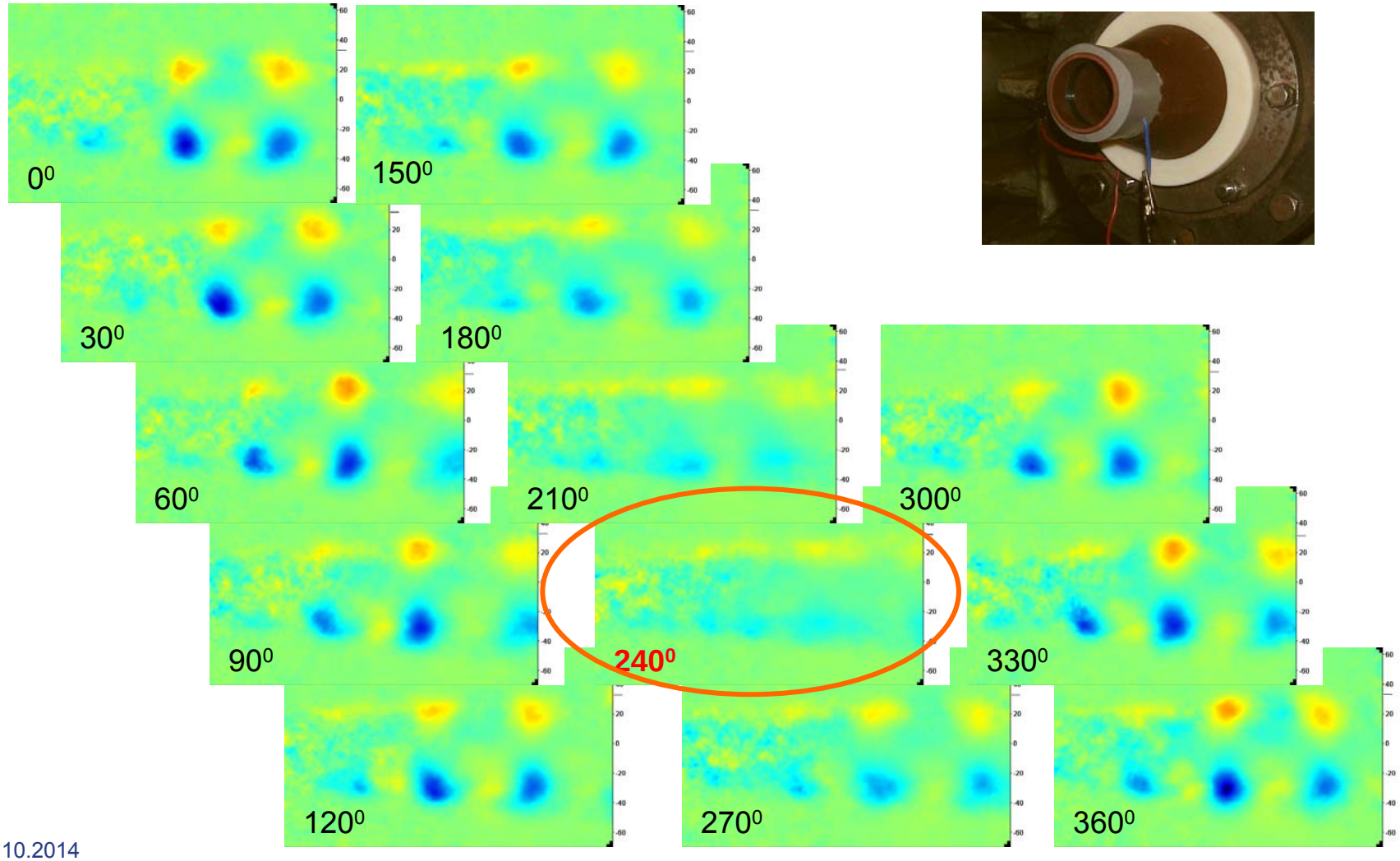

Plasma actuators based on high frequency dielectric barrier discharge

Phase-locked PIV measurements showed that plasma actuator excitation lead to instability waves/vortex rings formation in the jet shear layer for all elaborated types of plasma actuators.

The variation of the phase shift between the adjusted acoustical and plasma excited sources leads to maximal amplification or maximal attenuation (shifted by 180^0) of the coherent structures.

The proposed system of actuators allows effective controlling of artificial instability waves (AIW) in the whole shear layer of the jet.

Possible design of closed-loop control system for SNIW

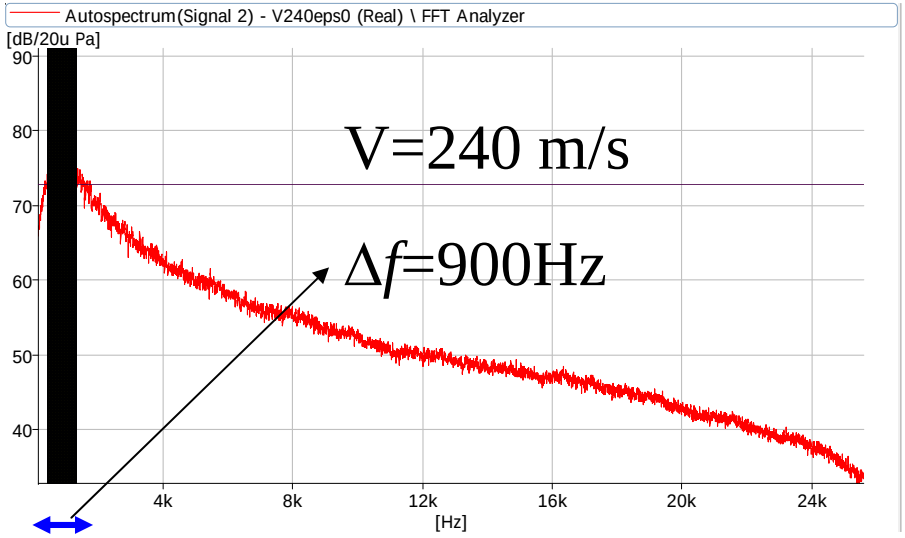

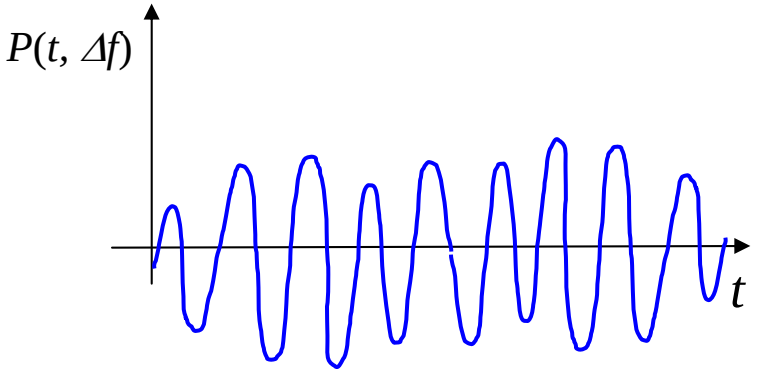

Round jet: **V=240** m/s, Micr. 40 deg.

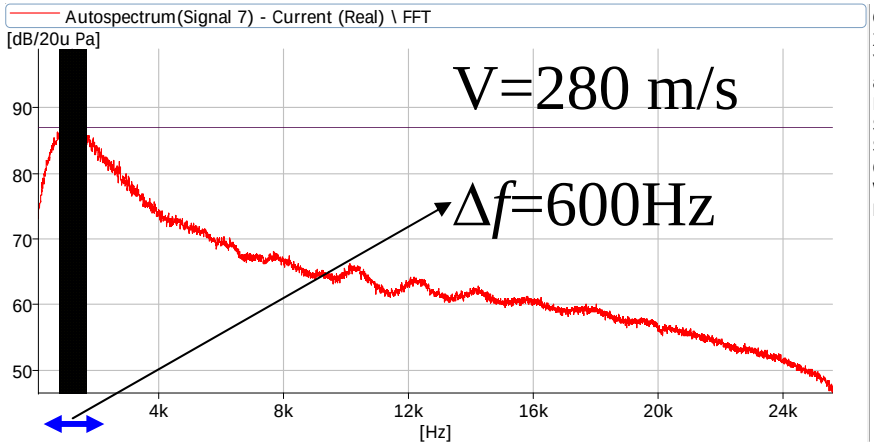

Round jet: **V=280** m/s, Micr. 40 deg.

Prospects

Proposed approach

In supersonic jet one of the mechanisms of sound radiation is identified and is ready to noise control strategy formulation. We issue the same mechanism exists in **hot high speed subsonic** jet.

The Main questions are:

Strategy of excitation?

Original assumptions?

Physical principle for control?

Approaches?

Plasma actuators for jet noise control

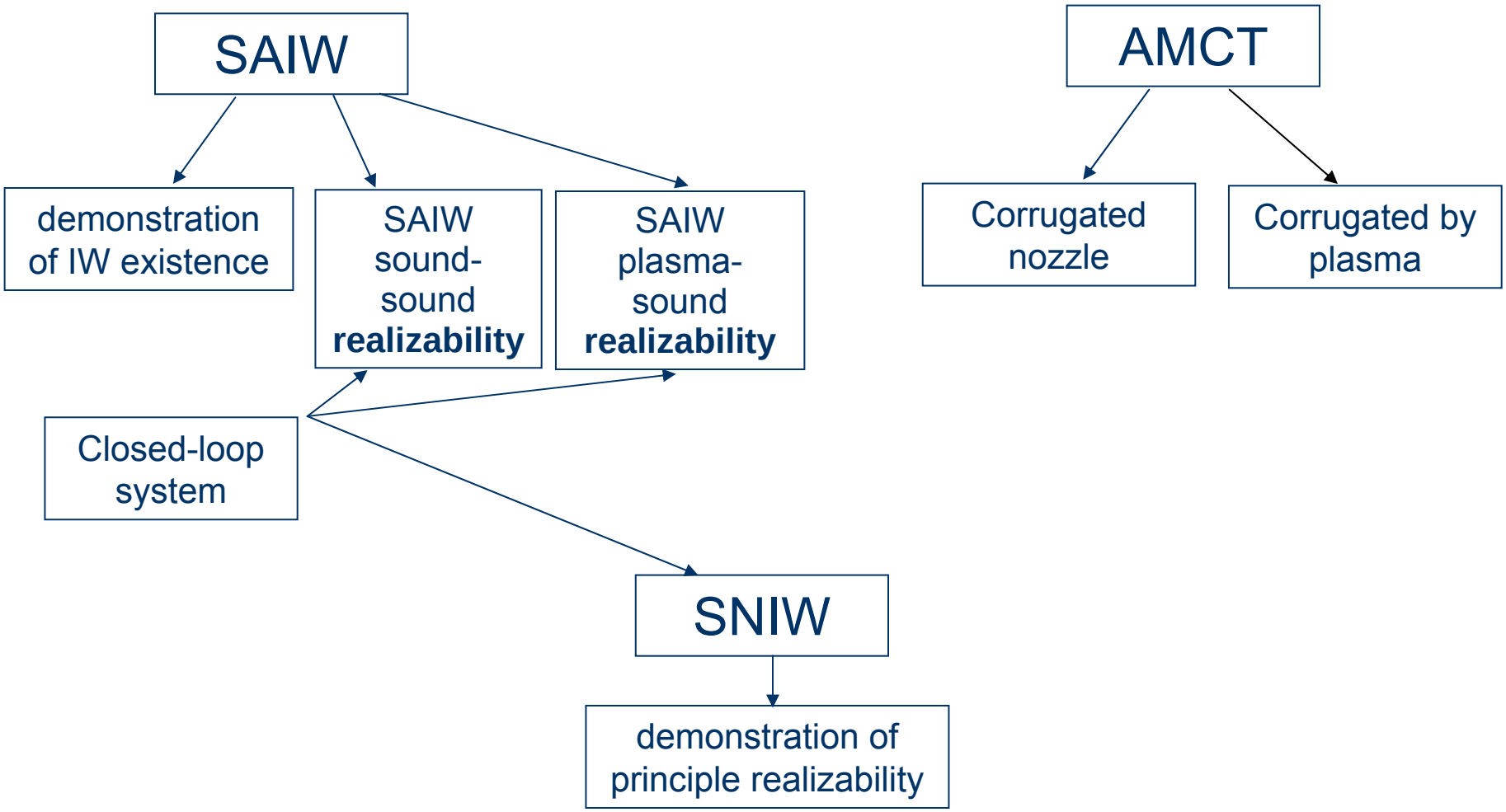

SAIW and SNIW

Formulation of active control strategy is realized with two steps:

(i) suppression of artificially excited instability wave (SAIW);

(ii) on this base the formulation of control strategy for natural instability waves (SNIW) developing downstream in free high speed jet (suppression of natural instability wave);

Experimental system SAIW is designed and manufactured.

This system contains closed-loop system.

AMCT

AMCT (azimuthal mode coupling technique):

(i) demonstration of principle realization AMCT on the base of corrugated nozzle;

(ii) demonstration of principle realization AMCT on the base of plasma-actuator.

Acknowledgements:

This work was carried out partly under:

- EU FP7 Project **Openair**,
- Coordinated EU-RF FP7 Project **ORINOCO,**
- Ministry of Industry and Trade of Russian Federation,
- Russian Foundation for Basic Research